IMPROVEMENTS IN DESIGN PROCEDURES FOR GROUND SOURCE AND HYBRID GROUND SOURCE HEAT PUMP SYSTEMS

By

JAMES R. CULLIN

Bachelor of Science in Mechanical Engineering

Bachelor of Science in Aerospace Engineering

Oklahoma State University

Stillwater, Oklahoma

2006

Submitted to the Faculty of the
Graduate College of
Oklahoma State University
in partial fulfillment of
the requirements for
the Degree of
MASTER OF SCIENCE
December 2008

IMPROVEMENTS IN DESIGN PROCEDURES FOR GROUND SOURCE AND HYBRID GROUND SOURCE HEAT PUMP SYSTEMS

Thesis Approved:

Dr. Jeffrey D. Spitler

Thesis Adviser

Dr. Daniel E. Fisher

Dr. Afshin J. Ghajar

Dr. A. Gordon Emslie

Dean of the Graduate College

ACKNOWLEDGEMENTS

This work is the culmination of a great deal of effort over the past two and a half years. There are a number of people whose contributions to this work I would like to acknowledge, because without them, this would not have been possible.

First, I would like to thank my advisor, Dr. Jeff Spitler, for his invaluable knowledge in the thermal systems field. I am extremely grateful for the opportunity to pursue research under his guidance. I would also like to thank the other members of my committee, Dr. Dan Fisher and Dr. Afshin Ghajar, for their insight and input into my research and this thesis.

I would also like to thank my fellow graduate students who have helped over the past several years. Specifically, the input of Jason Gentry and Xiaowei Xu has provided the cornerstone for much of this research.

To all of the faculty and staff in the Mechanical and Aerospace Engineering department at OSU and I thank them as well for the lessons learned during my studies both as a graduate student and as an undergraduate. Their collective

enthusiasm for teaching has driven me to pursue my advanced degrees, as I want to learn as much as possible from the great minds at this university.

I am especially thankful for the constant support given to me by my parents, John and Celia Cullin, and my sister, Nyssa Cullin, throughout my studies at OSU. Your unwavering support has made this entire effort possible, and you have made me into the person I am today.

Finally, I would like to acknowledge the impact that Cassandra Mickelson has had upon my life in the past year. Thank you for standing beside me through this effort; my life has become richer and more complete with you in it. The newfound energy you have given me has had just as much of an effect on this work as anything else, and I cannot thank you enough for that.

TABLE OF CONTENTS

Chapter Page

LIST OF TABLES

Table Page

LIST OF FIGURES

Figure Page

Figure Page

CHAPTER I

INTRODUCTION

As energy costs rise, it is highly desirable to have more energy efficient systems in both the residential and commercial sectors. Greater efficiency means less energy consumption, which in turn obviously results in less cost. Ground source heat pump (GSHP) and hybrid ground source heat pump (HGSHP) systems are one way to do this for heating and cooling applications. For any energy system, the capacity to accurately size the system is extremely important. An accurate simulation in the design stage leads to a system that is neither too large nor too small, as it can heat and cool the needed space with equipment that is neither too small (thus requiring supplemental heat addition or rejection to meet the demand) or too large (resulting in an oversized, less efficient system and increasing the first cost).

A ground source heat pump system consists of one or more heat pumps connected to a ground loop heat exchanger (GLHE). The GLHE uses the ground as both a heat source and a heat sink; in summer, heat can be rejected to the ground, while heat is extracted from the ground in the colder winter months. Thus, the heat transferred to and from the ground on an annual cycle is important. If there is an imbalance between the heating and cooling loads on the system, the ground temperature will drift either upward or

downward, thereby reducing the efficiency of the system. Other factors influencing the efficiency of the system include the thermal properties of the working fluid, ground, and the grout filling the boreholes. The upward or downward drift in temperature can be mitigated by increasing the individual borehole depth or adding additional boreholes—either of which adds to the total heat exchanger length—or by changing the configuration of the borefield, which alters the thermal interaction between the boreholes. Although there are multiple orientations and types of ground loop heat exchangers, only vertical, closed-loop GLHEs will be examined within the scope of this study.

When the imbalance between heating and cooling becomes large, a supplemental heat extraction or heat rejection device may be introduced as an alternative to significantly increasing the size of the ground loop heat exchanger. This creates a hybrid ground source heat pump system, with a portion of the heating and cooling loads being handled by the GLHE, and the rest by the supplemental device. Supplemental heat rejection can be accomplished by adding a cooling tower, fluid cooler, pond heat exchanger, or another similar device, while supplemental heat addition can be achieved by introducing something like a boiler or a solar collector.

In designing both ground loop heat exchangers and the associated GSHP systems, simulation of the system is critical. Simulation allows for an accurate depiction of the behavior of the GSHP system with respect to a wide variety of parameters. Simulation, as a consequence, leads to a design which meets the needs of the system, without being

grossly oversized or undersized. Without simulation, design engineers may rely on faulty assumptions or rules of thumb that can, and often, result in inefficient systems.

The design of a ground source heat pump system typically involves specifying the details (including depth, number, and configuration of boreholes) for the associated ground loop heat exchanger. Additionally, thermal properties of the ground, working fluid, and materials used are needed, as well as a description of the heat pump or heat pumps. For a hybrid ground source heat pump system, the design problem expands to also include specifying the size and type (either a heat source or a heat sink) of the supplemental heating or cooling device.

Several options are available for simulating GSHP and HGSHP systems. While some of these simulation methods can be quite accurate, they are not necessarily useful for design purposes, when a practicing engineer requires accurate results in as little time as possible. The tradeoff between increasing accuracy at the cost of simulation time and, as a result, feasibility from a design perspective, must be carefully considered. A simulation that is extremely accurate, but requires a significant amount of computation time as well as very detailed inputs by the user, is most likely not practical for an engineer designing a real-world system. Thus, it is the purpose of this work to introduce improvements in the design procedures for both GSHP and HGSHP systems that balance accuracy against feasibility for use by a design engineer. Additionally, since any simulation is not useful unless it has been experimentally validated, the GSHP simulation presented in this work will also be validated against experimental data. What follows is a brief overview of the

chapters of this work. It should be noted that since this work focuses on improvements in existing design procedures, a full literature review is not presented here; instead, the relevant literature is introduced when it is relevant to the particular improvements being discussed.

Chapter 2 presents the GLHEPRO software used to simulate and size ground source heat pump and hybrid ground source heat pump systems. The software was last formally described by Spitler [2000], and it has since undergone many enhancements. Updates have included a revised computation of the borehole thermal resistance, a new way to determine the thermal response over short time steps, and the capability to accurately simulate large, rectangular borefields. While some of the work since the last description of the software has been performed by others, special attention is paid to the specific contributions made by this author.

Chapter 3 suggests a new methodology for identifying peak loads for use in monthly ground source heat pump system simulation. Previously, little guidance has been available in identifying an appropriate duration over which to apply a monthly peak heating or cooling load. Additionally, it is possible that the absolute maximum heating or cooling load is not the best representation that could be used to obtain the most accurate prediction of the system's behavior. This chapter proposes a procedure that can be used by a practicing design engineer to more accurately represent the peak load behavior for a GSHP system. The method is tested for three building types in multiple locations, and compared to results from an hourly simulation and design process.

Chapter 4 describes a new procedure for designing a hybrid ground source heat pump system. This procedure sizes both the ground loop heat exchanger and supplemental heat extraction or rejection device for the HGSHP system by using a numerical optimization technique coupled with the existing GSHP simulation methodology. Computationally, the procedure does not require a great deal of resources to execute, which is an advantage for a practicing engineer. The new methodology is then briefly compared to other available methods for sizing HGSHP systems.

Chapter 5 presents an experimental validation of the GLHEPRO software described in Chapter 2. Eighteen months of experimental data from the hybrid ground source heat pump test facility located at Oklahoma State University are used in the validation. In addition to comparing the monthly average (at the end of the month) fluid temperatures, monthly maximum and minimum temperature comparisons are also made, as these are the values which will determine the size of a GSHP system. Additionally, considerable effort is made to explain the ways in which the simulation fails to accurately represent the experimental behavior, with suggestions proposed as to how improvements may be made in the future.

Overall, this work attempts to enhance the state-of-the-art for the simulation of ground source and hybrid ground source heat pump systems, especially with regard to simulation for the purposes of design. New simulation and design methodologies are proposed, and

are compared to what is currently available. The validation of a monthly GSHP design tool serves to demonstrate that the new methods are accurate for simulation purposes.

CHAPTER II

SOFTWARE FOR THE DESIGN OF GROUND SOURCE AND HYBRID GROUND SOURCE HEAT PUMP SYSTEMS

2.1 Introduction

GLHEPRO is a design tool used to simulate ground source heat pump (GSHP) systems, and to size the ground loop heat exchangers (GLHEs) in those systems. It is a Microsoft Windows application, consisting of a graphical interface implemented in Visual Basic and a simulation engine written in the FORTRAN programming language. GLHEPRO is designed to be straightforward and easy to use, requiring little from the user except the building heating and cooling loads, descriptions of system components such as the GLHE and the heat pumps, and the physical properties of the soil, grout, pipes, and so forth.

A detailed description of GLHEPRO has been presented in the past by Spitler [2000], but certain aspects of the design tool have been either updated or changed completely since that time. Thus, this is an effort to describe GLHEPRO at its current state in development. It should be noted that, since this tool is an ongoing project, part of the revisions to the program since Spitler last described it have been developed by others, including Young [2001], as well as Xu and Spitler [2006]. What follows is a description

of the design tool, with special attention paid to the revisions made since Spitler [2000] last presented the program.

2.2 Background

The basis for the approach used in GLHEPRO is the g-function, a set of non-dimensional response factors developed by Eskilson [1987]. The starting point for the g-function is the temperature response to a step input heat pulse for an individual borehole. For this single borehole, the temperature around the borehole as a function of time can be computed using a transient two-dimensional finite difference method in radial-axial coordinates. Eskilson then used superposition principles to determine the effects of boreholes in multiple borehole systems. The results of these superposition computations can be combined to create a set of nondimensional time and temperature response values, cumulatively called the g-function, which represents the thermal behavior of a specific borehole system as a function of time and heat input. Presently, there are a wide variety of configurations for which these g-functions are available. Figure 2-1 [used with permission from Spitler 2000] depicts the nondimensional response as a function of time for various borehole configurations.

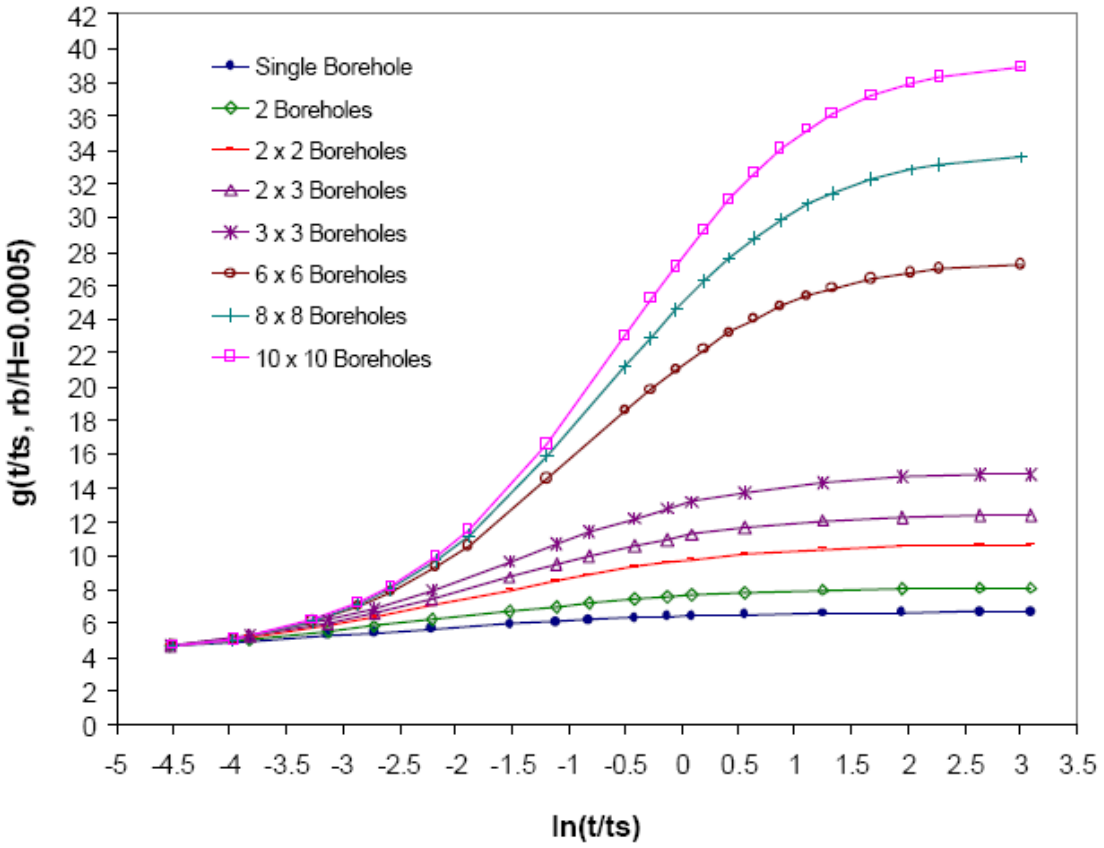

Figure 2-1: G-function temperature response factors for various borehole configurations

Since GLHEPRO deals with both monthly average loads as well as peak hourly loads, it is necessary to have a g-function that is applicable at both long and short time steps. Eskilson's g-functions have a minimum time step to which they are applicable; for common applications, this value is often on the order of several hours, which is greater than the one-hour interval necessary in computing the response to peak loads [Spitler 2000]. For some applications, this minimum time step may be even higher, on the order of days or even months. Additionally, much of the data developed by Eskilson does not cover time periods shorter than several weeks. While Hellström and Sanner [1994] expanded this data by extrapolating to shorter times using a line source solution, this is

still not sufficiently fine to compute the effects of peak loads, which can occur over times as short as a single hour. For shorter time steps, the method developed by Xu and Spitler [2006] may be used. The values of the g-function at short time steps are computed via a one-dimensional finite volume method, with the volumes chosen to preserve the thermal resistance of the borehole and the thermal mass of the grout and fluid. Xu [2007] showed that this method closely matches a more accurate two-dimensional model. By joining together the long and short time step g-functions, a complete profile of the temperature response of the borehole system to a heat input may be created, and this forms the basis of the simulation method used in GLHEPRO.

Using the full short and long time step g-function profile, the temperature response at any point may be determined by superimposing the responses to each individual load. For example, consider four months of heat rejection as shown in Figure 2-2 [figure used with permission from Spitler 2000]. The first month's pulse is applied for the entire simulation, the second month's from the second month onward, and so forth, with each pulse equaling that month's value less the value from the previous month.

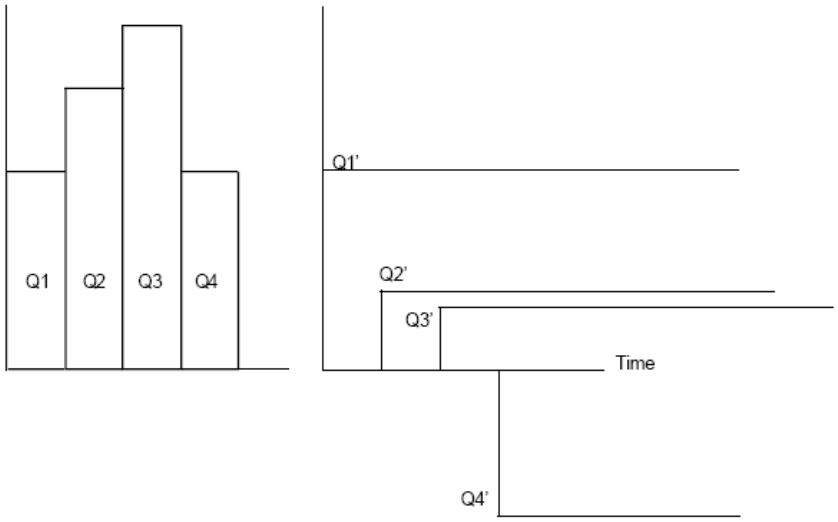

Figure 2-2: Superposition representation of four months of heat rejection pulses

The superposition principle then gives the temperature at the end of the n^{th} month as

$$T_{borehole} = \sum_{i=1}^{n} \frac{(Q_i - Q_{i-1})}{2\pi k} g\left(\frac{t_i}{t_s}, \frac{r_B}{H}\right) + T_{UG} \qquad (2\text{-}1)$$

Where:

$T_{borehole}$ is the borehole wall temperature [°C];

Q_i is the heat flux entering the ground per unit length of pipe [W/m];

n is the current time of interest [s];

k is the ground thermal conductivity [W/m-K];

g is the value of the g-function at the specified point [-];

t_i is the time at the i^{th} time step [s];

t_s is the time scale [s];

r_B is the borehole radius [m];

H is the depth of the borehole [m]; and

T_{UG} is the undisturbed ground temperature [°C].

For each month in the simulation, the temperature response in the ground due to the heating and cooling loads is determined according to Equation 2-1. In designing a GSHP system, this simulation will need to be run iteratively to determine the correct depth to meet constraints on the entering fluid temperature of the heat pump; this will be discussed in subsequent sections.

2.3 Program Input

Specification of the ground loop in GLHEPRO, including the soil and fluid properties, is accomplished through the main program window, shown below in Figure 2-3. There are four main types of inputs required for the simulation of a ground source heat pump system: characteristics of the borehole, thermal properties of the ground, thermal properties of the working fluid, and information about the heat pump, including the heating and cooling loads.

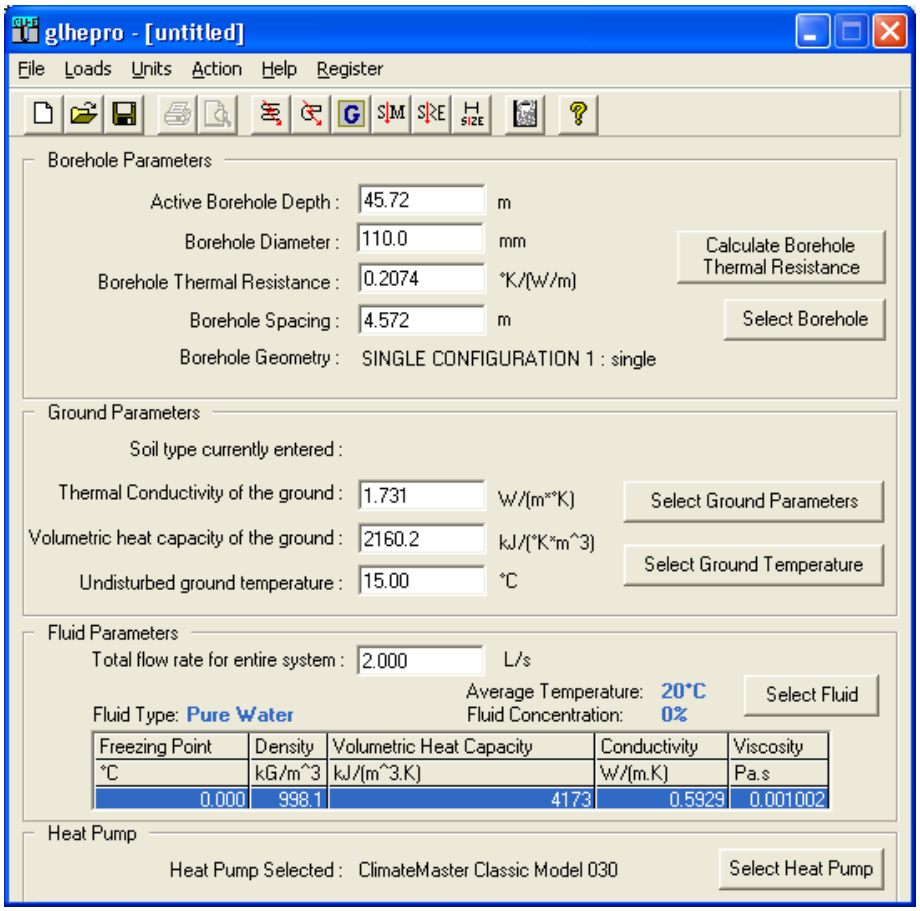

Figure 2-3: GLHEPRO main window

2.3.1 Borehole Parameters

The “Borehole Parameters” section gives values to the parameters that deal strictly with the borehole. The active borehole depth is that part of the total depth of a single borehole that facilitates heat transfer between the working fluid and the soil. In other words, it is the total borehole depth minus any upper portion used for piping to the rest of the system, or discounted due to the effects of varying ground geology. For a simulation, this value is input by the user; for sizing of GSHP systems, this value is determined automatically. The borehole diameter is, obviously, the diameter of the borehole, including any casing used. The borehole thermal resistance is the resistance to heat transfer between the

working fluid and the borehole wall. Although this is a very important parameter in the simulation of the system, it does not need to be provided by the user; instead, it is calculated internally. More details on this borehole thermal resistance will follow in a later section. Next, the borehole spacing is simply the distance between the centers of two adjacent boreholes; the magnitude of the spacing governs to what degree boreholes interact with others nearby. A larger borehole spacing will result in needing either fewer boreholes or less depth per borehole, when all other parameters are the same for cases in which the annual heat extraction and rejection are not balanced. The last element of this section, the borehole configuration, determines how many boreholes are present in the system, and in what configuration they are placed. GLHEPRO includes a library of numerous different configuration options, including line, L-shaped, U-shaped, and rectangular, with boreholes numbering up to around 900 in the rectangular configuration.

2.3.1.1 Large Rectangular Borefield Configurations

Because g-function data for borehole configurations of more than about 400 boreholes are not currently available, the development of an explicit equation, or a set of explicit equations, defining the g-function for a particular family of configurations would be extremely useful. Data for rectangular borefield configurations of up to 400 boreholes was obtained from Hellström [Hellström and Sanner 1994]; the data was generated via a complex 2-D numerical method. To model the data more simply, it was first noted that the relationship between the size of a rectangular borefield, as represented by the number of boreholes in one dimension regardless of the other dimension, and the g-function, as well as the relationship between the ratio of the numbers of boreholes in the two

dimensions and the g-function, were roughly quadratic in nature. Thus, the g-function data were fitted to the quadratic equation

$$g_{est}\left(\ln\left(t/t_s\right), B/H\right) = a_1 + a_2 \cdot \frac{C}{I} + a_3 \cdot \left(\frac{C}{I}\right)^2 + a_4 \cdot \frac{E}{I} + a_5 \cdot \left(\frac{E}{I}\right)^2 + a_6 \cdot \frac{C}{I} \cdot \frac{E}{I} \qquad (2\text{-}2)$$

Where:

g_{est} is the estimated value of the g-function;

$ln(t/t_s)$ is the dimensionless time;

B/H is the ratio of borehole radius to borehole depth;

C is the number of corner boreholes;

E is the number of edge (perimeter, non-corner) boreholes;

I is the number of interior boreholes; and

a_1-a_6 are the model coefficients

The ratio C/I is representative of the overall size of the borefield, since $C = 4$ for any rectangular field. E/I, then, is a measure of the deviation from squareness of the rectangular field, since E will have its minimum value for any arbitrary total number of boreholes when the field is square. The above quadratic equation fit was performed for each combination of boreholes X in an X by Y field ($X < Y$), and radius-to-depth ratio B/H. This resulted in a set of coefficients that can be used to generate g-function values for any rectangular borefield with at least 100 boreholes and between ten and twenty boreholes in each direction, without the need to store discrete values for each possible borefield configuration.

Testing of the resulting modeled g-functions versus the data already on hand from Hellström was performed both inside and outside of the interval of the equation fit. Individual g-function values differed from the available data by no more than 0.5%; a plot of the modeled g-functions versus available data at a fixed *B/H* ratio of 0.10 is shown in Figure 2-4. For configurations slightly below the equation fit interval, the g-functions show a bit of variation, but still produce very similar results to the available data. Proceeding farther below the interval (7x9 and 5x7 model curves in Figure 2-4) starts to produce a discontinuity at the transition between the short and long time step g-function values; this becomes quite pronounced the farther from the original interval. Additionally, the g-function curves begin to experience discontinuities in slope and other non-realistic behaviors. Above the equation fit interval (23x27 and 30x30 model curves), the shapes of the g-function curves look reasonable, as well.

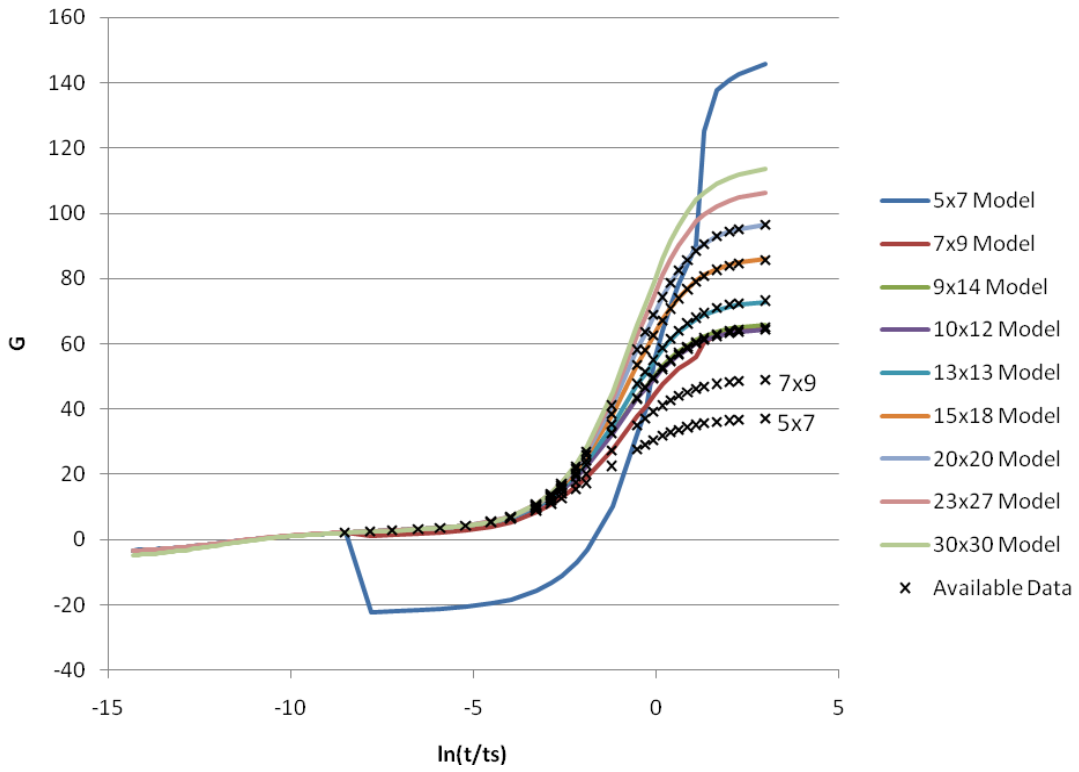

Figure 2-4: Modeled and actual g-function data

The differences in temperature caused by using the modeled g-functions are also small. For a sample office building, the system was simulated using a variety of 10 by *Y* rectangular borefields, with *Y* ranging from 10 to 40. Additionally, the spacing ratio *B/H* was varied between three different values. The error in the heat pump entering fluid temperature for the 300th month of the simulation is shown in Figure 2-5. For the larger *B/H* ratios, the temperature difference is almost zero, while for *B/H* = 0.03, it is somewhat larger but still within 0.05°C for all cases except the 10x10 configuration. That point is the first in the model, and experiences a small but noticeable difference between the model and the actual value for longer times. Thus, the difference is somewhat larger than for the other configurations and *B/H* ratios.

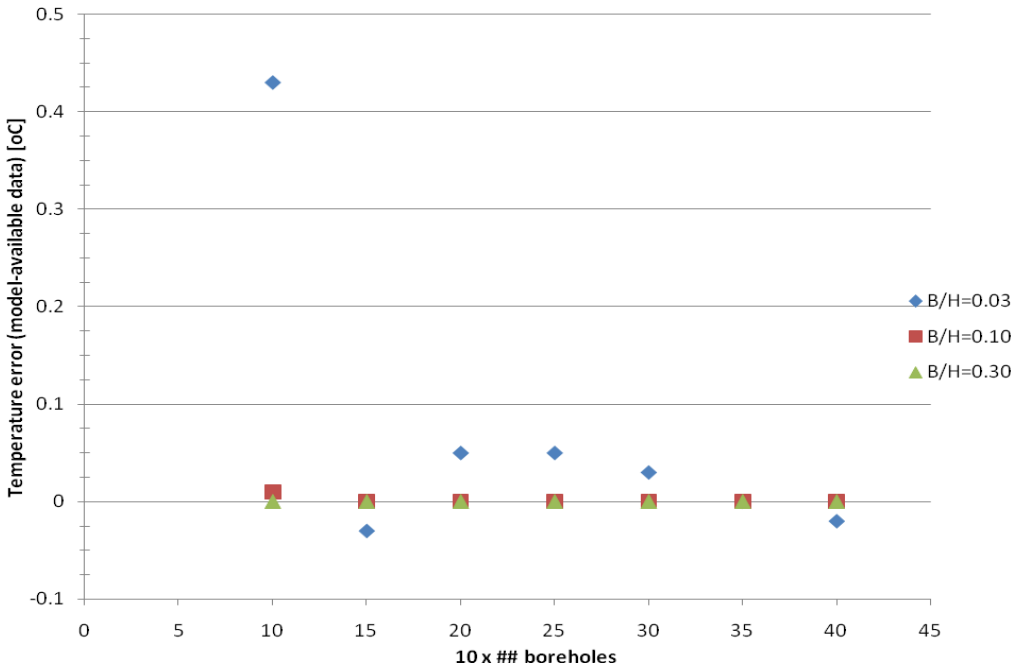

Figure 2-5: Modeled g-function temperature simulation error

To compare the capabilities of the modeled g-functions for the purpose of sizing a GLHE, systems were sized for a variety of building types and locations with various numbers of boreholes, as shown in Figure 2-6. In addition to comparing the model to Hellström's data, a third "block method" was used to size the boreholes. This block method split both the borefield and the load into pieces; for example, for a 10x30 borehole system, a 10x10 system was sized using a third of the load. It was assumed that this size would carry over to the 10x30 system with the entire load, since the additional thermal interaction effects due to the increased number of boreholes becomes rather insignificant for borefields this large (in other words, the effect of one borehole on another in a 10x10 system is nearly identical to that in a 10x30 system). As can be seen from Figure 2-6, all three methods produced nearly equivalent sizes for all cases, with the block method occasionally sizing a system a bit smaller due to the small amount of

borehole interaction that cannot be considered by using that method. Overall, the curve-fit model of the g-function for large rectangular borefield configurations performs quite well when compared to the data generated using a detailed numerical model.

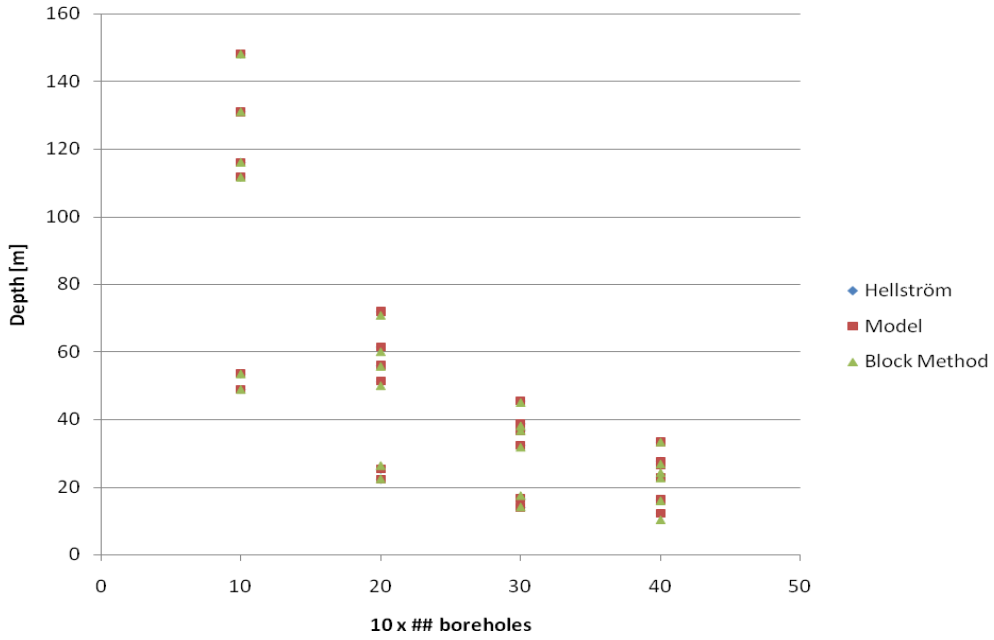

Figure 2-6: Modeled g-function system sizing comparison

2.3.1.2 Individual Borehole Geometry

In order to determine the borehole thermal resistance accurately, the geometry of an individual borehole is needed; for simplicity, it is assumed that all boreholes in the system are equivalent. The input screen for the borehole geometry is shown in Figure 2-7. The borehole diameter *d* is carried over from the main window. The shank spacing *s* is defined as the distance between the outside walls of the two ends of the U-tube. Several options are available for selection, including no separation (the pipes touch) and full separation (each pipe rests against the borehole wall); these selections mirror those used by Paul [1996]. The U-tube inside and outside diameters can be specified either

manually, or from selection of a variety of common pipe sizes, such as SDR11, Sch.40, PN6, and PN10. The flow rate per borehole and fluid factor are used in determining the borehole thermal resistance and short time step g-function values, which will be discussed later.

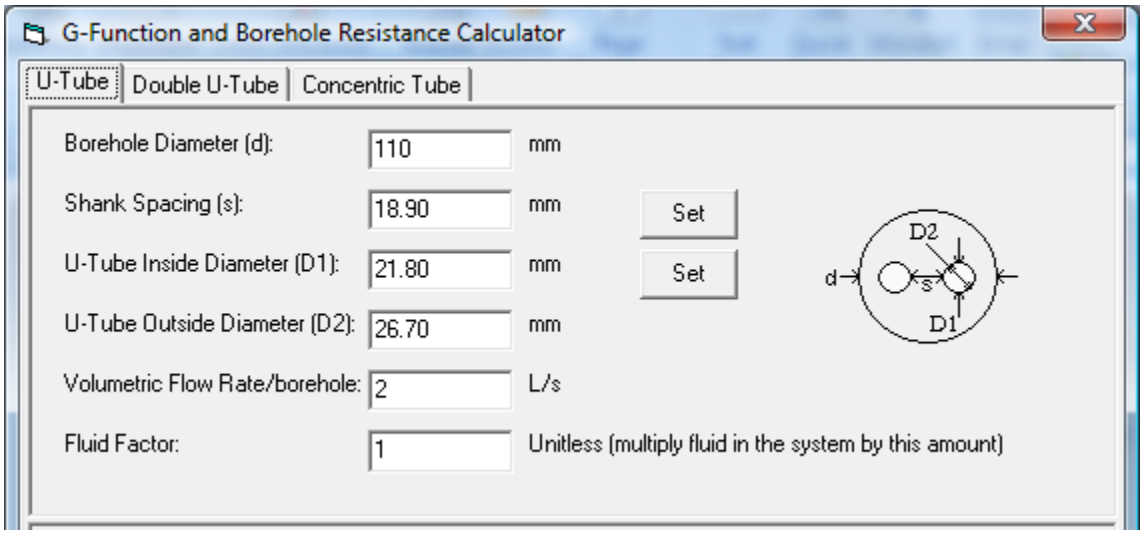

Figure 2-7: GLHEPRO borehole geometry inputs

Inputs for the double U-tube and concentric tube ground heat exchangers are similar. For the double U-tube, pipe sizes must obviously be specified for both pipes. Additionally, the available shank spacing options are no longer based on the work of Paul [1996]; instead, they are empirically based on what is physically possible. For instance, zero spacing is impossible, assuming all ends of the U-tubes are equally spaced, because pipes would be overlapping. For the concentric tube, both inner and outer pipe sizes are necessary, but no shank spacing is required since the second pipe is inside the first.

2.3.2 Ground Parameters

The "Ground Parameters" section gives the thermal properties of the soil. The thermal conductivity and volumetric heat capacity can be determined through any of several different methods, including laboratory analysis [Stolpe 1970; Mitchell and Kao 1978], use of a thermal probe [Hooper and Chang 1953; Falvey 1968; Mitchell and Kao 1978], classification by soil type [Bose 1988; Bose 1989], and in-situ testing [Austin 1998; Austin et al. 2000; Witte et al. 2002; Sanner et al. 2005]. GLHEPRO also includes a limited library of several common soil types, with typical values for thermal conductivity, density, specific heat, and volumetric heat capacity for each soil type. There are also several options for determining the undisturbed ground temperature. First, a working fluid could be circulated through the borehole until reaching steady state; the steady state temperature would also be the undisturbed ground temperature [Gehlin and Hellström 2004]. Second, GLHEPRO includes a map of the continental United States showing underground water temperatures, which are roughly equivalent to the ground temperatures, as a set of isotherms. A new option is the possible estimation of the undisturbed ground temperature from the average annual *air* temperature, which will now be discussed in more detail.

2.3.2.1 Estimation of Undisturbed Ground Temperature

It seems possible to use the average annual air temperature as a preliminary estimate of the undisturbed ground temperature. The approximation—that the ground is, on average, 1.4 °C warmer than the average annual air temperature—was developed as a result of a mapping approach taken by Signorelli and Kohl [2004]. This mapping approach first fit

both ground and air temperatures (in the form of yearly averages) as third degree polynomials against altitude. The values for both temperatures were taken from meteorological stations around Switzerland. Once the air temperature was modified to exclude subzero values (as these were likely to be snowy intervals, in which the snow would insulate the ground), a nearly constant difference between air and ground temperature with respect to altitude above sea level was found—the ground was, on average, 1.4°C (2.5°F) warmer than the air. This difference was applied to a previously generated map of the average annual air temperature in Switzerland, and compared to existing ground temperature data from borehole systems scattered throughout the country. A maximum deviation of 2°C was found during this verification.

By comparing available ground temperature references to available annual average temperatures for a variety of locations around the continental United States, it would seem that the air temperature might be a reasonable approximation for the undisturbed ground temperature in areas outside of Switzerland as well. As shown below in Table 2-1, the difference between the two varies a bit more substantially than Signorelli and Kohl found for Switzerland, however. Fargo shows a much larger difference, most likely due to the potential for snow cover insulating the ground; Houston is as much of an extreme climate as Fargo on the other end of the temperature scale. Very moderate climates such as Los Angeles and Seattle, which are tempered by incoming sea breezes, would seem to reduce the differences in these locations. Phoenix seems to be an outlier, but the cool, clear nights present an opportunity for radiative heat loss from the ground, which might serve to explain at least a part of the negative differential.

Table 2-1: United States ground/air temperature comparison

City	Annual Avg. Temp. (°F)*	Ground Temp. (°F)^	Difference (°F)
Atlanta, GA	61.3	64	2.7
Chicago, IL	49.0	51	2.0
Denver, CO	50.3	52	1.7
Detroit, MI	48.6	51	2.4
Fargo, ND	41.0	47	6.0
Houston, TX	67.9	74	6.1
Kansas City, MO	53.6	55	1.4
Los Angeles, CA	63.0	64	1.0
New York, NY	54.7	56	1.3
Oklahoma City, OK	60.0	62	2.0
Phoenix, AZ	72.6	68	-4.6
San Francisco, CA	57.1	59	1.9
Seattle, WA	52.8	53	0.2
		AVERAGE	1.85

* Air temperatures taken from http://www.worldclimate.com

^ Ground temperatures estimated from map in Collins [1925]

Further research would be needed to establish good explanations for the range of differences seen here. Presumably, such factors as vegetation, humidity, radiation to the sky, solar radiation incident on the ground, snow cover, etc. all have an effect. Results taken from measurements in the Czech Republic and Portugal [Šafanda et al. 2006] seem to be in line with the 2.5 °F empirical estimation for normal (i.e. grass) vegetation.

There is also an energy balance method developed by Pikul [1991], based on thermal resistances, to compute the ground temperature using the air temperature as one of the inputs. However, many of the secondary inputs, such as vapor pressures, soil moisture, and vegetation height, are extremely difficult to compute or measure, especially in more

developed locales. They also vary substantially with the seasons. Results of this method seem to vary significantly, with deviations on the order of ±2.5 °C (4.5°F) from measured data. Consequently, this method is, at the present time, both too complex and too inaccurate to be of much use in a design tool.

2.3.3 Fluid Parameters

Finally, the "Fluid Parameters" section defines the working fluid, both in terms of volumetric flow rate and fluid thermal properties. GLHEPRO contains several choices for working fluid and allows the concentration of the fluid as well as the mean temperature to be specified. Then, the necessary thermophysical properties, including density, conductivity, viscosity, volumetric heat capacity, and freezing point may be computed by means of empirical curve fits based on mixture type, concentration, and temperature [Melinder 1999; Khan 2004]. The option is also available to manually add the working fluid if the thermophysical properties are known, and the fluid is one not already available for selection.

2.3.4 Heat Pump/Load Specification

In GLHEPRO, only one heat pump may be selected, so that heat pump must be representative of all the heat pumps in the system, if there are multiple types. The heat pump model is a simple coefficient-based model, with second-order equation fits between the heat of rejection versus cooling capacity, the heat of absorption versus heating capacity, and the power consumption versus both the heating and cooling capacities:

$$q_{rej} = QC \cdot \left(a + b \cdot EFT + c \cdot EFT^2\right) \tag{2-3}$$

$$P_c = QC \cdot \left(d + e \cdot EFT + f \cdot EFT^2\right) \quad (2\text{-}4)$$

$$q_{extr} = QH \cdot \left(u + v \cdot EFT + w \cdot EFT^2\right) \quad (2\text{-}5)$$

$$P_h = QH \cdot \left(x + y \cdot EFT + z \cdot EFT^2\right) \quad (2\text{-}6)$$

Where:

q_{rej} is the heat rejected to the ground by the heat pump [kW];

QC is the system cooling load [kW];

Q_{extr} is the heat extracted from the ground by the heat pump [kW];

QC is the system heating load [kW];

EFT is the heat pump entering fluid temperature [°C]; and

$a - z$ are the model coefficients.

Since the heat extracted from or rejected to the ground is based on the heat pump entering fluid temperature, and this temperature is not known prior to the simulation, iteration must be performed at each step. An initial EFT is assumed and used to compute the heat extraction/rejection rates; these rates are used to compute the EFT, and the cycle continues until convergence.

Heating and cooling loads are specified as monthly energy consumptions. GLHEPRO assumes that the total monthly load is equally distributed over each hour of the month. Peak loads are specified by providing a magnitude for each month in heating and cooling, as well as separate durations in hours for the heating and cooling peaks. In addition, loads may be specified that act directly on the ground loop; this can be used to include any loads that are not seen by the heat pump.

2.4 Methodology

2.4.1 Borehole Resistance/STS G-function Computation

GLHEPRO requires two additional components before it can begin any simulation of the ground source system: the borehole thermal resistance and the g-function profile for short time steps. These are computed consecutively, as the short time step g-function values depend on the borehole thermal resistance.

The borehole thermal resistance is the resistance between the working fluid and the wall of the borehole, and consists of three component resistances. The conductive resistance due to the pipe is computed based on the pipe thermal conductivity using the familiar expression for the conductive resistance in a hollow cylinder [Incropera and Dewitt, 1990],

$$R_{cond,pipe} = \frac{\ln(r_o / r_i)}{2\pi k} \tag{2-7}$$

Where:

$R_{cond,pipe}$ is the thermal resistance due to conduction in the pipe, per unit length of pipe [K-m/W];

r_o is the outside radius of the pipe [m];

r_i is the inside radius of the pipe [m]; and

k is the thermal conductivity of the pipe [W/m-K].

Second, the thermal resistance between the pipe and the wall of the borehole, including the effects of any grout used, may be computed using the multipole method [Claesson

and Bennett 1987; Bennett et al. 1987]. The multipole method is a very accurate analytical method that compares favorably to a two-dimensional finite volume numerical model with boundary-fitted coordinates [Rees 2000; Young 2004]. It is implemented in GLHEPRO as an external FORTRAN routine. Because the only requirements of the multipole method are circles of homogeneous composition, such as an outer soil boundary representing the area affected by the borehole or a grout-filled borehole containing the piping, there is no restriction requiring only one U-tube. It is because of this flexibility that GLHEPRO was adapted to include support for both double and concentric U-tube systems, as well as the original single U-tube system. The only major difference between a double U-tube or concentric-tube system is the setup for the multipole thermal resistance calculation. A more extensive discussion on the implementation of the multipole method can be found in the work by Young [2004].

Finally, the last component is the convective resistance between the working fluid and the pipe wall. Since flow in the borehole may not always be turbulent, Xu and Spitler [2006] implemented a method for dealing with the entire possible range of Reynolds numbers. Gnielinski's correlation [1976] is used to compute the convection coefficient based on the Nusselt and Reynolds numbers when the flow is turbulent (Re>2300), while using the constant value Nu = 4.364 when the flow is laminar. To ensure a continuous curve at transition, a linear interpolation between the constant laminar Nusselt number and the Nusselt number from Gnielinski's correlation is performed whenever the Reynolds number falls between 2200 and 2500. With the convection coefficient known, the convective resistance between the fluid and the pipe may be computed as

$$R_{conv} = \frac{1}{2\pi r_i h} \tag{2-8}$$

Where:

R_{conv} is the thermal resistance due to convection in the pipe, per unit length of pipe [K-m/W];

r_i is the inside radius of the pipe [m]; and

h is the convection coefficient between the fluid and the pipe wall [W/m^2-K].

The approach to computing the short time step g-function values has been substantially updated since the design tool was last presented by Spitler [2000]. Whereas before, the short time step values were computed directly using a transient two-dimensional finite volume model developed by Yavuzturk [1999], Xu and Spitler's method [2006] uses a one-dimensional model that directly accounts for convective resistance and fluid thermal mass using the Gnielinski convection correlation and fluid factor approaches, respectively. By carefully controlling the inputs, the results of the simplified one-dimensional calculations closely match those of a much more detailed two-dimensional simulation. To account for the thermal mass of the fluid, an additional term, called a "fluid factor" by Xu and Spitler [2006], may be introduced. This factor is basically just a multiplier on the amount of fluid in the system; by adding this extra fluid, the effects of any temperature change due to a heating or cooling load are damped somewhat. Using these values, the thermal response for short times can be computed numerically using a one-dimensional model; these values are kept in the same form as the g-function, and can be utilized in the same way. This approach maintains computational efficiency without sacrificing accuracy.

2.4.2 Simulation Approach

The simulation approach in GLHEPRO remains the same as was presented in Spitler [2000], and will be summarized here. The borehole wall temperature at each time step is computed via the superposition of the temperature changes caused by the load pulses from the current and every previous time step. These are weighted by the value of the g-function at the nondimensionalized time corresponding to each particular time step, as described in Equation 2-1. Next, the temperature of the working fluid can quickly be determined by using the borehole resistance,

$$T_f = T_{borehole} + R_B \cdot Q_i \tag{2-9}$$

Where:

T_f is the temperature of the working fluid [°C];

R_B is the borehole thermal resistance [K/(W/m)]; and

other quantities are as described in Equation 2-1.

Finally, the heat pump entering and exiting fluid temperatures are calculated by assuming that the temperature change between inlet and exit is linear. Thus, the heat pump entering fluid temperature is computed as

$$T_{in} = T_f - \frac{Q \cdot H \cdot NB}{2 \cdot \dot{m} \cdot c_p} \tag{2-10}$$

while the heat pump exiting fluid temperature is determined by

$$T_{out} = T_f + \frac{Q \cdot H \cdot NB}{2 \cdot \dot{m} \cdot c_p} \tag{2-11}$$

Where:

T_{in} is the heat pump entering fluid temperature [°C];

T_{out} is the heat pump exiting fluid temperature [°C];

NB is the number of boreholes in the system [-];

$\dot{m}$ is the mass flow rate of the working fluid [kg/s];

C_p is the specific heat of the working fluid [J/kg-K]; and

other quantities are as described in Equations 2-1 and 2-9.

While knowing the temperature of the working fluid due to an average load over the course of the month is certainly useful knowledge, the extreme temperatures entering the heat pump are perhaps more important, as they can be used to determine whether the heat pump will function adequately and efficiently. The handling of the peak load for each month, to obtain a maximum and minimum heat pump entering fluid temperature for the month, has changed substantially since Spitler [2000]. Spitler [2000] used a simple analytic approximation to the line source method to determine the temperature change due to the peak load. With the short time step g-function values calculated with the method of Xu and Spitler [2006], the same approach used to compute the "average" temperatures for the month may be utilized. The only difference in determining the peak temperature as opposed to the monthly temperature, then, is that the peak load—or, rather, the difference between the peak load and the average load for the month—is used instead of the total load for the month averaged over the month. The actual value for the peak load, and the duration for which this load is applied, are very important to the accuracy of the simulation; choosing these values requires some effort, and a method for doing so is presented in Chapter 3.

2.4.3 Sizing Technique

The ability to determine a suitable depth for the boreholes in a ground loop is perhaps the most important feature of GLHEPRO. Instead of explicitly specifying a size for the ground loop, the user may provide upper and lower limits for the heat pump entering fluid temperature. GLHEPRO then begins the sizing procedure by making an initial guess at the borehole depth and simulating to determine the actual maximum and minimum heat pump entering fluid temperature. The depth is then adjusted incrementally until there is one depth that results in one of the design constraints exceeded and one depth that results in both constraints met; this guarantees that the desired borehole depth is somewhere between the two values. With the solution thus bracketed, the technique of modified false position [Dowell and Jarratt 1971] is used to refine the guess until convergence within a design tolerance of ±0.01 degrees (Celsius or Fahrenheit, depending on the unit system). The convergence here rarely requires more than a few iterations, meaning that the overall sizing routine takes only a matter of seconds to produce the desired results on a typical personal computer.

2.4.4 Hybrid System Sizing Technique

In addition to sizing regular GSHP systems, GLHEPRO has been modified to also size HGSHP systems. For a hybrid ground source heat pump system, "sizing" requires finding not only the necessary borehole depth, but also the required size of the supplemental heat extraction or heat rejection device. For any HGSHP, it is possible to have a range of combinations of borehole depths and supplemental device sizes, as shown in Figure 2-8, that maintain the heat pump entering fluid temperature within the allowable

limits. For example, in a system in which the borehole depth is constrained by cooling, a larger cooling tower will reduce the needed size of the borehole. This might move the solution from point 1, a pure GSHP system, to point 2, which is a hybrid system with a supplemental heat rejection device. On the other hand, for a system in which an additional heat source is required, the optimal HGSHP system might be at point 2'. In both cases, the solution could be anywhere along the curve, but it is not known in advance what the shapes of these curves might look like, or where the best solution might occur.

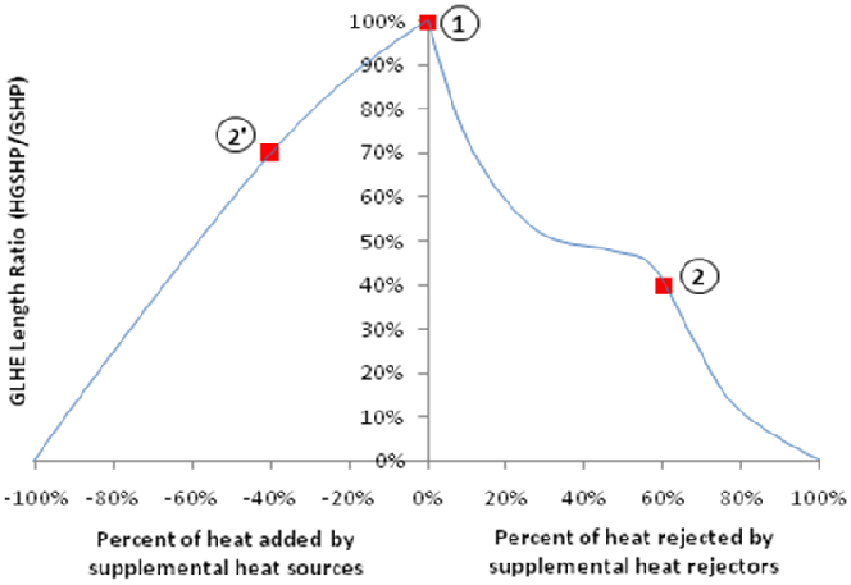

Figure 2-8: Potential HGSHP design points

The task, then, is to find the most optimum combination of values of the ratio of GLHE length between the HGSHP system and its base GSHP system (defined as the smallest system that will capably handle all heating and cooling loads, without any supplemental devices), and the percentage of heat added or rejected by the supplemental devices. This

is the subject of Chapter 4 of this work. A thorough discussion of the HGSHP design procedure can be found there.

2.5 Conclusions and Recommendations

A previously developed program for the simulation and sizing of ground loop heat exchanger systems has been revised to incorporate a number of improvements and new features. The most important updates and changes to the methodology include refined calculation of the borehole thermal resistance using the multipole method, more accurate estimation of the convective resistance via an improved convection correlation, consideration of thermal mass of the fluid in predicting peak temperature response, addition of double U-tube and concentric tube heat exchangers in addition to the original single U-tube option, expansion of the g-function approach to large rectangular borefields, and approximation of undisturbed ground temperature when more detailed data is not available. As a whole, GLHEPRO provides developers of ground loop heat exchanger systems with a simple and quick way to simulate the systems they are designing.

Possibilities for the further refinement of GLHEPRO include the option for hourly simulation, which would increase the level of accuracy as compared to a monthly simulation. However, this option must be carefully considered, as any substantial increase in computation time—such as what a full transition to an hourly simulation time step would cause—would likely be unacceptable for a practicing design engineer.

Additionally, the current method of sizing a hybrid system does not directly simulate the supplemental heat rejection or extraction device; it simply specifies the required size. Modifications could be made to the program that would allow for the inclusion of a variety of supplemental devices, such as cooling towers and boilers, thereby creating a full hybrid system design simulation. Also, this program could be easily adapted to handle the design of horizontal ground heat exchangers; however, a suitable simulation and design methodology would first need to be developed.

CHAPTER III

REPRESENTATION OF LOADS FOR GROUND SOURCE HEAT PUMP SYSTEM SIMULATIONS

3.1 Introduction and Background

The design of ground heat exchangers for ground-source heat pump systems is a critical part of the overall system design. As the ground heat exchanger is a large part of the overall system cost and perhaps nearly all of the incremental cost when compared to, say, a water loop heat pump system, correct sizing is very important. If the size is too large, the capital cost of the system may preclude selection. If the size is too small, the system will, sooner or later, fail due to excessive heat pump entering fluid temperatures.

A number of design tools [Hellström and Sanner 1994, Katsura et al. 2006, Kavanaugh and Rafferty 1997, Morrison 2000, Spitler 2000] are now available. They all rely on a simulation of system operation over the expected life of the system, though the simulation may be more or less simplified compared to a detailed hourly simulation [Yavuzturk and Spitler 1999, Xu and Spitler 2006, Thornton, et al 1997.]. They all depend on inputs such as ground thermal properties, heat pump performance parameters, borehole completion details, and building heating and cooling loads. It is the last

category of inputs that is the focus of this chapter. In order to keep user input tractable, all of the tools, with one exception, rely on a representation of the loads that is simplified compared to the 8760 hourly building loads that would be generated by a building energy analysis program. Several of the tools [Hellström and Sanner 1994; Spitler 2000] rely on a representation of the loads as monthly total cooling and heating loads, upon which monthly peak cooling and heating loads are superimposed. The monthly peak loads are specified as a rectangular pulse with the magnitude and duration. Users have been expected to exercise engineering judgment in order to determine the peak pulse magnitude and duration. The degree to which this expectation is met in practice is questionable, and the purpose of this chapter is to propose a methodology for obtaining the simplified load representation and to validate this methodology against detailed hourly simulations. Adoption of this methodology will allow improved design of ground heat exchangers.

3.1.1 Design Tools

The first ground heat exchanger (GHE) design tools date back to work done by Eskilson [1987]. For a single borehole, Eskilson used a transient two-dimensional finite difference method in radial-axial coordinates to determine the temperature field surrounding the borehole as a function of time. For multiple borehole configurations, Eskilson used superposition to determine the effect of multiple boreholes on one another when each borehole is at the same temperature. These results are then used to create a single non-dimensional temperature response to a step input, called a g-function, for the specific configuration (including layout, spacing, and the ratio of borehole radius to borehole

depth). These g-functions are represented as a set of discrete points relating the non-dimensionalized temperature response to dimensionless time. Eskilson integrated this work into several small design tools, which could, for example, determine the minimum or maximum temperature in a borehole system, or use these minimum and maximum temperatures with the heat rejection and extraction rates to determine a suitable size for the boreholes.

Further revisions upon Eskilson's tools were made by Hellström and Sanner [1994]. The original version of their program sought to combine some of Eskilson's tools into one larger program that could be used for the design of a GSHP system. In this tool, loads were represented as a set of twelve monthly average heat extractions or injections, plus a single peak pulse applied in the month with the highest heating or cooling load. Later updates to this program improved some accuracy concerns [Hellström et al. 1997; Knoblich 1997], and the most recent version has slightly changed the way that loads are represented [Hellström and Sanner 2000]. Now, the loads can be represented either as annual totals with monthly percentage distributions, or as monthly averages. Peak loads can either be generated from a seasonal performance factor, or input directly. The peak loads are approximated as square pulses lasting for a specified duration, and it is assumed that the energy content of the peak pulse has no effect on the long-term behavior of the system; in other words, the peak load is solely used to determine the monthly extreme temperature. No guidance is given as to how users should choose the duration of the peak pulse.

A similar approach is also used independently in another design tool [Marshall and Spitler 1994; Spitler 2000]. Again, Eskilson's response factor methods are utilized so that a wide variety of borehole systems may be simulated. Users input building heating and cooling loads and the corresponding rates of heat extraction from and heat rejection to the ground are computed using an equation-fit heat pump model. The square pulse approximation for peak loads is used in this tool as well; the temperature change due to the peak load is computed via a simple analytic expression. A default peak load duration was suggested based on the short time response of several cases, but the selection of this value was otherwise left to the user's engineering judgment.

Another approach, originally developed by Kavanaugh [1992], is that of Kavanaugh and Rafferty [1997], which also appears in the ASHRAE HVAC Applications Handbook [2007]. This method is based on the analytic solution of the temperature of a buried cylinder which may be used to determine effective ground thermal resistances for annual, monthly, or daily heat pulses. Loads are represented as a combination of an annual heat transfer rate to the ground, an average monthly heat transfer rate during the peak heating and cooling months and a maximum heat transfer rate for a short period of time during the design day. The duration of the maximum heat transfer rate is stated as possibly being as short as one hour, though four hours is recommended. The basis for the recommendation is not stated. There are two key differences between this approach and the others described in this section:

1. For this approach, the model has been formulated to solve for a length that will meet the peak cooling load and a length that will meet the peak heating load

without exceeding the user-specified temperature limits. The other approaches iteratively adjust the ground heat exchanger length in order not to exceed the user-specified temperature limits.

2. For this approach, rather than simulate a multi-year period of operation, heat exchanger lengths are determined for a single year, but a temperature penalty is introduced for borehole-to-borehole interference resulting in long-term heat build-up (or draw-down) in the borefield. The temperature penalties are tabulated for several combinations of load profile, borehole separation and borehole grid pattern.

A recently developed design tool [Katsura et al. 2006; Nagano et al. 2006] utilizes approximations to the cylinder-source approach and is claimed to be capable of treating interaction between arbitrarily-configured boreholes, including systems where not every borehole is identical, as long as the boreholes are far enough apart. The temperature response of the ground loop as a whole is then determined with a flow rate weighted average of the responses from the individual boreholes. Unlike the other design tools described above, this tool utilizes hourly loads. The authors quote a computation time of 40 seconds on a notebook computer for a two-year simulation with an unspecified number of boreholes. Because ground heat exchanger designs are often made for periods of 20 years or longer, the actual time for a design simulation may be somewhat longer. When combined with the iteration required to size the ground heat exchanger, it is anticipated that the computation time for an actual design could be unacceptable for many users. However, because the authors do not give computation times for real-world

design problems, it is difficult to reach a judgment on this matter. Certainly, it may be expected that as computers get faster, the iterative use of hourly simulations for ground heat exchanger designs will become increasingly more practical.

3.1.2 Required Design Inputs

Since every GSHP design tool utilizes a simulation of the ground loop heat exchanger, it is necessary for the user to specify the ground thermal properties, borehole completion method and loads on the ground heat exchanger or loads on the system heat pumps. Among the necessary inputs are:

- Soil thermal conductivity—Can be found through several different methods, including laboratory analysis [Stolpe 1970; Mitchell and Kao 1978], use of a thermal probe [Hooper and Chang 1953; Falvey 1968; Mitchell and Kao 1978], classification by soil type [Bose 1988; Bose 1989], and in-situ testing [Austin 1998; Austin et al. 2000; Witte et al. 2002; Sanner et al. 2005].
- Undisturbed ground temperature—Can either be measured or reasonably estimated [Gehlin and Hellström 2003; Signorelli and Kohl 2004].
- Other soil thermal properties—Typically found from tabulated reference. Further research into accurate in situ measurement of properties such as specific heat and density is needed.
- Fluid thermal properties—Can be computed from empirical equation fits based on mixture concentration and temperature [Melinder 1999; Khan 2004].
- Pipe and grout thermal properties—Generally available from the manufacturer.

- Heat pump description—Some representation of the performance of the heat pump is necessary. This can be done, for example, by using equation fits of heat extracted or rejected and power consumed versus the input heating or cooling load.
- Heat pump loads—A representation of the loads is obviously needed. In applications such as this, the loads are commonly computed on an hourly basis, and obviously vary continuously over the operation of the system. How, then, should heating and cooling loads be represented for the best results when using a design tool?

3.1.3 Representation of Loads

All of the design procedures, whether based on a detailed simulation or a model formulated to solve for design length, require some representation of the heating and cooling loads over the life of the system. Generally, these would be computed with a building simulation program or building energy analysis program, which would give the results for a typical meteorological year as a series of 8760 hourly loads. In lieu of knowing the actual future weather, this sequence, applied on a recurring basis for ten, twenty, or more years, is used as an estimate of future loads.

However, with the exception of the work described by Katsura et al. [2006] and Nagano et al. [2006], the building heating and cooling loads are aggregated in a manner that allows many fewer time intervals or time steps to be analyzed. In the case of Kavanaugh

and Rafferty [1997], there will be a total of five time intervals utilized: a one year period, two one-month periods, and two short intervals, on the order of one to four hours. In the case of the methods reported by Hellström and Sanner [1994] and Spitler [2000], thirty-six time intervals are used: twelve monthly periods and twenty-four short intervals representing monthly peak heating and cooling loads. In either case, the combination of longer intervals and short time intervals is supposed to be an approximate representation of the actual building heating and cooling loads, as illustrated in Figures 3-1 and 3-2. Figure 3-1 shows one year's worth of hourly heating and cooling loads for an office building in Albuquerque, with the convention that the heating loads are shown as positive and the cooling loads are shown as negative.

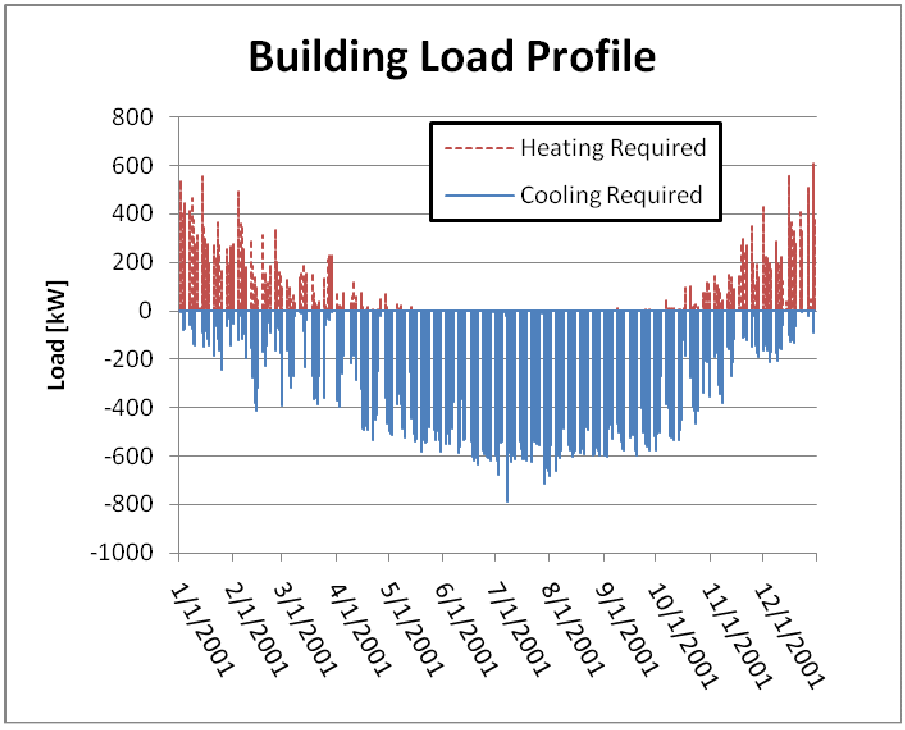

Figure 3-1: Albuquerque office building annual load profile

Figure 3-2 shows two days worth of hourly cooling loads (now with the convention that the cooling loads are positive) for the day containing the annual peak cooling load and the previous day. Also shown is the approximate load profile made up by combining the monthly average load and the monthly peak load. There are obviously several differences; first, the thermostatic setback control drops the actual load to zero for almost the entirety of the first of the two days shown, while the approximate profile assumes a constant base load over the month equivalent to the average hourly load for the month. Secondly, the rectangular pulse shape of the peak load in the approximate profile is markedly different from the shape of the actual hourly load profile. The magnitude and duration of the peak profile may be adjusted, but it will never exactly match the actual peak load profile. The choice of magnitude and duration that best represents the actual peak load profile is the subject of this work.

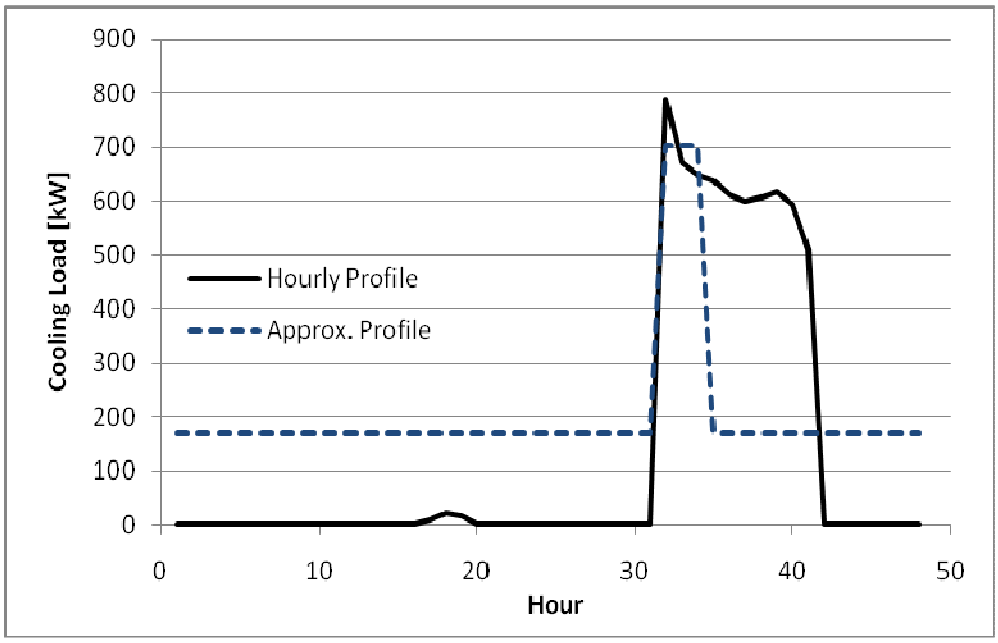

Figure 3-2: Albuquerque office building – two days containing annual peak cooling load

Users of design tools are expected to use a building simulation or building energy analysis program to find the average monthly loads and peak loads. With hourly values for all heating and cooling loads, the average monthly loads can be readily determined. However, little or no guidance has been given as to how the user should select the peak load and, particularly, the peak load duration. Figure 3-3 shows two days of hourly cooling loads, containing the annual peak cooling load, for an office building located in Baltimore, MD. From the shape of the load profile, a peak load duration of a single hour seems reasonable; indeed, this is a good approximation for this case, as designing the ground heat exchanger via a monthly simulation with this peak duration yields a total ground loop length within 5% of that found by using an hourly simulation. Here, relying on engineering judgment to determine the peak load and peak load duration appears feasible, although the accuracy of the user's approach without additional guidance may still be low.

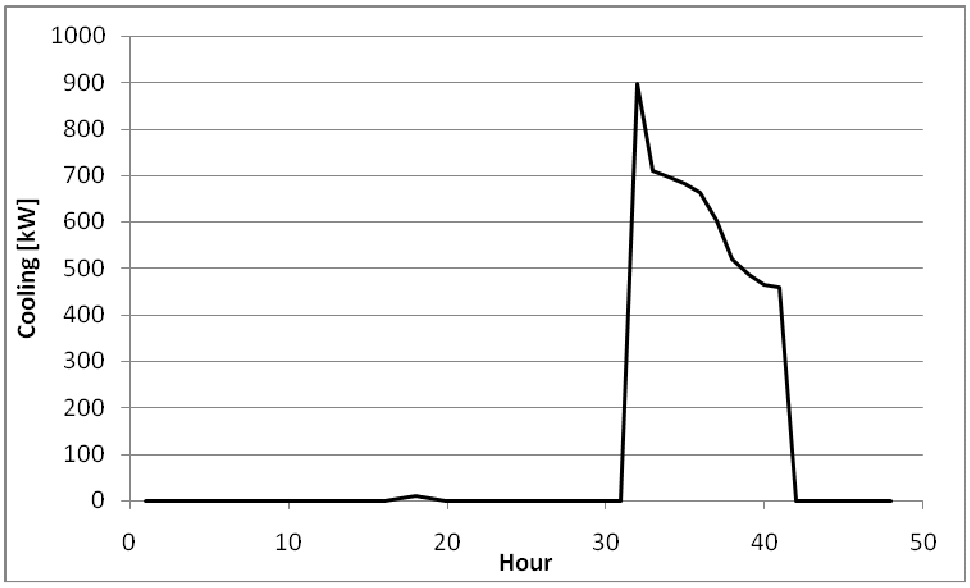

Figure 3-3: Office building in Baltimore, MD – two days containing annual peak cooling load

Figure 3-4 shows two days of hourly cooling loads, containing the annual peak cooling load, for a hotel located in Memphis, Tennessee. Here, the lack of a clear, distinct peak complicates the selection of the peak load and peak load duration. Should the user choose the absolute maximum peak occurring at hour 41 with a duration of one hour, or should that peak be applied over more than one hour? Furthermore, if a multi-hour peak is selected, should the value of the peak load be taken as the maximum, or should it be an average value over the duration? At best, it seems that it would be difficult for a typical user of a ground heat exchanger design program to apply engineering judgment to this problem and come up with a reasonable representation of the loads.

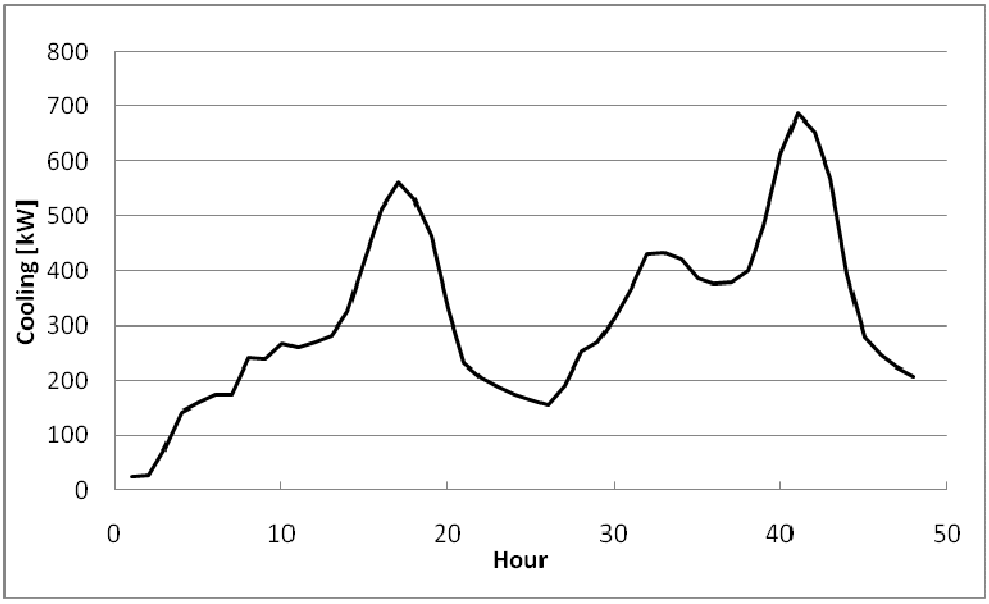

Figure 3-4: Hotel building in Memphis, TN – two days containing annual peak cooling load

Furthermore, as shown by Young [2004], the design of ground heat exchangers can be quite sensitive to the peak load. Consider the case of the motel in Memphis, loads for which are shown in Figure 3-4. This site uses a 225 borehole ground heat exchanger arranged in a 15-by-15 square, and the heat pump entering fluid temperature constraints

were set at 40°C and 5°C. Using the absolute maximum peak cooling load and applying it for one hour results in a borehole depth of 85m per borehole; however, applying the peak load for three hours increases the required size to 94m. This is an increase of more than ten percent, which will obviously result in a noticeable increase in the cost of the system. Further increasing the peak load duration will cause further oversizing. If instead the peak cooling load were to be averaged over the three-hour period containing the maximum load, the required borehole depth would be 90.5m. Without performing an hourly simulation to better determine the behavior of the system, it is not possible to say which of these three options are the best, or if another option is better than any of the three.

To summarize, in some cases it may be possible for users to make a reasonable representation of the peak load and peak load duration based on the daily load profiles, but for some combinations of buildings and locations, this is not possible. Because the design of the ground heat exchanger can be quite sensitive to the representation of the peak load, a procedure for determining an acceptable peak load magnitude and duration would be quite useful, both in reducing the requirement for subjective judgments in the design process and in improving the accuracy of the design procedure. This chapter proposes such a method and verifies the accuracy of the method against detailed hourly simulations.

3.2 Proposed Methodology

In this section, a proposed methodology for choosing an appropriate peak load magnitude and duration is set forth. The proposed methodology takes advantage of the linear nature of the governing partial differential equations, which allow superposition of the temperature responses to heat inputs. More specifically, while the actual fluid temperature leaving the ground heat exchanger at a certain point in time strongly depends on the history of heat rejection and extraction over the duration of operation, the temperature rise over the day is mainly dependent on the heat rejection and extraction over the day. The heat rejection and extraction of the day before will have a slight influence on temperature rise over the day. The heat rejection and extraction from two days before, three days before, etc. will have a rapidly diminishing influence.

Therefore, it is possible to find the day on which the peak load occurs, run an hourly simulation for a one or two day period, find the resulting temperature rise over the day, and compare this to the resulting temperature rise due to a rectangular pulse. The magnitude and duration of the rectangular pulse can then be adjusted to match the temperature rise of the peak load day. Once the "best-fit" magnitude and duration are determined, they can be used as part of the design simulation, where the entire history over twenty or more years of operation will be utilized.

The primary advantage of this approach is that the one- or two-day hourly simulation can be performed very quickly, much faster than, say, a twenty-year hourly simulation. In

turn, this maximizes the accuracy of the simulations utilized for design, with twelve monthly and twenty-four short intervals per year. These simulations also run much faster than a twenty-year hourly simulation. The primary disadvantage is a minimal loss of accuracy when compared to running a twenty-year hourly simulation.

With this introduction, each step will be discussed briefly below, along with the assumptions involved.

3.2.1 Peak Day Determination

The days with the annual peak cooling load and annual peak heating load can be readily identified with a simple algorithm. To be clear, though, these are not necessarily the days on which the peak heat pump entering fluid temperatures are encountered. For example, it is possible that the peak cooling load occurs on a day in August, while the peak entering fluid temperature may not occur until a hot day in late September. This will depend on the entire history of operation. If the load profile on the peak load day is similar to the load profile on the peak temperature day, though, this will be a good approximation. This will often be the case for many buildings, as a peak entering fluid temperature day is likely to be similar to a peak cooling load day in terms of occupancy and other internal heat gains, solar irradiation, etc.

3.2.2 Construction of Rectangular Pulses

The peak loads are approximated as square heat pulses. While, in theory, any combination of magnitude and duration that gives an equivalent temperature response to

the actual load profile might be used, an approach that remains as close as possible to the actual load profile is probably preferred. Therefore, two different ways of constructing these square pulses were explored, which were termed “average over duration” and “maximum during duration”. “Average over duration” uses the specified duration that has the highest average load over that duration, which by necessity will include the maximum load for the day (and thus the year as well). The use of the averaging method for the same cooling design day as before is shown in Figure 3-5. In contrast with the averaging method, “Maximum during duration” uses the absolute maximum load and applies it every hour for the specified duration. If an approximated profile using the maximum method were to be plotted in Figure 3-5, it would be seen as a horizontal line extending to the right from the maximum value of the cooling load.

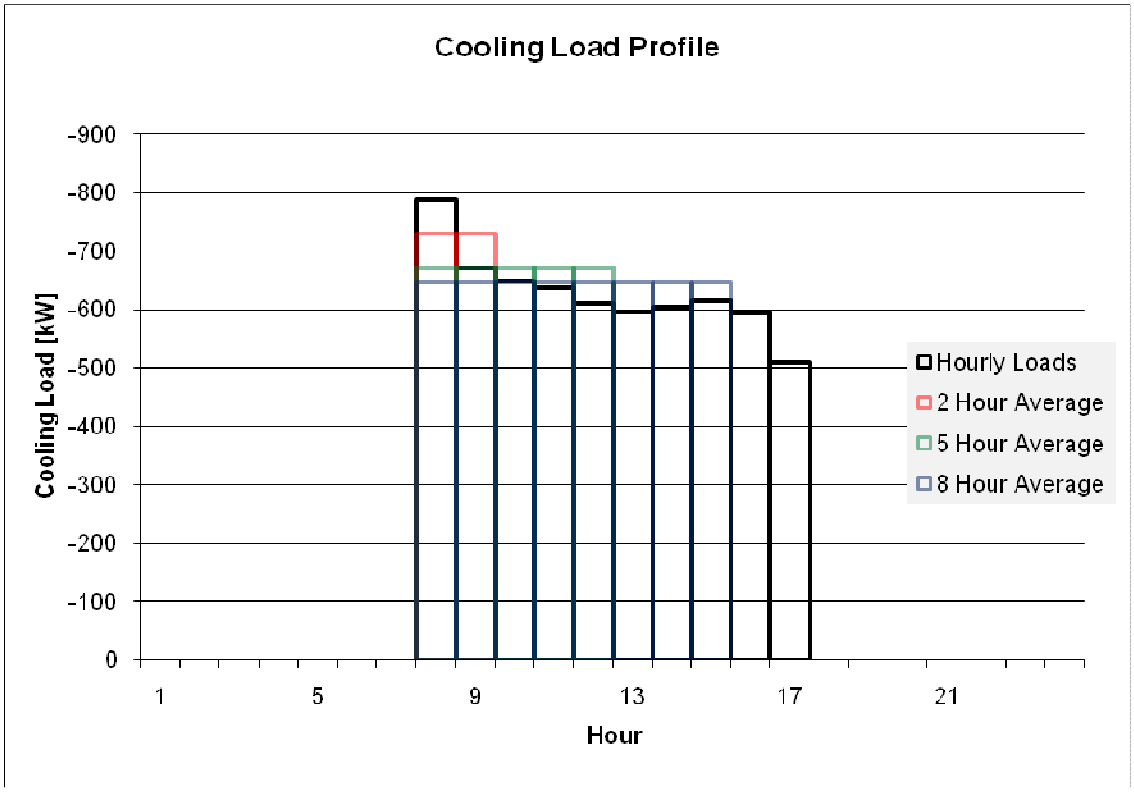

Figure 3-5: Cooling design day with several possible peak approximations

3.2.3 Computation of the Temperature Response for Selection of Peak Load Magnitude and Duration

With the two sets of loads for the heating and cooling peak days—the actual hourly loads as well as the peak approximations—the temperature responses may be computed using the short time step approach described by Xu and Spitler [2006]. This is a one-dimensional finite volume method; the volumes representing the borehole are chosen so that the borehole resistance, computed with the multipole method, is correctly maintained. Likewise, the thermal mass of the fluid and grout is also carefully conserved. However, the distribution of thermal mass and resistances among the individual volumes is necessarily an approximation. As shown by Xu [2007], the short-time response matches a detailed two-dimensional model quite closely.

The computation of the temperature response was first implemented in a spreadsheet, independent of any ground heat exchanger design tool. In the interest of avoiding redundant user inputs, it is useful to know which borehole parameters have a significant effect on the analysis. Initially, characteristic values representative of a typical system were selected, and a parametric study was performed to determine the effect of varying each parameter on the end choice of optimum peak duration. It was found that no single parameter had a significant effect on the choice of peak duration. Of the parameters, only the thermal mass of the fluid, which is denoted by the fluid factor [Xu and Spitler 2006], and, to a lesser degree, the thermal resistance of the borehole, had any noticeable effect of the nondimensionalized temperature response, and this effect was only on the order of a

couple percent, at most. Therefore, it is really only necessary to read the 8760 hourly cooling and heating loads into the spreadsheet; it is not necessary to input the shank spacing, borehole diameter, grout and soil thermal conductivities, etc.

In order to simplify interpretation of the results, it is convenient to plot the temperature response of both the actual daily load profile and the rectangular profile in non-dimensional form, as shown in Figure 3-6. Temperatures are nondimensionalized by dividing the temperature change at any individual hour by the maximum temperature change during the simulation with the actual load profile. This leads to a desired value of 1 when attempting to find the most suitable magnitude and duration. Nondimensionalizing the temperature in this way is done because the temperature *change*, and not the true value of the temperature, is desired; thus, the far history and undisturbed ground temperature are unneeded at this step.

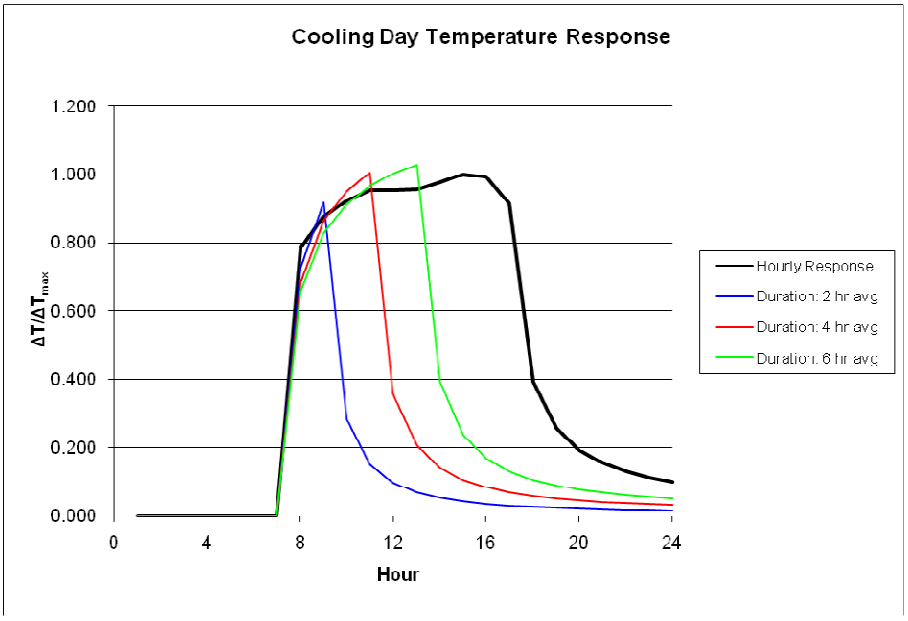

Figure 3-6: Sample hourly temperature response for actual and rectangular load profiles

At present, the user interface allows the user to choose between the "average over duration" and "maximum during duration" magnitudes and then three candidate durations. This may be repeated iteratively until the best fit is found. This procedure could, and perhaps should eventually, be automated. By doing this manually, some insight into the physics of the design may be developed. Whether or not this benefit outweighs the time savings to be had in automating the calculation is an open question.

As a final step, once the desired method and duration are known, the peak heating and cooling loads for every month are determined using the method selected by the user, except this time using only the loads for each month instead of the entire year. As discussed above, since the peak entering fluid temperature may not occur on the same day or in the same month as the peak load, the choice of magnitude using the user's selected approach and duration is an approximation.

3.2.4 Computation of the Temperature Response within the Design Simulation

Once the peak magnitudes and durations have been established, the design simulation can be run. A fuller description of the simulation can be found in Xu and Spitler [2006]; the design tool is described by Spitler [2000]. A brief description follows.

The temperature response for the full and approximated load profiles is obtained by the application of the short time step g-functions. The g-function approach determines the temperature response to a series of step heat pulses, as given for the n^{th} time period by

$$T_{borehole} = T_{ground} + \sum_{i=1}^{n} \frac{Q_i - Q_{i-1}}{2\pi k} \cdot g\left(\frac{t_n - t_{i-1}}{t_s}, \frac{r_b}{H}\right) \quad (3\text{-}1)$$

Where $T_{borehole}$ is the average temperature of the wall of the borehole, in °C;

T_{ground} is the undisturbed ground temperatures, in °C;

Q is an individual step heat pulse, in W/m;

k is the ground thermal conductivity, in W/m-K;

t_i is the time at the end of the i^{th} time period, in s;

t_s is the time scale $H^2/9\alpha$, in s;

r_b is the borehole radius, in m; and

H is the borehole depth, in m.

The values of the g-functions are computed based on the approach of Xu and Spitler [2006], in which a one-dimensional numerical model is used to determine a set of discrete values for the g-function at short time steps. This 1-D model uses a detailed computation of the borehole thermal resistance, variable convective resistance, and consideration of the thermal mass of the fluid in the borehole to find g-function values for time steps of less than one hour.

When the simulation is run in the design tool, an "average" fluid temperature for the entire month is computed based on the applying the total heating and cooling loads for the month as a fixed value. This temperature is not the average over the month, but rather the temperature at the end of the month if the monthly load were applied as an

average value over the month. It might also be thought of as, approximately, the average entering fluid temperature for the last day of the month. The maximum and minimum temperatures for each month are determined by superimposing the temperature response of the peak loads on this end-of-month temperature. For each month, the peak temperatures are computed with the equation

$$T_{fluid,peak} = T_{fluid,avg} - \frac{Q_{rej,peak}}{H \cdot NB}\left(R_b + R_q\right) \quad (3\text{-}2)$$

Where:

$T_{fluid,peak}$ is the end-of-the-month peak fluid temperature in the ground loop at the end of the month, averaged over the U-tube, in °C;

$T_{fluid,avg}$ is the average monthly fluid temperature in the ground loop, in °C;

$Q_{rej,peak}$ is the peak heat rejection rate due to the peak load pulse, in W;

NB is the total number of boreholes in the ground loop;

R_b is the thermal resistance of the borehole, in m-K/W;

and R_q is the thermal resistance term due to the duration of the peak load, in m-K/W.

The peak heat rejection rate $Q_{rej,peak}$ is determined by dividing the peak load by the presumed COP of the heat pump, then subtracting the monthly average heat rejection component. Since the COP is a second order equation fit of the entering fluid temperature specific to the heat pump being used, and this is a value that is being determined, determining the temperature response to the peak load requires some iteration.

The thermal resistance due to the peak load duration, R_q, is given by

$$R_q = \frac{g\left(\frac{t}{t_s}, \frac{r_b}{H}\right)}{2\pi k} \tag{3-3}$$

Where:

g is the short time step g-function value for the peak load;

t is the duration of the peak load, in s;

and other variables are as described earlier.

With the peak temperature in the borehole fluid known, the temperature exiting the ground loop heat exchanger and entering the heat pump—the location for which design temperature limits are provided for the system design—is determined by performing a simple $Q = \dot{m} c_p \Delta T$ computation. This is done assuming that the temperature change between the borehole inlet and borehole exit (presumed to be equivalent to the heat pump inlet) is linear.

Placing the peak load at the end of the month is an assumption that can cause the simulation to over predict or under predict the temperature response. If, for example, the monthly peak cooling load for a month late in the cooling season—when the average cooling load is reduced significantly from the previous month—occurs at the beginning of the month, it will cause higher peak temperatures than if it occurs at the end of the month. The assumption that it occurs at the end of the month will thus tend to yield lower peak temperatures; if that month is the peak temperature month, the resulting

ground heat exchanger size will be smaller than needed to meet the temperature limit. In other months, the effect may be the opposite.

The advantage of assuming that the peak load occurs at the end of the month is in avoiding excess input in a design tool. This seems like an acceptable tradeoff for a small loss in accuracy. The actual impact of this approximation will be quantified later in the chapter.

3.3 Validation

The proposed methodology was used to size ground loop heat exchangers for an office building, school, and hotel complex in multiple different locations. In order to validate the methodology, the results were then compared to hourly simulations. For each combination of building and location, a monthly simulation, using the proposed peak load methodology, was performed in order to find the GLHE length that allowed specified heat pump entering fluid temperature constraints to be met. Then, using the hourly simulation, the actual heat pump entering fluid temperature extremes were found; by iteratively adjusting the ground loop size for the hourly simulation, a percent error was determined for each case, representing the difference in ground loop sizes between the hourly and monthly simulations.

3.3.1 Validation Background

The results of the peak load analysis procedure were validated using an hourly simulation to confirm the results of the approximated loads in a monthly simulation. The hourly simulations were performed using the HVACSIM+ modular simulation environment [Clark 1985], with the Visual Tool graphical user interface [Varanasi 2002]. The system in HVACSIM+ consists of a ground loop heat exchanger model and a simple heat pump model. The ground loop heat exchanger model uses the g-function approach originated by Eskilson [1987], and consists of both long time step and short time step values [Xu and Spitler 2006]. This model was validated based on twelve months of experimental data obtained at the Oklahoma State University hybrid ground source heat pump research facility [Gentry et al. 2006; Xu 2007]. The test facility uses three vertical boreholes, each approximately 250 feet deep. The complete design of the hybrid ground source heat pump test facility is discussed in more detail by Hern [2002].

Additionally, the HVACSIM+ simulation utilizes a simple equation-fit heat pump model [Tang 2005]. The coefficients for the model as used in this work were based on catalogue values for the heat pump brand and model used in the test facility; they were modified very slightly so that the heat pump model became a simple first-order, constant coefficient (i.e., fixed COP) model. The COPs were approximately 3 in heating and 5 in cooling. This simplification allowed the results to be spot-checked quickly and easily to ensure that the outcomes of the simulation were sensible.

The monthly simulations, and subsequent ground loop sizing, were performed using the ground heat exchanger design tool GLHEPRO [Spitler 2000], which was presented in Chapter 2. This tool utilizes the same approach to simulate the ground loop as the HVACSIM+ model; in fact, the coding is much the same, except with a monthly time step instead of an hourly time step. In addition to the ground loop heat exchanger model, the tool includes the capability to specify a heat pump by its basic heating and cooling coefficients, again much the same as HVACSIM+. One of the main advantages of the monthly simulation tool is the capability to determine, via iterative simulation, a suitable ground loop length so that specified entering fluid temperature bounds to the heat pump are not exceeded.

3.3.2 Building Descriptions

The peak load approximation was used for three different buildings, each in a variety of locations. The first building is a three-story office building, 48.8m (160 ft) in each of the plan dimensions and 9.1 m (30 ft) tall. The second building is a school building consisting of multiple classrooms and several larger common areas, such as a cafeteria. The third and final building is a hotel complex consisting of three identical buildings, each 10 stories (about 24.4m or 80ft) tall and approximately 50.3m (165 ft) by 18.3m (60 ft) in the plan dimensions. For each combination of building and location, the heating and cooling loads for every hour of the year were found by simulating the building in the EnergyPlus program [DOE 2007].

The basic ground loop designs for both the office and motel buildings were quite similar. As a starting point, the system contains 144 vertical boreholes, arranged in a 12-by-12 grid, with the boreholes 7.62m (25ft) apart. The boreholes themselves are 128 mm in diameter, and use 1" Schedule 40 pipe. Typical ground and grout thermal properties were assumed (k_{ground} = 3.50 W/m-K, $(\rho c_p)_{ground}$ = 2160 kJ/m^3-K; k_{grout} = 0.744 W/m-K, $(\rho c_p)_{ground}$ = 3900 kJ/m^3-K), with the undisturbed ground temperature varying by location. The operating fluid was a 20% solution of ethylene glycol, with a total flow rate of 57.6 L/s for the office building and 250 L/s for the hotel complex; this value varies due to the differences in the total loads between the buildings. The initial design limits on the entering fluid temperature of the heat pump were set at 35°C and 5°C. After sizing the system using this initial configuration, modifications were made so that the individual borehole depth would be between around 80m. The number of boreholes was increased or decreased as needed, with the goal of keeping a square or near-square borefield configuration. In addition, for some of the more extreme climates (e.g. Houston, Miami), there was not enough difference between the undisturbed ground temperature and the constraining heat pump EFT limit to assure a reasonable number of boreholes. Thus, an approximate temperature differential of 20°C (cooling) or 10°C (heating) between the undisturbed ground temperature and the heat pump entering temperature design limit was desired, and the heat pump EFT limits were modified as needed to maintain this temperature differential.

The ground loop design for the school building is like those for the office and hotel buildings, but on a slightly smaller scale. As the school is much smaller, comparatively,

than either of the other buildings, fewer boreholes will be needed. The flow rate through the entire system was set at 20 L/s, regardless of other system characteristics; the fluid is the same 20% ethylene glycol solution. Again, the target borehole length was 80m, so the number of boreholes was adjusted for each location to generate a ground loop near this value. Also, the heat pump design constraints were occasionally adjusted, as before, to prevent the borehole depth from becoming too large.

3.4 Results and Sources of Error

For each case, the ground loop was sized using GLHEPRO with the monthly load profile using the peak load approximation that has been developed. Then, the ground loop parameters were imported into HVACSIM+, and an annual hourly simulation was run iteratively to determine the borehole length required to just reach, but not exceed, the heat pump entering fluid temperature limitations. Thus, a percent difference in the borehole length, representing the amount of oversizing by the monthly simulation as compared to the hourly simulation, can be computed. For the office, school, and motel buildings described above, results are summarized in Tables 3-1 through 3-3, respectively. For each location, the undisturbed ground temperature is listed, as well as the maximum (T_{max}) and minimum (T_{min}) EFT limits on the heat pump, which are used to size the ground loop. For the dominant mode (heating or cooling), the temperature differential between the heat pump EFT limit corresponding to the dominant mode and the undisturbed ground temperature is also listed; this gives a rough idea of the amount of heat that can be rejected or extracted from the ground. Next are the number of boreholes

in the ground loop, and the length per borehole as determined by the monthly simulation design tool. The HVACSIM+ maximum or minimum temperature, depending on the dominant mode, is the extreme temperature found by performing an hourly simulation using the borefield designed by the monthly simulation. The "ΔT exceeded" is the temperature differential between the extreme temperature found by the hourly simulation and the respective heat pump EFT constraint; a negative value signifies that the system is oversized, since the detailed simulation never reaches the limits imposed on the heat pump EFT. Finally, the HVACSIM+ design length is the length required to just meet, but not exceed, the design constraints on the heat pump EFT from the hourly simulation, while the "% Oversized" is the difference between the hourly and monthly design lengths, which shows by how much the monthly simulation oversizes that system.

To improve the accuracy of the nondimensionalized temperature response, an additional day of load data was added into the simulation, using the day before the peak load occurs. This was done because, using only 24 hours of loads, the square wave pulse was occasionally not coming sufficiently close to the hourly profile to obtain the most accurate results. In several cases, such as the Baltimore office building and some of the school cases, this made the peak response due to the square wave closer to that of the full hourly profile. In cases such as this, the effect is a reduction in the oversizing by 1-2% (e.g., from 7% oversized to 5%). For other cases, the day prior to the peak load day has very little load, and so considering this day in the simulation has a miniscule effect, not resulting in a change of selection for the peak magnitude and/or duration. Since the

computation time added by considering the second day is trivial, the additional day is used in all the results shown in Tables 3-1 through 3-3.

Table 3-1: Office building results comparison

Location	Undisturbed Ground Temp. [℃]	T_{max} [℃]	T_{min} [℃]	Dominant mode	ΔT_{clg} [℃]	ΔT_{htg} [℃]	# of BHs	GLHEPRO Design Length [m]	HVACSIM+ T_{max} [℃]	HVACSIM+ T_{min} [℃]	ΔT exceeded [℃]	HVACSIM+ Design Length [m]	% Oversized
Albuquerque	12.22	35	5	Cooling	22.78	---	10x16	91.65	34.81	---	-0.19	91.15	0.5%
Baltimore	13.89	35	5	Cooling	21.11	---	12x13	88.98	33.49	---	-1.51	84.73	5.0%
Boise	11.11	35	5	Heating	---	6.11	12x13	88.78	---	5.21	-0.21	86.37	2.8%
Burlington	7.78	35	0	Heating	---	7.78	12x13	85.37	---	0.44	-0.44	81.36	4.9%
Chicago	11.11	35	0	Cooling	23.89	---	11x12	75.79	35.15	---	0.15	76.79	-1.3%
Duluth	5.00	35	-5	Heating	---	10.00	12x12	81.43	---	-4.76	-0.24	79.87	2.0%
El Paso	18.33	40	5	Cooling	21.67	---	13x13	85.89	39.52	---	-0.48	84.64	1.5%
Fairbanks	2.78	35	-5	Heating	---	7.78	16x16	89.68	---	-3.34	-1.66	83.41	7.5%
Helena	7.78	35	0	Heating	---	7.78	10x11	84.68	---	0.59	-0.59	78.70	7.6%
Houston	23.33	45	5	Cooling	21.67	---	12x12	83.92	43.55	---	-1.45	81.44	3.0%
Memphis	17.22	40	5	Cooling	22.78	---	13x14	87.76	39.09	---	-0.91	85.54	2.6%
Miami	25.56	45	5	Cooling	19.44	---	12x12	80.46	44.80	---	-0.20	79.88	0.7%
Phoenix	20.00	45	5	Cooling	25.00	---	13x14	86.74	44.32	---	-0.68	85.17	1.8%
Salem	11.67	35	5	Cooling	23.33	---	11x11	84.45	34.30	---	-0.70	81.64	3.4%
San Francisco	15.00	35	0	Cooling	20.00	---	12x12	81.27	34.52	---	-0.48	79.53	2.2%
Tulsa	16.67	40	5	Cooling	23.33	---	12x13	86.10	39.44	---	-0.56	84.73	1.6%
												Average	2.9%

Table 3-2: School building comparison results

Location	Undisturbed Ground Temp. [℃]	T_{max} [℃]	T_{min} [℃]	Dominant mode	ΔT_{clg} [℃]	ΔT_{htg} [℃]	# of BHs	GLHEPRO Design Length [m]	HVACSIM+ T_{max} [℃]	HVACSIM+ T_{min} [℃]	ΔT exceeded [℃]	HVACSIM+ Design Length [m]	% Oversized
Albuquerque	12.22	35	0	Heating	---	12.22	6x7	83.53	---	1.11	-1.11	76.68	8.9%
Baltimore	13.89	35	0	Heating	---	13.89	7x7	83.95	---	1.16	-1.16	77.60	8.2%
Boise	11.11	35	0	Heating	---	11.11	6x10	81.04	---	0.89	-0.89	75.26	7.7%
Burlington	7.78	35	-5	Heating	---	12.78	6x10	88.60	---	-4.19	-0.81	84.38	5.0%
Chicago	11.11	35	0	Heating	---	11.11	8x8	85.75	---	0.67	-0.67	81.85	4.8%
Duluth	5.00	35	-5	Heating	---	10.00	9x9	86.00	---	-4.39	-0.61	81.16	6.0%
El Paso	18.33	35	0	Cooling	16.67	---	6x6	76.39	33.52	---	-1.48	70.21	8.8%
Fairbanks	2.78	35	-5	Heating	---	7.78	10x12	83.40	---	-4.74	-0.26	80.80	3.2%
Helena	7.78	35	-5	Heating	---	12.78	8x8	81.60	---	-4.45	-0.55	78.74	3.6%
Houston	23.33	40	0	Cooling	16.67	---	5x6	75.70	38.17	---	-1.83	67.92	11.5%
Memphis	17.22	35	0	Heating	---	17.22	5x7	76.57	---	1.62	-1.62	70.00	9.4%
Miami	25.56	40	0	Cooling	14.44	---	6x7	76.69	38.75	---	-1.25	69.50	10.3%
Phoenix	20.00	35	0	Cooling	15.00	---	7x8	87.11	33.22	---	-1.78	77.00	13.1%
Salem	11.67	35	0	Heating	---	11.67	7x8	80.63	---	0.85	-0.85	75.24	7.2%
San Francisco	15.00	35	0	Heating	---	15.00	5x8	76.73	---	0.96	-0.96	72.28	6.2%
Tulsa	16.67	35	0	Heating	---	16.67	6x6	79.57	---	1.67	-1.67	72.40	9.9%
												Average	7.7%

Table 3-3: Hotel complex results comparison

Location	Undisturbed Ground Temp. [℃]	T_{max} [℃]	T_{min} [℃]	Dominant mode	ΔT_{clg} [℃]	ΔT_{htg} [℃]	# of BHs	GLHEPRO Design Length [m]	HVACSIM+ T_{max} [℃]	HVACSIM+ T_{min} [℃]	ΔT exceeded [℃]	HVACSIM+ Design Length [m]	% Oversized
Albuquerque	12.22	40	0	Cooling	27.78	---	14x14	72.83	38.72	---	-1.28	70.33	3.6%
Baltimore	13.89	40	0	Cooling	26.11	---	12x13	81.69	37.56	---	-2.44	72.81	12.2%
Boise	11.11	40	0	Cooling	28.89	---	12x13	76.54	37.29	---	-2.71	69.34	10.4%
Burlington	7.78	35	0	Heating	---	7.78	13x13	83.47	---	0.17	-0.17	81.73	2.1%
Chicago	11.11	35	0	Heating	---	11.11	11x11	80.25	---	0.59	-0.59	75.82	5.8%
Duluth	5.00	35	-5	Heating	---	10.00	14x14	86.65	---	-4.56	-0.44	82.50	5.0%
El Paso	18.33	45	0	Cooling	26.67	---	14x14	84.51	42.54	---	-2.46	76.06	11.1%
Fairbanks	2.78	35	-7	Heating	---	9.78	18x18	82.70	---	-6.22	-0.78	75.95	8.9%
Helena	7.78	35	-5	Heating	---	12.78	11x12	75.23	---	-3.79	-1.21	68.15	10.4%
Houston	23.33	45	0	Cooling	21.67	---	15x16	77.61	42.78	---	-2.22	67.78	14.5%
Memphis	17.22	40	0	Cooling	22.78	---	14x14	83.62	37.93	---	-2.07	76.00	10.0%
Miami	25.56	45	0	Cooling	19.44	---	15x16	80.15	43.32	---	-1.68	73.19	9.5%
Phoenix	20.00	45	0	Cooling	25.00	---	15x16	79.36	42.81	---	-2.19	72.21	9.9%
Salem	11.67	35	0	Cooling	23.33	---	12x12	84.38	32.85	---	-2.15	76.87	9.8%
San Francisco	15.00	40	0	Cooling	25.00	---	11x12	82.79	37.67	---	-2.33	73.56	12.5%
Tulsa	16.67	40	0	Cooling	23.33	---	14x14	81.96	38.16	---	-1.84	75.31	8.8%
												Average	9.0%

Overall, the results show a reasonably close agreement between the monthly and hourly simulations when determining the required ground loop length. The positive values for the percent error indicate that the monthly simulation is oversizing the ground loop slightly, which of course will result in slightly more capacity than is required. The school and hotel tend to show higher errors than the office, as a result of violations of one or more assumptions. Only one case, the Chicago office building, is undersized. The differences between the loop length in the monthly and hourly simulations can be better understood by examining the sources of error that produce them. These errors stem from the assumptions and approximations used in determining the peak load magnitude and duration; when they do not hold, the methodology does not produce as accurate of a result. The various sources of error will now be discussed individually.

3.4.1 Peak Load Does Not Occur at End of Month

In the monthly simulation, the peak load is applied to the ground loop at the end of the month, after the total load for that month has been applied. If the peak load does actually occur at the end of the month—say, within a few days—this assumption works fairly well. However, when the peak load occurs toward the middle or, worse still, at the beginning of the month, larger errors may result. One example of this is shown below in Figure 3-7, which shows the occurrence of the peak response for the Albuquerque office building when simulated with both hourly and monthly time steps. Also shown is the peak temperature response if the same peak load were placed on the 21st day of the month, which coincides with the actual peak temperature. The monthly results shown in the figure were determined by breaking the monthly load profile (the total load for the month plus the single peak) down to an hourly basis, and simulating based on those hourly loads. Even for this particular case, where the oversizing error is quite small, there is a small but noticeable difference between the two peak temperatures. For the hourly simulation, the maximum heat pump entering fluid temperature attained is 24.30°C. Using the peak load at the end of the month, the maximum temperature is slightly overpredicted at 24.64°C, while placing the peak load at the end of the day of the actual peak results in a much closer 24.35°C. It should be noted that, although this is the first year of the simulation and would not be used directly for a system design, plots of subsequent years would show similar behavior. Even for this case, where the oversizing error is just 0.5%, accounting for this discrepancy by adding 0.34°C (24.64°C – 24.30°C) to the upper temperature limit to allow for the difference in peak load timing, the

oversizing error drops to 0.1%. For this case and others using the office building, the timing of the peak load is a significant source of error.

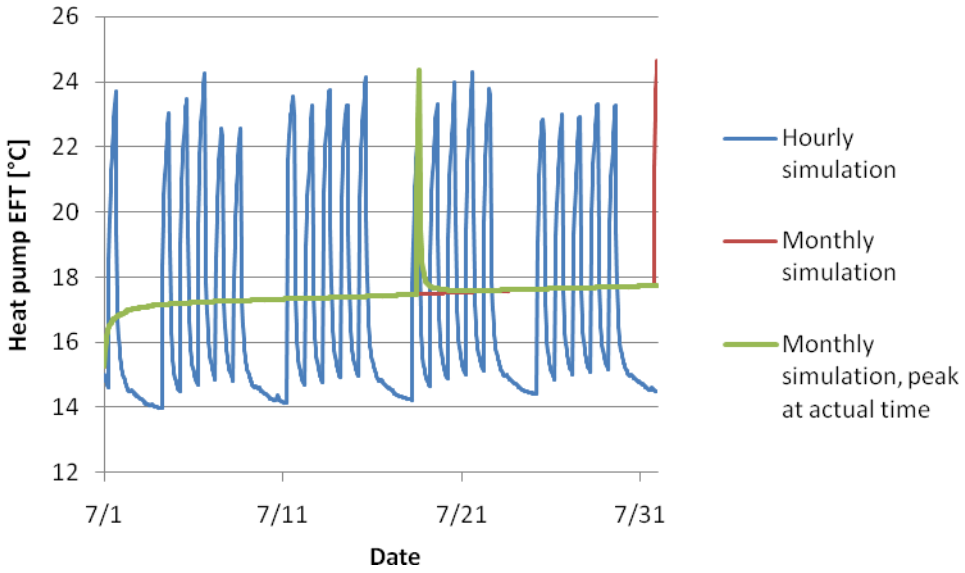

Figure 3-7: Albuquerque office peak load behavior

For the heating-constrained school cases, the peak load occurs in January toward the beginning of the month; this occurs because the warm-up period for the load generation program uses the first day of the simulation, which was on a weekend setback schedule. Consequently, the first load on the daily operation schedule is quite significant, and is the largest individual heating load for the year. Because, in each case, January has both the highest total monthly load *and* the highest peak load, this month drives the size of the ground loop for the heating cases. Since the peak load is assumed by GLHEPRO to occur after the entire month's heating loads, the net effect is that the fluid in the system is at a lower temperature than in reality, which leads to the oversizing of the ground loop to compensate. A couple of ways to rectify this error were explored, including using the peak load that occurs after a certain date (say, for example, the tenth day of the month),

or simply using the peak load from the last day of the month. Both of these reduced the oversizing error by between one and three percent, but there was no consistency in which refinement would result in the most improvement.

One way that the importance of the peak load can be quantified is by the ratio of the peak cooling load to the average cooling load for the month, or, similarly, the ratio of the peak heating load to the average heating load for the month. For the school cooling cases (El Paso, Houston, Miami, and Phoenix), the ratio of peak cooling to average cooling was less than the ratio of peak heating to average heating for the school heating cases. Because of this, the peak maximum temperature in the cooling cases is more dependent on the system's behavior in the immediate past in addition to the peak load. This is easily handled in an hourly simulation, but must be carefully considered when using a monthly simulation. For the monthly simulation, it is harder to match the behavior of this peak within the limits of the monthly simulation methodology; in other words, the timing of the peak load in the monthly simulation—at the very end of the month—inhibits the accuracy of the simulation. The three highest errors for the school, all more than 10% oversized, occur in cooling cases. The matching of the time of month that the peak load occurs serves to explain some of the error in these school cooling cases.

For the cooling cases mentioned above, the absolute peak cooling load occurs in the middle of the month, and the resulting ground loop sized by the monthly simulation is somewhat oversized; by selecting a "peak" load from the end of the month (which will be slightly smaller than the absolute greatest load for the month), the sizing errors can be

reduced substantially. This can be seen in Figure 3-8 for the Phoenix school case. While the peak temperature of 30.94°C does occur during the last week, there is still enough cooling load remaining that the monthly simulation cannot match this temperature. In this case, selecting the peak from the last day of the month, which is still more than 90% that of the maximum load for the month, results in a peak simulated maximum heat pump EFT of 31.04°C, as compared to the 31.97°C produced by using the absolute maximum load for the duration specified by the temperature change-matching methodology.

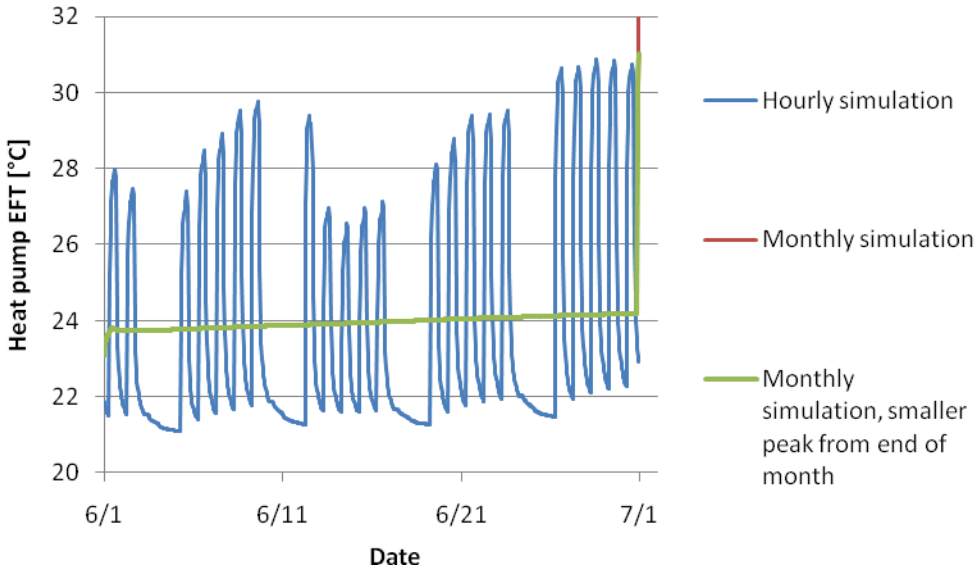

Figure 3-8: Phoenix school peak load behavior

As with the school, one of the factors in the oversizing of the hotel cases is the fact that the peak loads do not occur at the end of the month, as GLHEPRO assumes. Again, this leads to oversizing of the ground loop—GLHEPRO applies the peak after the entire month's loads have also been applied, so the resulting temperature will be more extreme (higher in cooling months and lower in heating months) than is actually the case. However, for the hotel, the error can be better accounted for by noting that applying a

square peak load pulse may not best fit with the particular details of the hotel load profile, as discussed in the next section.

It is also possible that the peak load occurs at the beginning of a cooling month at the end of the season, when the fluid temperature in the ground loop is decreasing over the course of the month. In this instance, the fluid temperature in the monthly simulation would be too low when the peak load is applied, leading to an undersized system. However, if this were to occur it is unlikely that the peak heat pump entering fluid temperature would occur at this same time; this is a separate source of error that will be discussed later.

3.4.2 Square Peak Heat Pulse Not Ideal Match for Load Profile

Another factor contributing to the error, particularly for the hotel complex, is the adequacy of the square heat pulse approximation. This is especially true for cooling cases, which, as seen from Table 3-3, have a higher discrepancy in temperature between GLHEPRO and HVACSIM+. The typical heating profile has a higher initial load due to morning startup, and a somewhat lower, consistent load sustained throughout the day. Consequently, the temperature response peaks with this startup load, then rises steadily throughout the course of the day.

However, the typical cooling load profile, which is shown below in Figure 3-9, demonstrates two separate periods of activity, one in the morning and another, of greater magnitude, in the evening. Obviously, a square pulse of the nature used in the approximation is not a very close approximation to this sort of profile. Figure 3-10

shows the temperature responses of both the hourly load for the peak load day and the day prior for the hotel in San Francisco, as well as several square pulse approximations for various peak load durations, scaled to show the nondimensionalized temperature near the maximum value. For peak magnitudes computed using the averaging method, there is no duration which results in a temperature change equivalent to the full load profile. For the peaks computed using the maximum method, the closest nondimensionalized temperature to unity, 0.98, occurs for the 2-hour duration. If all approximations were satisfied, one might expect a slightly undersized system since the peak temperature does not quite meet the hourly simulated value. However, this system is actually oversized by 12.5%. For this case, and many of the cooling-constrained hotel cases, the peak load occurs at or quite near the end of the month and coincides with the peak temperature, so these approximations are satisfied. Thus, the only major approximation not met is that the peak load can be adequately represented with a square wave; this incorrect approximation is the chief cause of error for these cases.

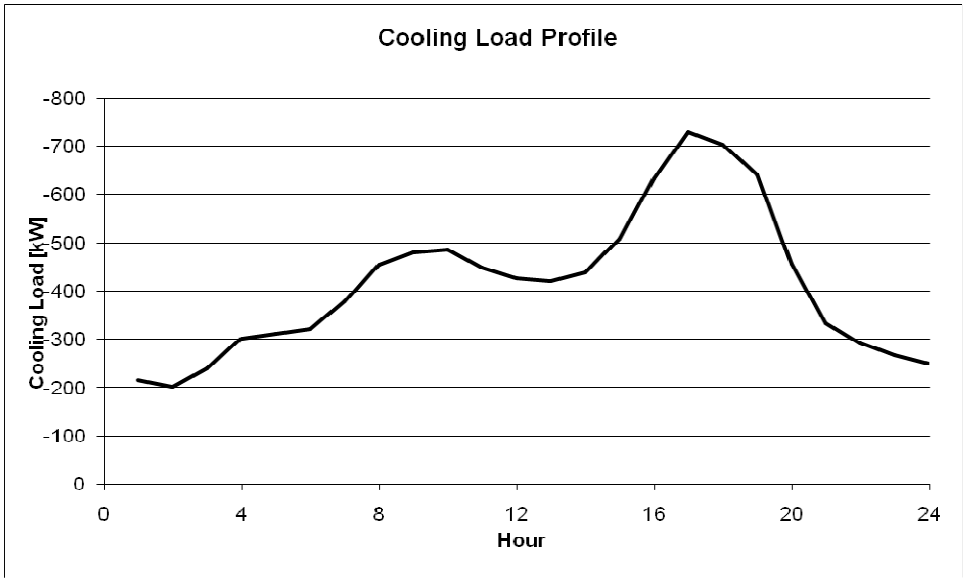

Figure 3-9: Typical hotel cooling load profile

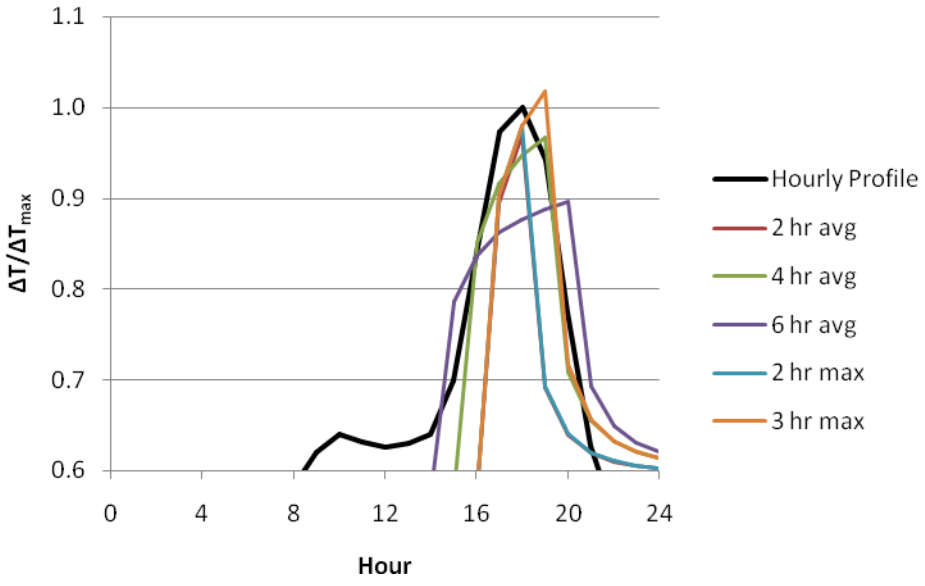

Figure 3-10: Hotel temperature response for different peak load approximations

Figure 3-11 shows the temperature response due to the peak load in the first year for the Memphis hotel when it is simulated with a GLHE size of 76.0m per borehole (the HVACSIM+ design length from Table 3-3) using different approximations to the peak load. Although the maximum temperature actually occurs on 17 August when simulated hourly, the temperature results for this day and the previous have been translated to the end of the month to facilitate visual comparison. When simulated on an hourly basis, the first year maximum heat pump EFT is 30.82°C. On a monthly basis, with the peak load applied at the end according to the methodology presented earlier, the maximum EFT jumps to 31.62°C; this will obviously lead to oversizing, as the maximum temperature predicted is too high. If instead the full peak day (17 August) were placed as the last 24 hours of the month, the temperature becomes 30.79°C, while adding another day previous

(16 August, which is the day of the second-highest load) bumps the temperature up slightly to 30.91°C. Simply adding the peak load that would produce the equivalent temperature change onto the average load as a square heat pulse may not necessarily be the most accurate option, as this shows. By using the monthly simulation for ten years, with the one day of loads at the end, the maximum temperature is 38.02 °C. By considering this difference from the maximum constraint as extra range available in the sizing tool (i.e., sizing to 41.98 °C instead of 40 °C), the GLHEPRO design length is reduced to 77.63m; this is a reduction in oversizing from 10.0% to just 2.1%.

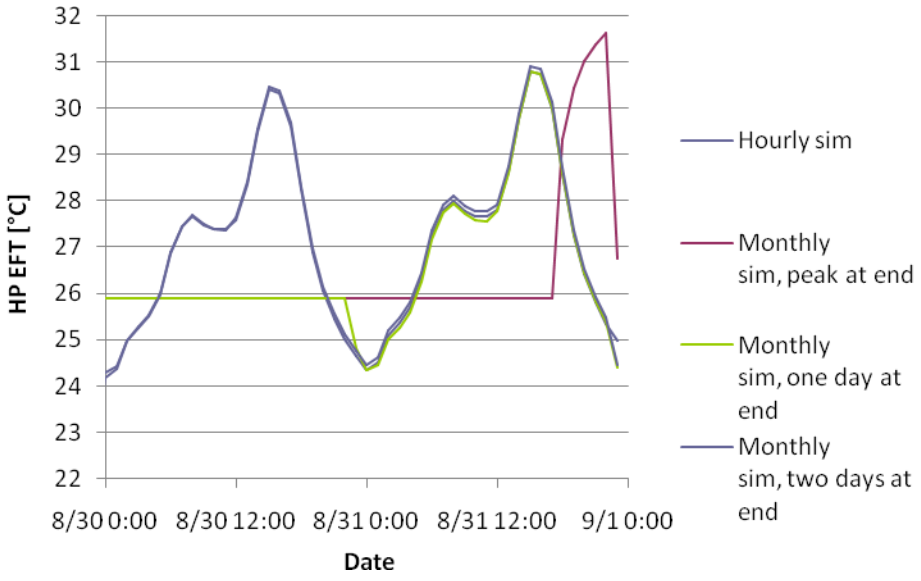

Figure 3-11: Hotel temperature response for different peak load approximations

3.4.3 Peak Temperature Day Misidentified

One of the assumptions made by this methodology in determining the response to the peak load is that the peak temperature occurs on the same day as the peak load. In some cases, the peak temperature response occurs in a different month entirely from the peak

load; this can occur because the peak temperature is a consequence of sustained buildup of high loads, while the peak load is simply a spike with much lower loads following. This is the case for both the Baltimore and Houston office buildings. For Baltimore, the peak cooling load occurs in the month following the maximum temperature, and that load is basically an outlier in magnitude: it is about 20% higher than any other individual hourly load for the entire year. The end result is an overprediction of the influence of the peak load on the system, which causes the oversizing. Much the same occurs in the Houston office case, but the difference in loads, and consequently in the oversizing of the system, is smaller. For Baltimore, replacing the outlier load by a more reasonable value causes the peak temperature response to shift to the month in which it appears in an hourly simulation, and drops the GLHEPRO design length to 87.07m. This corresponds to a decrease in the oversizing of the system from 5.0% to 2.8%.

Additionally, even if the peak temperature occurs in the same month as the peak load, they may not occur on the same day. If the two days have substantially different shapes—for example, one has a single, pronounced one-hour peak, while the other has a slightly smaller peak sustained over multiple hours—then the peak responses may be significantly different. Following this example, the sustained load is likely to cause a buildup to a more extreme temperature over the duration of the load than the response due to the single hour peak. Sizing the system based on the single peak will result in an undersized system.

To further explore the effect of misidentifying the peak day, the peak load approximation procedure was run for individual months instead of the entire year, and in some cooling-constrained cases, such as the Memphis and Tulsa office buildings, the duration does vary from month to month over the summer months. For example, in the Tulsa case, the best approximation for the peak duration, using the entire year's loads, was 9 hours (averaging method). For the other cooling months, however, the duration varied from between the 9 hours suggested by analyzing the full year down to 6 hours. Using a duration improperly suited to the actual peak will result in an oversizing of the system, as can be seen from the results. However, performing this additional analysis comes at the cost of more computation time in determining those peak values, and more user time in transferring the values into the monthly simulation; additionally, while reducing the error in the non-design months is a desirable task, doing so has no impact on the final design of the system. Finally, as the monthly simulation is refined more and more to analyze hourly effects, it becomes closer to a pure hourly simulation, which may not be desirable from a speed standpoint for design purposes.

3.4.4 Whole Numbers for Hours Restrict Peak Selection

For simplicity, the selection of the peak load duration was restricted to an integer number of hours. While the theory behind the simulation does not require an integer duration, choosing such a duration reduces the time required from a designer's standpoint, in the amount of time required to choose a good duration, as the methodology is currently implemented. However, fully automating the procedure, which is likely a desirable task for the future, would remove this hindrance.

To explore the effects of using a fractional number of hours in the choice of a peak duration, a selection of cases was chosen to represent a variety of building and climate types. The results of this exploration are shown in Table 3-4. In each case, the non-integer duration was chosen to the nearest 0.05 hours. In two of the cases, the error decreased, while in one (the Burlington hotel) it remained unchanged because the particular selection of peak duration was extremely close for that case. For the Baltimore hotel, the peak duration changed from 6 hours to 6.05 hours, which produced a 2.0% increase in the amount of oversizing. For the Salem hotel, however, the change in design length was less than 1m, while the peak duration changed from 5 hours to 5.45 hours. Even when the hourly profile is not matched as closely by an integer number of hours, there are other factors obviously in play. Overall, the change in accuracy does not appear to be worth the additional complexity to account for a fractional peak load duration.

Table 3-4: Non-integer peak duration results

Site	Design Length (Integer Duration)	% Oversized	Design Length (Non-Integer Duration)	% Oversized	Change in %Oversized
Hotel, Baltimore	81.69	12.2%	83.14	14.2%	2.0%
Hotel, Burlington	83.47	2.1%	83.47	2.1%	0.0%
Hotel, Salem	84.38	9.8%	84.96	10.5%	0.7%
Office, Duluth	81.43	2.0%	79.95	0.1%	-1.9%
School, Houston	75.70	11.5%	75.51	11.2%	-0.3%
School, Phoenix	87.11	13.0%	87.36	13.5%	0.5%

3.5 Conclusions and Recommendations

A methodology for approximating the peak loads—both magnitude and duration—for the monthly simulation of a ground source heat pump/ground loop heat exchanger system has been presented. This methodology has been implemented as an easy-to-use spreadsheet tool, with the ability to quickly transfer the results into the simulation tool GLHEPRO. Results for three real buildings in various locations were validated against a detailed hourly simulation, with results overall fairly good. Several likely sources of error were identified, mostly due to incorrect assumptions: the day with the peak load is not the same as the day with the peak temperature response; the peak load does not occur at, or even near, the end of the month; and the peak load cannot be completely represented as a square wave pulse. It was shown that accounting for these sources can reduce the oversizing error by more than half in some cases; it is not quite clear, however, how the various causes of error interact, as most cases did not strongly exhibit more than one.

This methodology could be improved by changing the way that peak loads are interpreted—looking at alternatives to the square heat pulse approximation—but this would also require modifications to the design tools used to simulate the systems being considered. A more reasonable approach might be to adapt the peak loads from month to month, so that the approximated peak load for every month does not have to look the same.

CHAPTER IV

DEVELOPMENT OF AN ALGORITHM FOR SIZING HYBRID GROUND SOURCE HEAT PUMP SYSTEMS

4.1 Introduction

Ground-source heat pump (GSHP) systems offer an attractive alternative for residential and commercial heating and cooling applications because of their higher energy efficiency as compared to conventional systems. However, the higher first cost of GSHP systems has been a significant constraint for wider application of the technology, especially in commercial and institutional applications. Compared to rooftop unitary systems in commercial applications, the first cost of a GSHP system is 20% to 40% higher [Kavanaugh and Rafferty 1997]. Many commercial and institutional buildings have high internal heat gains and thus are generally cooling-dominated, having a GSHP system that rejects more heat to the ground than it extracts on an annual basis. Though less typical, some commercial and institutional buildings are heating-dominated, with GSHP systems that extract more heat from the ground than they reject to the ground on an annual basis. Depending on the imbalance between heat rejection and heat extraction, the ground temperature surrounding the heat exchanger may rise or fall over the system operation period. This will negatively impact the system performance, as heat pump

COPs will vary with the change in temperature. This effect may be mitigated by increasing the ground loop heat exchanger (GLHE) size, which will further increase the first cost of the system.

One option to reduce the size of the GLHE, and therefore the first cost of the system, is to reduce the imbalance in the ground thermal loads by incorporating a supplemental heat source or sink into the system. GSHP systems that incorporate a supplemental heat source or sink have been termed "hybrid ground source heat pump systems" (HGSHP systems). Supplemental heat rejection can be accomplished with a cooling tower, fluid cooler, pond heat exchanger, pavement heating system, etc. Supplemental heat sources could be solar thermal collectors, boilers, greenhouses, and so on.

The GSHP design problem involves specifying both a borehole depth and a borehole configuration (i.e., both number and configuration of boreholes). Typically, the system is designed with a specific borehole configuration in mind, and if the results of the GLHE sizing prove inadequate—which might occur if the resulting borehole length is either too large or unreasonably small—a new configuration is selected and the process is repeated. Several procedures are available for sizing the vertical ground loop heat exchanger [Hellström and Sanner 1994; Kavanaugh and Rafferty 1997; Morrison 2000; Spitler 2000], and a detailed description of a design tool used for this purpose is presented in Chapter 2.

This chapter presents a new method for designing a hybrid ground source heat pump system; as the majority of systems in which a HGSHP is needed utilize a cooling tower, the focus will be on such systems. Practically, though, any supplemental device may be used with the methodology presented here. In addition, the new HGSHP design procedure will be briefly compared with the lone existing procedure, as well as with a much more detailed design algorithm based on cost optimization. A more detailed comparison of these three design procedures is forthcoming.

4.2 Background

4.2.1 Design of HGSHP Systems

Designing a hybrid ground source heat pump system requires sizing not only the ground loop heat exchanger but also a supplemental heat source or sink. The only published procedures for sizing HGSHP systems are given by Kavanaugh and Rafferty (1997) and Kavanaugh (1998). Some publications have investigated HGSHP systems with different supplemental heat sources or sinks as well as control strategies for the HGSHP system [Chiasson et al. 2000a; Chiasson et al. 2000b; Chiasson and Yavuzturk 2003; Chiasson et al. 2004; Khan et al. 2003; Yavuzturk and Spitler 2000]; however, none present a general design process for the HGSHP system.

One possibility for representing the design domain of an HGSHP system is with reference to the base GSHP system designed to meet all of the system heating and cooling loads, as shown in Figure 4-1. The vertical axis in Figure 4-1 represents the size

of the HGSHP system ground loop heat exchanger compared to the base GSHP system ground loop heat exchanger. For positive values, the horizontal axis represents the ratio of heat rejected over the year by the supplemental heat source to that rejected over the year by the GSHP system ground loop heat exchanger. Conversely, for negative values, the horizontal axis represents the ratio of heat added by the supplemental heat source to that extracted over the year by the GSHP system ground loop heat exchanger. Point 1 in this figure thus represents the base GSHP system, with no supplemental heating or cooling. For a typical HGSHP system, with a cooling tower to reject excess heat, the design might be represented by point 2, where the ground heat exchanger size is about 40% of the base GSHP system and about 60% of the annual heat rejection is done with the cooling tower. Point 2' would represent an HGSHP system where, say, a boiler or a group of solar collectors is used to provide additional heat to the loop. Here, the ground heat exchanger is about 70% of the base GSHP system and about 40% of the required annual heat transfer to the loop is provided by the supplemental heat source. In practice, there is a wide range of feasible solutions, ranging from a system with the entire load handled by the ground loop, to a system with no ground loop at all. This range is represented by the curves in Figure 4-1. These curves do not depict the actual shape of the feasible solutions, since this will vary depending on all the parameters in the system; instead, the curves just serve as examples of what a feasible solution curve might look like. The goal of the design procedure, then, is to find a feasible solution as near as possible to the optimum system design.

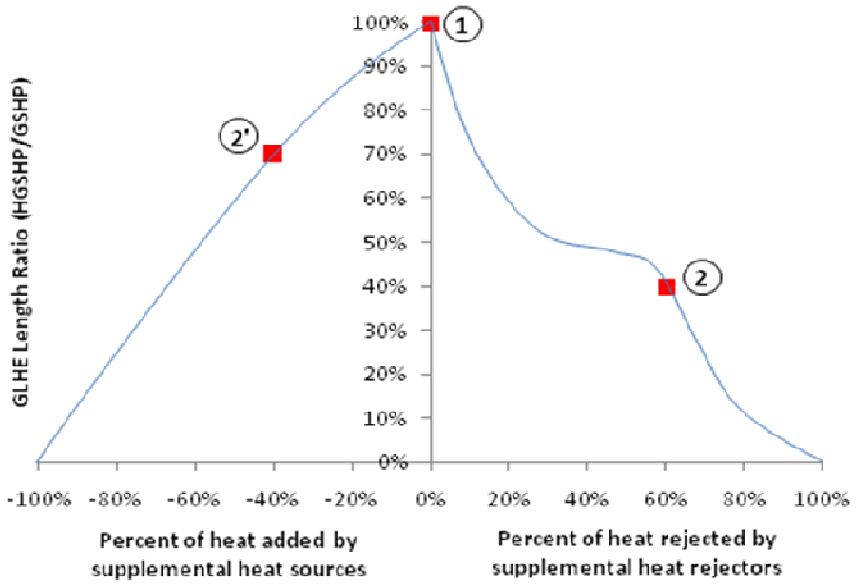

Figure 4-1: Conceptual diagram of HGSHP system design procedure

4.2.2 "Dominated" Versus "Constrained"

Before attempting to understand existing design procedures, or develop a new one, it is extremely useful to briefly consider some of the terminology that is used to describe the design of GSHP and HGSHP systems. One such term used to describe GSHP systems is "cooling-dominated", which is usually taken to mean that the ground loop heat exchanger of the GSHP system will reject more heat (usually significantly more) to the ground than it extracts on an annual basis. As a result, the ground temperature surrounding the heat exchanger will rise over the system operation period. Similarly, a "heating-dominated" system has the ground loop heat exchangers extracting significantly more heat from the ground than it rejects on an annual basis, and the ground temperature will consequently fall over the system operation period.

However, it is not necessarily the case that, for a cooling-dominated system, the required ground heat exchanger size will be determined by the cooling requirements. The required size depends not only on the system heat rejection and extraction demands, but also on allowable heat pump entering fluid temperatures (EFTs) and the undisturbed ground temperature. It is entirely possible that, due to a small difference between the EFT limits placed on the heat pump and the undisturbed ground temperature, a GSHP system design may be constrained by one mode of operation (heating or cooling), while the "dominant" mode is the opposite. For this reason, two new terms are introduced: "heating-constrained" and "cooling-constrained"; these terms describe systems for which the designs are driven by the system heat extraction or rejection, respectively.

The allowable minimum and maximum heat pump entering fluid temperatures will depend on the equipment, the heating and cooling loads of the spaces served by the equipment, and whether or not antifreeze is being used. Consider a case where, with antifreeze, the minimum allowable heat pump EFT is -6.7ºC and the maximum allowable heat pump EFT is 43.3ºC. When pure water is used as the working fluid, the allowable minimum heat pump EFT might only be 6ºC in order to prevent freezing. These upper and lower temperature limits are used to size the ground loop heat exchanger so that its exiting fluid temperature—the entering fluid temperature to the heat pump—does not exceed either limit. As an example, consider a GSHP system for a cooling-dominated building in both Tulsa, Oklahoma, where the undisturbed ground temperature is about 15ºC, and in Chicago, Illinois, where the undisturbed ground temperature is about 10ºC. In both locations, pure water is used as the working fluid. The Tulsa ground heat

exchanger consists of 160 boreholes, each 89m deep, while the Chicago ground heat exchanger has 240 boreholes, each 90m deep. In Chicago, a third case is created by using antifreeze; this allows the ground heat exchanger to be reduced to 100 boreholes, each having of a depth of 91m. After the design of the GSHP system is complete, monthly entering fluid temperatures to the heat pump are determined with a simulation; these results are shown in Figure 4-2. The upper temperature limit of 43.3ºC for all cases and the two lower temperature limits, -4.1ºC and 6ºC, depending on the working fluid, are shown as horizontal dashed lines.

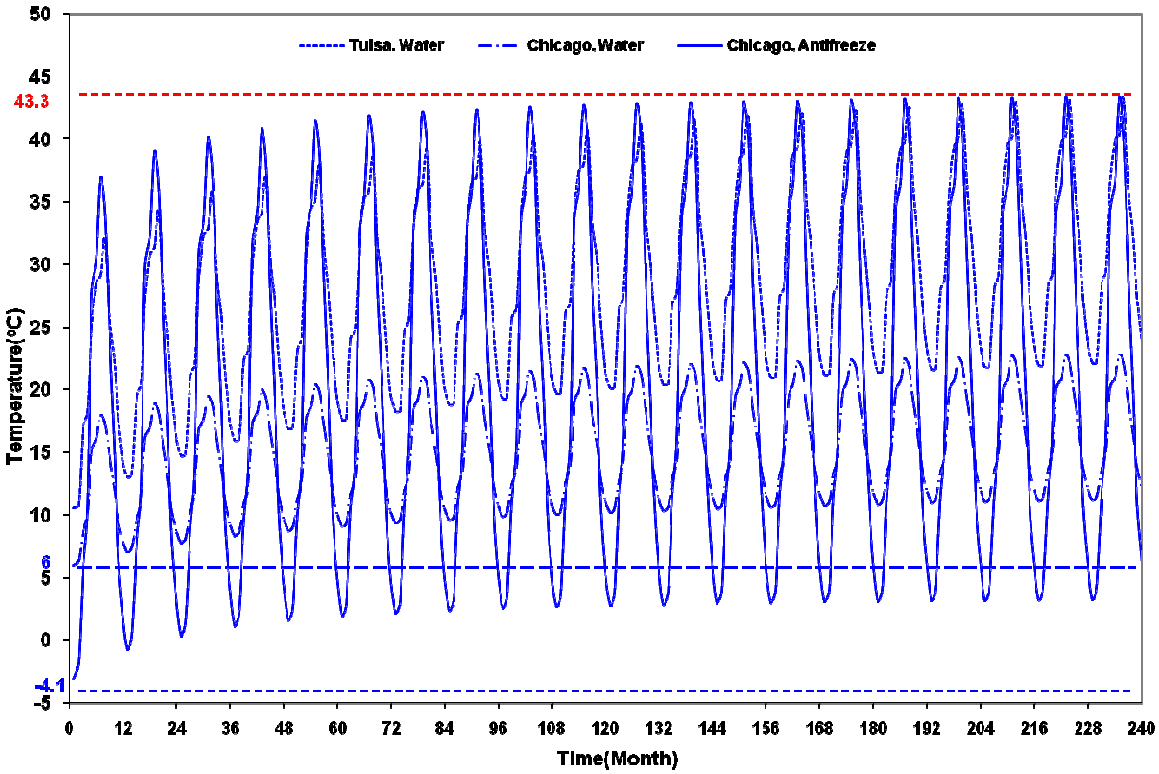

Figure 4-2: Heat pump entering fluid temperatures for different system designs

For the Tulsa case and the Chicago case with antifreeze, the resulting entering fluid temperatures are more or less as expected, hitting the upper limit in the later years, and

never hitting the lower limits. However, for the Chicago case with water, the lower limit is reached during the first year, while the upper limit is never even approached. Because there is a very small temperature difference (4°C in this case) between the undisturbed ground temperature in Chicago and the desired minimum entering fluid temperature, the ground loop heat exchanger must be very large; consequently, the upper limit is never approached, despite the building being cooling-dominated. Although this may be an unusual case, for which antifreeze should be used, it nevertheless illustrates the possibility that a building may be cooling-dominated yet heating-constrained. If sufficient antifreeze were utilized, the system would become cooling-constrained instead, as shown by the simulation in Chicago using antifreeze.

4.2.3 Existing HGSHP Design Procedure

Kavanaugh and Rafferty [1997] give what is currently the only available design procedure for sizing the borehole and supplemental heat source or sink of a HGSHP system; this procedure was later revised by Kavanaugh [1998]. The general procedure for designing a regular GSHP system involves computing one required GLHE length to satisfy the heating loads and another to satisfy the cooling loads, then using the larger of the two. For a cooling-constrained GSHP system, then, the required borehole length for cooling is greater than the required heating length. When designing an HGSHP system for this cooling-constrained system, the borehole length of the hybrid ground source heat pump system is sized to meet the heating loads of the system and is assumed to meet part of the system cooling loads, which is approximately equal in magnitude to the system heating loads. The additional system cooling loads are handled by the supplemental heat

rejection component(s). Similarly, for a heating-constrained GSHP system, the required borehole length for cooling is less than the required heating length, and the ground heat exchanger is sized to meet the system cooling loads and part of the system heating loads, with one or more supplemental heat input devices handling the remainder.

For sizing the HGSHP system components, Kavanaugh and Rafferty [1997] developed a procedure to calculate the required borehole lengths for cooling and heating. In this procedure, the peak block loads at the design day are required. Annual equivalent heating and cooling hours are required for calculation of the GLHE system heat extraction/rejection rate, which are found via a spreadsheet procedure. The effects of annual and peak (four-hour) heat pulses are used to compute the required borehole length for both heating and cooling. Next, the supplemental heat source or sink is sized from the difference between the two required borehole lengths. For a HGSHP system with a cooling tower as the supplemental heat rejecter, the capacity of the tower can be specified in terms of the fluid flow rate by assuming that the fluid has a 5.6 ºC temperature change through the heat pump condenser and cooling tower.

4.3 Proposed Design Procedure

A new procedure for designing a HGSHP system was developed for implementation in the ground loop heat exchanger tool presented in Chapter 2. These tools size the GLHE using a monthly time step coupled with a monthly peak-period simulation of the GSHP system. Using an analogous simulation which incorporates the presumed behavior of the

supplemental heat sink or source, combinations of ground loop heat exchanger size and the supplemental heat sink/source size can be evaluated. The proposed procedure follows from two observations of GSHP system design:

1. In general, the GLHE first cost tends to dominate the system life cycle cost. Therefore, designs that minimize the GLHE size tend to have the lowest life cycle cost.
2. In general, systems that minimize the GLHE size and make maximum use of the supplemental heat sink/source tend to, as a result, reach both the minimum and maximum heat pump entering fluid temperature limits.

Accordingly, the procedure attempts to adjust both the GLHE and supplemental heat sink/source sizes to come as close as possible to reaching both temperature limits over the lifespan of the system, without ever exceeding either limit. This requires some approximation regarding the behavior of the supplemental heat sink/source. Specifically, it is assumed that the portion of the heat rejection or extraction that is met by the supplemental heat sink/source can be reasonably approximated as constant. Thus, the system heat extraction and rejection ratios illustrated in Figure 4-1 are assumed to apply to both the annual heat rejection and extraction rates as well as the peak heat rejection and extraction rates. Using a boiler as a supplemental heat source, for example, may come very close to this approximation if the boiler were operated correctly. For a cooling tower, this is approximation would be less accurate, though it appears to be sufficiently accurate for design purposes. However, for a system with solar collectors as the supplemental heat source, one can imagine that the system might deviate significantly

from this approximation, so the use of this method cannot at present be recommended for such an application.

The procedure is implemented as described below.

4.3.1 Specification of GLHE and Supplemental Device Sizes

1. Calculate the required borehole length of the base GSHP system. Before any work can be done toward determining the optimum HGSHP system, the base GSHP system, without any supplemental device, must be sized. This is done to provide a starting point for the optimization step; this point is equivalent to point 1 in Figure 4-1. Additionally, this step determines whether the system is heating- or cooling-constrained, so that it is known whether a supplemental heat addition or heat rejection device is needed.

   To size the GSHP system requires several inputs, including loads on the heat pump, ground and fluid thermal properties, and constraints (maximum and minimum) on the heat pump entering fluid temperature. An initial borehole length is guessed, and the system is simulated with a monthly time step; among the outputs of the simulation are the simulated maximum and minimum entering fluid temperatures to the heat pump. These temperatures are compared to the constraints; the borehole length is adjusted; and the process is repeated until both the simulated maximum and minimum temperatures fall inside the applied constraints. Since this is a univariate problem in borehole length, the technique of modified false position [Dowell and Jarratt 1971] is

used to determine the solution. For more details on this GSHP simulation, see Chapter 2.

2. Determine the optimal HGSHP system. The determination of the borehole length and supplemental device size for the HGSHP system is treated as an optimization problem, with the goal of meeting both the maximum and minimum heat pump entering fluid temperature constraints simultaneously and as closely as possible. To simplify the formulation of the optimization, the borehole length and supplemental device size are treated as ratios, as shown in Figure 4-1. The length ratio is defined as the ratio between the borehole length for the HGSHP system and the borehole length for the GSHP system. Thus, the length ratio can have any value between 0 and 1, with a value of 1 indicating that the HGSHP borehole length is equal to the GSHP borehole length. The load ratio is defined as the ratio of cooling or heating loads met by the supplemental device to the total cooling or heating loads on the system. Heating or cooling loads are used depending on whether the system is heating- or cooling-constrained, using the knowledge obtained from the first step. The load ratio can take on any value between -1 and 1, with a negative sign indicating heat addition.

   For any combination of length and load ratios that results in a physically possible system (that is, the borehole length, and thus the length ratio, must be non-negative), the system can be simulated using the same simulation as for the base GSHP system. The length ratio is multiplied by the GSHP length to get the HGSHP borehole length, and the original monthly loads—both average and peak—for the constraining mode

are multiplied by the load ratio to obtain the new loads seen by the heat pump. Individual combinations of length and load ratios can be evaluated by comparing the simulated heat pump maximum and minimum entering fluid temperatures to the design limits. This is done via an objective function, given as

$$OF = (MaxEFT_{Cal} - MaxEFT_{Set})^2 + (MinEFT_{Cal} - MinEFT_{Set})^2 + Penalty \quad (4\text{-}1)$$

where the *cal* subscripted indicates the calculated (simulated) value, and the *set* subscript indicates the setpoint (constraint) value. The first two terms are the squares of the "errors" between the simulated and desired temperature extremes. The values are squared so that having one constraint being met while the other is exceeded does not produce a net zero effect. The purpose of the penalty term is twofold. First, as a consequence of squaring the temperature "errors" in the first two terms, exceeding the limits slightly achieves the same objective function value as being slightly within the limits. The penalty adds to the objective function in order to push the solution away from the region where the constraints are violated. The second purpose of the penalty term is to prevent physically impossible or implausible systems from being considered. This is done by adding a large value to the objective function if the GLHE length is either negative or exceeds the size of the base-case GLHE, or if the size of the supplemental heat source/sink becomes negative. While negative lengths and capacities are obviously not physically possible, these values can potentially be encountered when searching numerically for a solution. Hence, this aspect of the penalty function seeks to avoid such values.

Starting from an initial guess of the length and load ratios and initial step sizes, the Nelder-Mead simplex method [1965] is used to adjust the values of the length and load ratios until the objective function is minimized. A large penalty is assessed if the length ratio ever becomes negative, which would correspond to a physically impossible negative borehole length, and the system is not simulated; this is done to attempt to force the algorithm back into the plausible solution domain. After completion of the simplex method, the process is repeated with the solution as one of the initial simplex points to refine the solution. (Although this may not be necessary with respect to significant figures, it is a general recommendation for usage of the method.) The end result is a combination of length and load ratios that, when simulated, give maximum and minimum heat pump entering fluid temperatures as close to the constraint temperature limits as possible. This step, the main body of the procedure, requires several minutes of computation time on currently available computer hardware

3. Compute the necessary capacity of the supplemental heat addition/rejection device. This final step simply requires multiplying the optimum load ratio by the maximum load in the constraining mode (heating or cooling). As discussed earlier, this is based on the assumption that the supplemental heat addition/rejection device, when sized to meet some fraction of the peak load, will meet that fraction during the rest of the year.

4.3.2 Specification of Cooling Tower for a Cooling-Constrained System

To evaluate the results of this design procedure, a selection of cooling-constrained systems will be used to compare results between procedures. For each system, a cooling tower will be selected, and a sub-hourly simulation will be performed to evaluate the energy consumption and life cycle cost of the systems. Because the design procedure developed by Kavanaugh [1998] does not explicitly account for high cooling tower inlet temperatures or low local wet bulb temperatures, and thus tends to oversize the cooling tower (or fluid cooler), a new algorithm has been developed in conjunction with Xu [2007] to more accurately determine the required size of the cooling tower.

The algorithm for sizing the cooling tower is based on the local peak wet bulb temperature and the peak ExFT of the heat pump. Assuming a peak heat pump ExFT coincident with the local peak wet bulb temperature (i.e., ExFT on the order of 100ºF - 115ºF), the practical cooling capacity of the cooling tower for the HGSHP system can be calculated, which will be greater than the cooling capacity of cooling tower at the nominal design conditions. Then, by looking at catalog data from a cooling tower manufacturer, a smaller size of cooling tower can be chosen for the HGSHP system. The detailed procedure is as follows:

1. Determine the local outdoor peak wet bulb temperature. There are several possibilities to determine the local peak wet bulb temperature. The website of the U.S. Department of Energy [DOE 2007] provides weather data for a Typical Meteorological Year (TMY) in more than 250 North American cities. The local

outdoor peak wet bulb temperature can be calculated from this data. Alternatively, the local outdoor peak wet bulb temperature can also be obtained from ASHRAE standard weather data [ASHRAE 2005]. In this study, the local outdoor peak wet bulb temperature is calculated from the TMY weather data.

2. Select the peak inlet fluid temperature of cooling tower. At this point, the peak heat pump ExFT is selected as the peak inlet fluid temperature of the cooling tower. Knowing the heat pump heat rejection rate and the fluid flow rate, the peak heat pump ExFT can be determined from a user-specified maximum heat pump EFT. Some heat pump manufacturers give the allowable ExFT of a heat pump as 110ºF - 120ºF. In this research, a temperature of 115ºF (46.1ºC) is selected as the peak inlet fluid temperature of the cooling tower.

3. Choose cooling tower from a database to meet the required capacity. Although cooling tower capacities can be represented in more than one way, it is convenient to use the effectiveness-NTU model [Webb 1984; Webb and Villacres 1984] to determine UA values for a range of cooling tower and place them in a database. Then, given the peak outdoor wet bulb temperature and peak cooling tower inlet fluid temperature, the database can be searched to find the cooling tower with the smallest UA value that meets the required heat rejection rate.

4.3.3 HGSHP Solution Domain

To provide some insight into the workings of the hybrid ground source heat pump design process, the objective function described in section 4.3.1 was evaluated for a wide variety of points, with load ratios ranging from -1.1 to 1.1 and depth ratios ranging from 0.0 to 1.1, to get an idea of the shape and tendencies of the solution domain. In other words, for any given system, the HGSHP system was simulated with a large number of different load and depth ratios, some of which are slightly outside the realm of feasibility. For instance, a depth ratio greater than 1 indicates a GLHE length greater than what is needed for a standard GSHP system, while a load ratio less than 0 for a cooling-constrained system would add an unnecessary supplementary heat input device. For a cooling-dominated and cooling-constrained office building in Tulsa, values of the objective function are shown in the 3D plot in Figure 4-3.

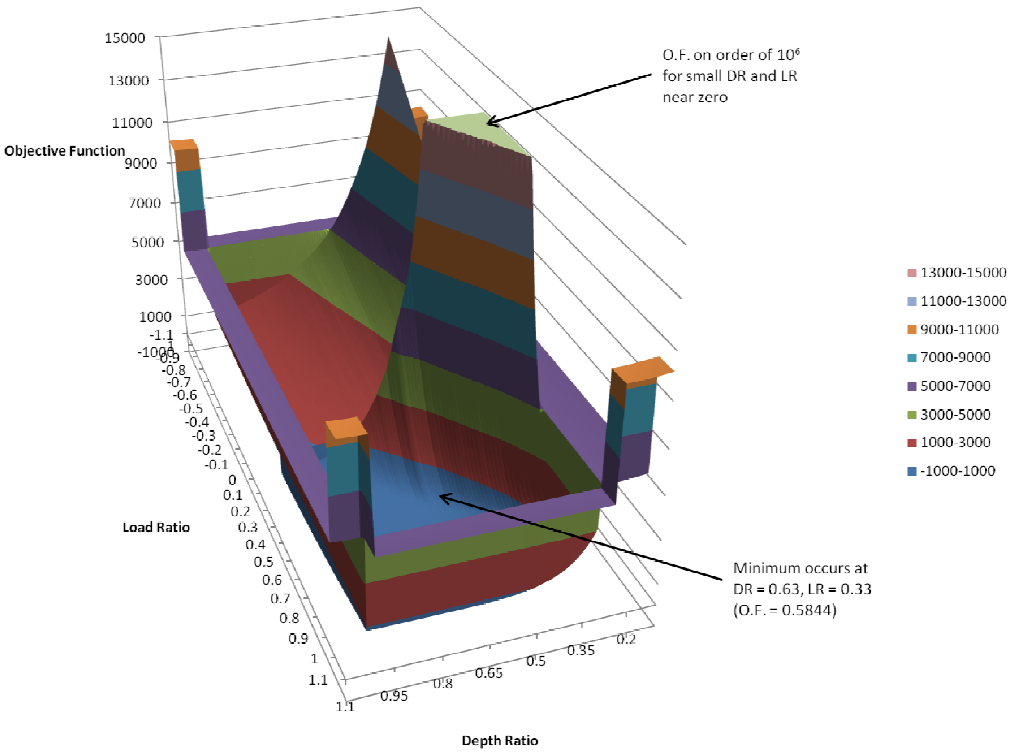

Figure 4-3: HGSHP solution domain for Tulsa office building

For depth and load ratios near the solution (depth ratio 0.63; load ratio 0.33), the objective function slopes gently into a bowl shape around the minimum. The slope greatly increases for small values of the depth ratio, especially as the load ratio approaches zero; these systems represent a very small GLHE, with nearly all of the heating and cooling loads handled by the ground. As a result, the heat pump EFT maxima and minima are significantly outside the specified limits, which cause the extraordinarily high objective function values. For negative load ratios, which depict a heating-constrained system, the objective function is set via the penalty to a large value, and increases the more negative the load ratio becomes. Since it would not make sense to add a supplemental heat source to a cooling-constrained system, these systems are not simulated, and the objective function calculated solely with the penalty. The shelf-like structure surrounding the bowl represents values of depth or load ratios that correspond to implausible systems—depths less than zero or greater than what is needed for a GSHP system, or supplemental devices that handle more than the actual load. Again, these systems are not simulated, because the systems are not practical designs.

Figure 4-4 shows two-dimensional cross-sections of the domain plot at various values of the depth ratio. This plot more clearly shows the variation in the objective function with respect to both ratios; there are also slightly different profiles for differing values of the depth ratio. While there is a definite discontinuity in the objective function between positive and negative load ratios, this does not really pose a problem in the optimization. This is because, due to the initial GSHP sizing step, it is known ahead of time whether the system is heating- or cooling-constrained; the optimization algorithm is initialized on

the correct side, so that as the load ratio decreases past the optimum, the algorithm pushes the solution back toward the optimum and away from any potential problems that might be caused by jumping to an incorrectly-signed depth ratio.

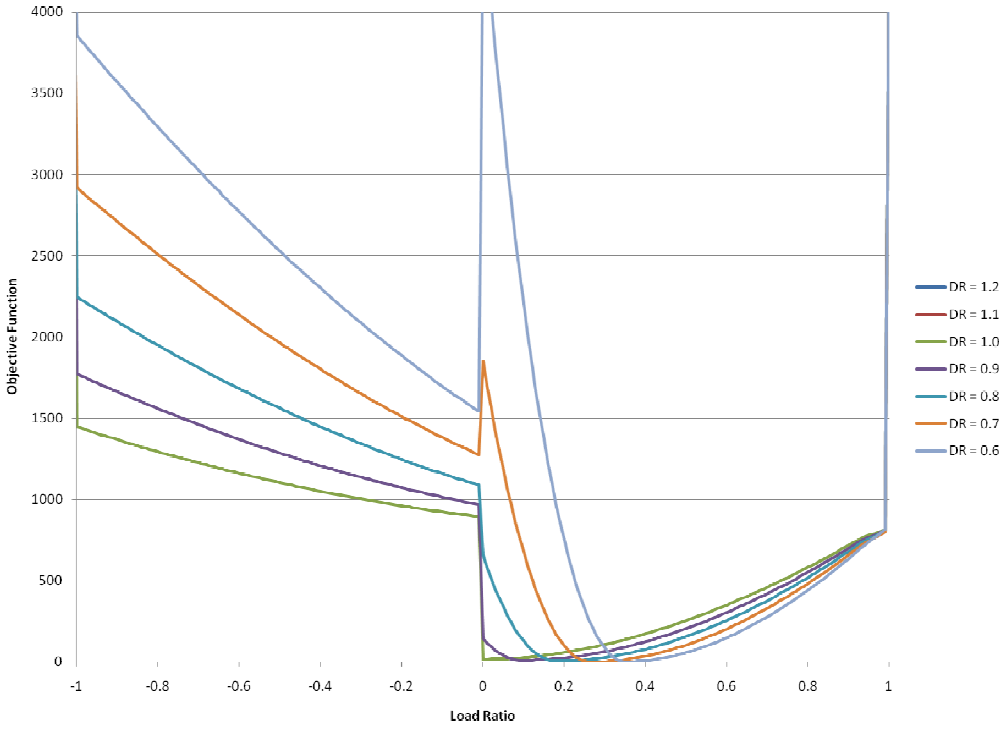

Figure 4-4: HGSHP Tulsa solution domain—2D cross-sections

Figure 4-5 shows the same cross-sections as Figure 4.4, zoomed in to show detail around the optimum. From this detail, it can be seen that the minimum is somewhere around a depth ratio of 0.7 and a load ratio of 0.27; this is indeed true, as the actual minimum is at 0.63 and 0.33. The area near the minimum, while sloping only gently, still has enough change to allow the optimization algorithm to efficiently hone in on the minimum.

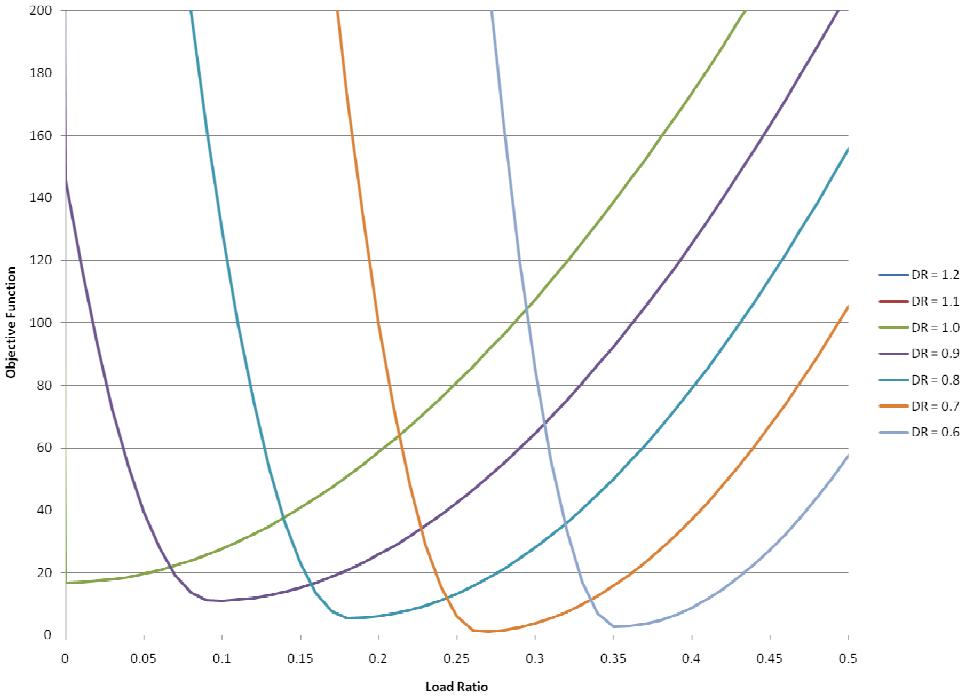

Figure 4-5: HGSHP Tulsa solution domain—zoomed 2D cross-sections

4.4 Evaluation of Algorithm

To evaluate the performance of this HGSHP design algorithm, results are compared to the existing method [Kavanaugh 1998], as well as to a life cycle cost optimization design method based on Gentry's [2007] experimentally validated hourly HGSHP simulation, which was developed by Xu [2007]. That method attempts to find the combination of GLHE length and supplemental device size (cooling tower capacity, in this case) that minimizes the 20-year life cycle cost of the system. Although this algorithm would be ideal from a design perspective, since it is an hourly simulation, it requires far too much time (on the order of hours) to complete, as compared to the several minutes required for either of the other two methods evaluated; it is used simply as a reference procedure

representing the absolute best possible design. The three methods were tested on an office building in two different locations; comparisons for more locations, and a brief exploration of cooling tower control strategies, will be the subject of future work.

4.4.1 Building Description

The test building is based on an actual 52-story office building evaluated by Feng [1999], although only three stories are used in this study. The building was modeled, and heating and cooling loads for the building were found, by Gentry [2007]. For this comparison, the building was modeled in both Tulsa, Oklahoma, and Baltimore, Maryland. More details about the building may be found in both Feng [1999] and Gentry [2007].

4.4.2 Results

The three different HGSHP system design methods described previously were used to design a HGSHP system for the office building in the two cities. The design results, including the total GLHE length and open-loop cooling tower size, are summarized in Table 4-1. The length of the base GSHP is shown for comparison. Additionally, the annual energy consumption and present value of the 20-year life cycle cost of each system are listed in the table. Several assumptions were made when calculating the life cycle cost:

- The cost of the ground heat exchanger is calculated at $6 per foot of the borehole [Kavanaugh 1998]. This amount includes horizontal runs and connections.

- The first cost of the cooling tower is calculated at $275 per ton of cooling tower capacity [Means 2006]. This amount includes other equipment and apparatuses required for controls.
- The cost of auxiliary equipment and materials for the cooling tower is estimated to be 10% of the first cost.
- Issues related to the maintenance of supplemental heat rejecters and related equipment are neglected.
- The cost of electricity is assumed to be $0.07 per kWh.
- A 6% annual percentage rate, compounded annually, is used for the present value analysis.

Table 4-1: HGSHP design procedure results comparison

City	Tulsa, OK				Baltimore, MD			
Design Method	Base GSHP	Kavanaugh	Proposed	Opt. Based	Base GSHP	Kavanaugh	Proposed	Opt. Based
Total GLHE Length (m)	14,228	9,845	7,923	7,353	12,363	11,658	8,774	7,774
Cooling tower capacity (tons)	---	109	44	17	---	52	21	12
Total annual energy consumption (kWh)	---	194,150	198,738	207,961	---	140,274	153,494	162,132
Present Value of 20-Year Life Cycle Cost ($)	---	382,708	328,768	316,788	---	377,467	318,211	300,775

Because the proposed HGSHP design method and the life cycle cost optimization design method are simulation-based, whereas Kavanaugh's method sizes the GLHE based on explicit equations, the proposed and life cycle design methods are able to give a more accurate depiction of the GLHE behavior. Consequently, these methods produce a

shorter GLHE length. Additionally, because Kavanaugh's method bases the determination of the cooling tower capacity on the assumption that the fluid is cooled from 35°C to 29.4°C, with a 25.4°C peak outdoor wet bulb temperature, it tends to oversize the cooling tower. In actuality, using Tulsa as an example, the peak outdoor wet bulb temperature is 26.7°C, while the peak heat pump ExFT is set at 46.1°C. Since there is a greater capacity for heat transfer than is assumed in Kavanaugh's method, the required tower size is smaller; both the proposed methodology and the life cycle cost optimization use the cooling tower database approach described in section 4.3.2, so they produce similar sizes.

While the proposed method, as well as the life cycle cost-based method, produces smaller cooling towers than Kavanaugh's method, the total system energy consumptions are slightly higher. This is because about 85% of the total energy consumption is from the heat pump, with another 5% or so from the main circulating pump; the remainder comes from running the cooling tower fan and secondary pump. As a result, since the cooling towers from Kavanaugh's method are oversized, the heat pump requires less energy to operate while still producing the required cooling.

Although the proposed method consumes a greater amount of energy, the life cycle cost is still less than for the existing (Kavanaugh's) method. For a 20-year life cycle, the first costs of the GLHE and cooling tower account for about 50% of the total life cycle cost. Therefore, although the systems designed by the proposed method consume more energy than the systems designed by Kavanaugh's method, the systems designed with the

proposed method have a lower average life cycle due to the savings in initial cost. The cost optimization design method has the lower life cycle cost in both cases, since that is the exact purpose of that method.

4.5 Conclusions and Recommendations

This study proposes a new simulation-based method for designing hybrid ground source heat pump systems. First, it was quickly demonstrated that the traditional terminology of a system being "heating-dominated" or "cooling-dominated" is not necessarily related to the mode of operation that constrains the design of a GSHP (or HGSHP) system. The algorithm proposed uses a standard optimization procedure to determine the GLHE and supplemental heat source/sink sizes that minimize the differences between the simulated heat pump EFT extremes and the desired limits, with the objective being to just meet both limits simultaneously. Details of the optimization step were presented, demonstrating that the optimization does indeed produce the best solution, as closely as can be determined from the specific formulation of the objective function used in the algorithm. Finally, the proposed design procedure was briefly compared to existing methodology using a 20-year life cycle cost as the basis for comparison. For the two cases examined, the proposed procedure performed quite favorably, coming much closer to the optimal life cycle cost than the existing design methodology.

More work is needed to further examine the effectiveness of this HGSHP design procedure. Such work is currently underway, using a wider variety of climate locations

for the comparison. Additionally, this work will attempt to evaluate the selection of cooling tower control strategies as it pertains to the system energy consumption and life cycle cost. Finally, other works focusing on the design of HGSHP systems are currently in progress, and comparison of these various procedures would be highly recommended.

CHAPTER V

VALIDATION OF GROUND SOURCE HEAT PUMP SYSTEM DESIGN SOFTWARE

5.1 Introduction and Background

GLHEPRO [Spitler 2000] is a simulation-based software tool for the design of ground heat exchangers used with ground-source heat pump systems. It utilizes simulation in an iterative fashion to adjust the size of the ground heat exchanger in order to meet minimum or maximum entering fluid temperature limits specified by the user. In order to keep computational time and input requirements to a reasonable level, heating and cooling loads are specified as monthly totals and monthly peak loads. This requires considerably less input than a full, multi-year, annual hourly simulation and also runs much faster. The accuracy of the design tool is limited by the accuracy of the underlying simulation. This chapter describes an experimental validation of the underlying simulation, utilizing experimental data from a hybrid ground source heat pump test facility located at Oklahoma State University.

5.1.1 Experimental Facility

The Oklahoma State University test facility was designed by Hern [2002]. The ground loop heat exchanger consists of four horizontal and one vertical borehole, each 4.5 inches (114.3 mm) in diameter and averaging about 246 feet (75 m) in length; however, only three of the vertical boreholes were in use during the time in which the experimental data used here was taken. The cooling capacity of the ground loop is supplemented by a three-ton evaporative cooling tower, connected to the loop via a plate heat exchanger in order to maintain a closed-loop system. Additional supplemental cooling was available via a pond loop heat exchanger, although it was not used in this particular experiment. Two Florida Heat Pump WP036 model water-to-water heat pumps are used in the facility; one is configured to operate in cooling mode, while the other operates in heating mode at all times. For the majority of the experiment, only one heat pump is in operation; later in the experiment, the two are run simultaneously for a short time.

A wide variety of flow rate and temperature data from the test facility's operation is available from March 2005 through August 2006. Data were recorded at one minute intervals, and then later post-processed into hourly averages. The experiment was run continuously except for very brief periods of computer downtime and regular system maintenance. For the purposes of validation, the values of interest are the ground loop entering and exiting fluid temperatures, as well as the flow rate through the ground loop.

5.1.2 Simulation Procedure

The simulation procedure is based on the g-function, a non-dimensional response factor developed by Eskilson [1987]. The g-function gives the temperature response to a series of step heat pulses as given for the n^{th} time period by

$$T_{borehole} = T_{ground} + \sum_{i=1}^{n} \frac{Q_i - Q_{i-1}}{2\pi k} \cdot g\left(\frac{t_n - t_{n-1}}{t_s}, \frac{r_b}{H}\right) \tag{5-1}$$

Where:

$T_{borehole}$ is the average borehole wall temperature, in °C;

T_{ground} is the undisturbed ground temperature, in °C;

Q is an individual step heat pulse, in W/m;

k is the ground thermal conductivity, in W/m-K;

t_i is the time at the end of the i^{th} time period, in s;

t_s is the time scale $H^2/9\alpha$, in s;

α is the ground thermal diffusivity, in m^2/s;

r_b is the borehole radius, in m;

and H is the borehole depth, in m.

While the original g-function response factors were created for a single borehole, Eskilson used superposition principles to compute the g-function values for a variety of systems with multiple boreholes; currently, there is a wide variety of borefield sizes and configurations with available g-function values. For time steps longer than a few hours, g-function data is tabulated, while the values of the g-functions for shorter time steps are computed based on the approach of Xu and Spitler [2006]. In this approach, a one-

dimensional numerical model is used to determine a set of discrete values for the g-function at short time steps. This 1-D model uses a detailed computation of the borehole thermal resistance, variable convective resistance, and consideration of the thermal mass of the fluid in the borehole to find the g-function values.

At each time step, the temperature at the borehole wall is computed via the above equation. The average fluid temperature in the ground loop is then determined by correcting for the thermal resistance in the borehole:

$$T_{fluid} = T_{borehole} - Q_n \cdot R_{borehole} \tag{5-2}$$

Where:

Q_n is the normalized heat extraction rate for the current (n^{th}) time step, in W/m;

and $R_{borehole}$ is the borehole thermal resistance, in K/W.

With the average fluid temperature known, the inlet and outlet loop fluid temperatures are determined:

$$T_{inlet} = T_{fluid} - \frac{Q_n \cdot H \cdot NB}{2\dot{m}c_p} \tag{5-3}$$

$$T_{outlet} = T_{fluid} + \frac{Q_n \cdot H \cdot NB}{2\dot{m}c_p} \tag{5-4}$$

Where:

$\dot{m}$ is the mass flow rate, in kg/s;

c_p is the specific heat of the working fluid, in J/kg-K;

and NB is the number of boreholes.

Loads on the ground heat exchanger may be entered in two forms. First, loads on heat pumps may be input, which are translated to loads on the ground heat exchanger with the use of a simple equation-fit heat pump model that computes the ratio of heat rejection to cooling provided or heat extraction to heating provided. Second, loads directly on the ground heat exchanger, unmediated by a heat pump, may be input. In this validation, the latter form is chosen because the hybrid ground source heat pump system has a cooling tower, which rejects some of the heat. Therefore, measured loads on the ground heat exchanger are utilized as inputs.

For each month, the total load for the month, as well as the peak hourly load, is specified for both heating and cooling. The total load is divided by the number of hours in the month, and this average is applied for every hour over the month to determine the response to the total load for the month. The peak loads are specified by both a magnitude and duration; the magnitude and duration are chosen so that the change in temperature due to the peak load, with respect to the monthly simulation, is as close as possible to the change in temperature due to the hourly loads, as determined by an hourly simulation. Since it is assumed that the peak loads only affect the peak temperatures, and not the averages for the month, only the changes in temperature—not the temperatures themselves—are compared to determine the magnitude and duration of the applied peak load. Additionally, the duration is chosen so that the response is most accurate for the month with the largest load; in other words, there is only one peak load duration for heating and one for cooling, and these are applied to every month.

5.2 Methodology

Eighteen months of experimental data from the test facility will be used in the validation. The heating and cooling loads across the ground loop heat exchanger were computed by simply multiplying the temperature differential across the GLHE by the measured mass flow rate and the specific heat of the working fluid (water). Hourly total loads were determined by adding the energy requirements for each data point and dividing by the total time of one hour. For comparison to the simulation results, peak temperature data was determined by taking the highest and lowest values when averaged over a ten-minute interval. The "average" temperature at the end of the month was determined by averaging all the temperature measurements for the final 48 hours of operation; this was done to obtain a valid comparison between the actual borehole temperature at the end of the month and the simulated value for the entire month.

The total loads for each month, as well as the peak loads and peak load durations, were calculated by a spreadsheet tool designed for this purpose; these loads are listed in Table 5-1. By examining the annual peak heating and cooling loads, a heating duration of five hours and a cooling duration of 3 hours were selected so that the temperature response to these peak loads during that month was as close as possible to the temperature change that would be seen from a detailed hourly simulation. Since the loads were computed using the temperature differential across the ground loop, the loads were input as pure ground loads; because the software is not currently equipped to handle simulation of

hybrid systems, the effects of the cooling tower could not accurately be accounted for otherwise.

Table 5-1: Monthly simulation load data

	Total Heating [kWh]	Total Cooling [kWh]	Peak Heating [kW]	Peak Cooling [kW]
Mar-05	1958.56	159.69	7.46	13.48
Apr-05	74.62	1319.74	0.5	8.97
May-05	65.78	1700.59	3.16	9.65
Jun-05	1.07	2704.18	0.96	12.53
Jul-05	12.95	3271.07	1.41	10.14
Aug-05	2.39	3775.13	0.54	10.25
Sep-05	22.7	3366.33	1.79	9.88
Oct-05	620.57	1133.41	4.77	9.4
Nov-05	451.9	1008.53	8.98	9.33
Dec-05	1504.1	0	9.21	0
Jan-06	1698.43	0	8.8	0
Feb-06	1608.62	0	7.54	0
Mar-06	613.08	702.25	8.51	16.92
Apr-06	543.93	1582.29	9.93	10.26
May-06	232.17	2607	8.59	9.8
Jun-06	91.24	2887.99	2.04	9.71
Jul-06	40.74	3990.2	2.33	13.41
Aug-06	23.02	3397.29	1.59	9.7

The parameters of the ground loop system, as well as the physical properties of the soil and heat pump specification, were taken directly from the values given by Hern [2002]. Since the three boreholes in use are all of slightly different depths, the average value was taken. The undisturbed ground temperature and soil conductivity were measured, and the borehole resistance was estimated based on in situ test results obtained by Hern. The soil heat capacity was unknown and could not be conveniently measured, so a value in the center of the known range of 1341-2683 kJ/m^3-K was used in the calculation of the borehole resistance; a sensitivity analysis suggested that selecting a heat capacity anywhere in this range would not appreciably change the borehole thermal resistance

value. The simulation input parameters are listed below in Table 5-2. As an internal check on all of this data, the borehole thermal resistance was computed within the simulation software, using the measured values as inputs, as 0.1622 m-K/W, which agrees with Hern's values of between 0.1618 and 0.1676. For the computation, it was assumed that the shank spacing—the distance between the two ends of the U-tube—was equal to the distance between the U-tube and the borehole wall. This is typical of most boreholes.

Table 5-2: Monthly simulation input data

Borehole depth	74.68	m
Borehole diameter	114.3	mm
Borehole spacing	6.1	m
Ground thermal conductivity	2.55	W/m-K
Ground heat capacity	2012	kJ/m^3-K
Borehole thermal resistance	0.1622	m-K/W
Undisturbed ground temperature	16.3	°C
Fluid flow rate	0.631	L/s

The monthly simulation was run using the load data from March 2005, the beginning of the experiment at the test facility, through August 2006. The resulting output, which includes the temperature of the fluid in the ground loop, as well as average, minimum, and maximum heat pump entering fluid temperatures for each month and the normalized rate of heat extraction (or absorption) by the ground loop, can then be compared to the experimental data from the test facility.

The simulation program, as typically used by GLHEPRO, assumes that the 12 monthly loads will recur over the entire period of operation specified by the user. For purposes of

validation, the program was modified to take monthly loads for the 18 months of operation.

5.3 Results and Sources of Error

For the initial simulation, using the eighteen consecutive months of data, plots of the simulation and experimental values of monthly maximum, minimum, and the heat pump entering water temperature at the end of the month, as well as the normalized average and peak borehole heat extraction rate, are shown below in Figures 5-1 through 5-4. The plots begin with month 3 because the experimental data begins in March; this convention was used simply to make comparison between the simulation results and the experimental data more intuitive. Figure 5-1 shows the monthly average and peak borehole heat extraction rates as measured during the experiment. Negative values indicate more heat rejection than extraction, i.e. the system is cooling dominated for that month. The peak heat rejection rate is zero for months 12-14 because there are no hourly cooling loads for those months.

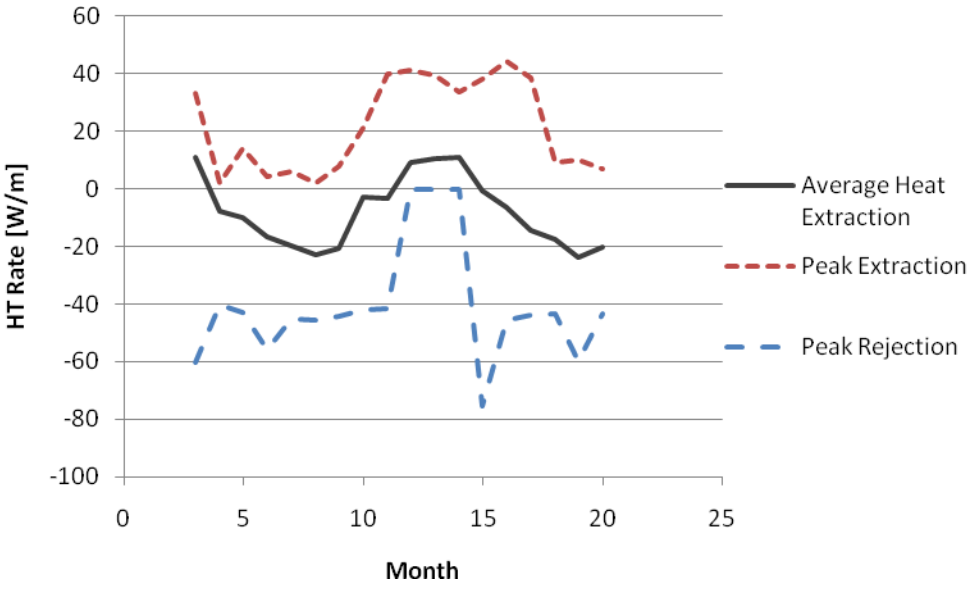

Figure 5-1: Monthly experimentally-measured heat transfer rates

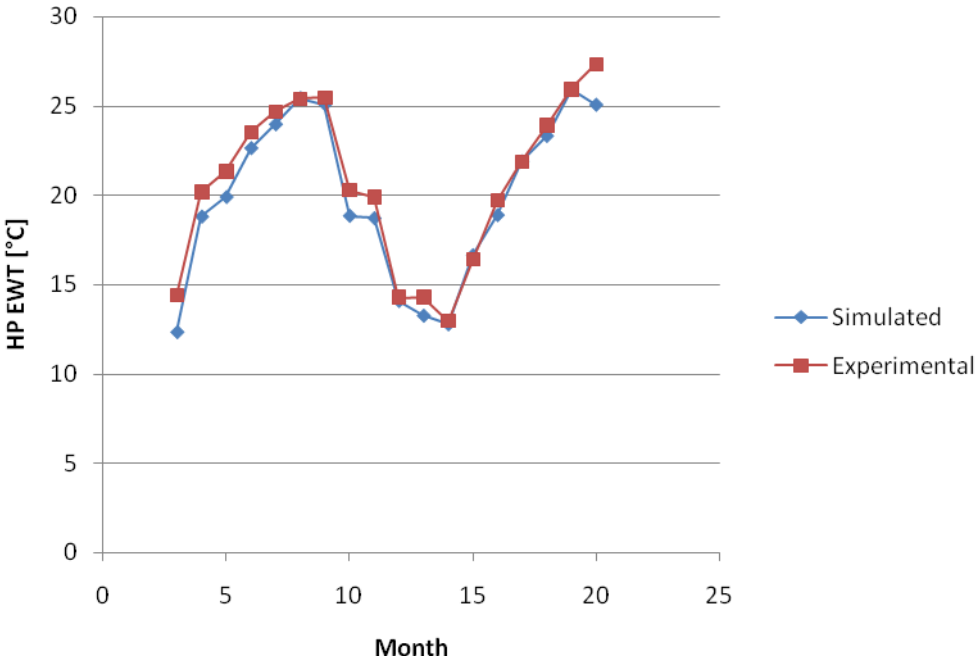

Figure 5-2: 18 month simulation results – end-of-month heat pump EWT

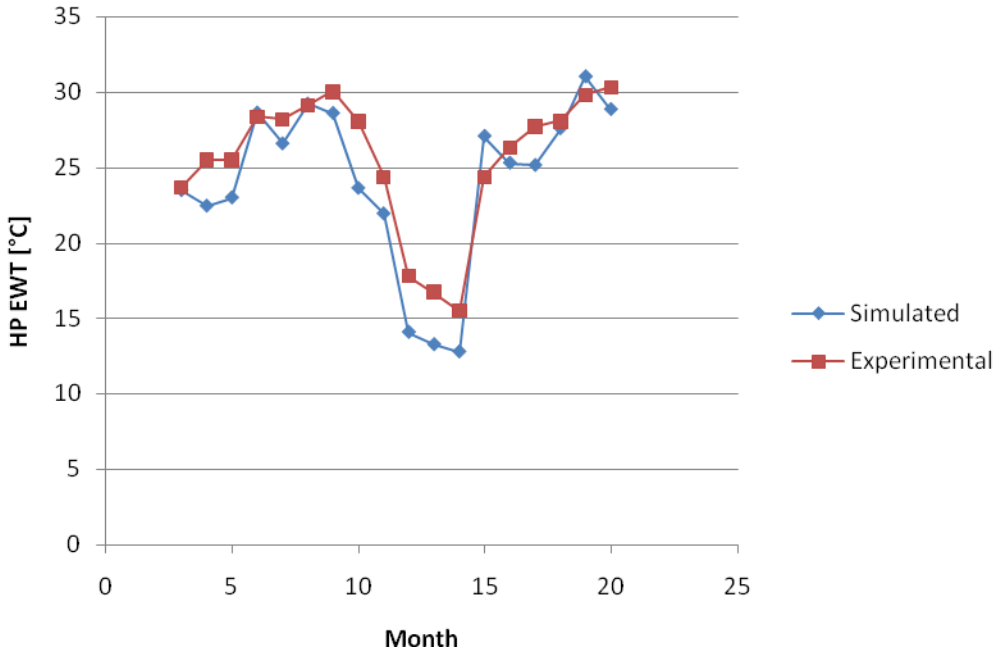

Figure 5-3: 18 month simulation results – maximum heat pump EWT

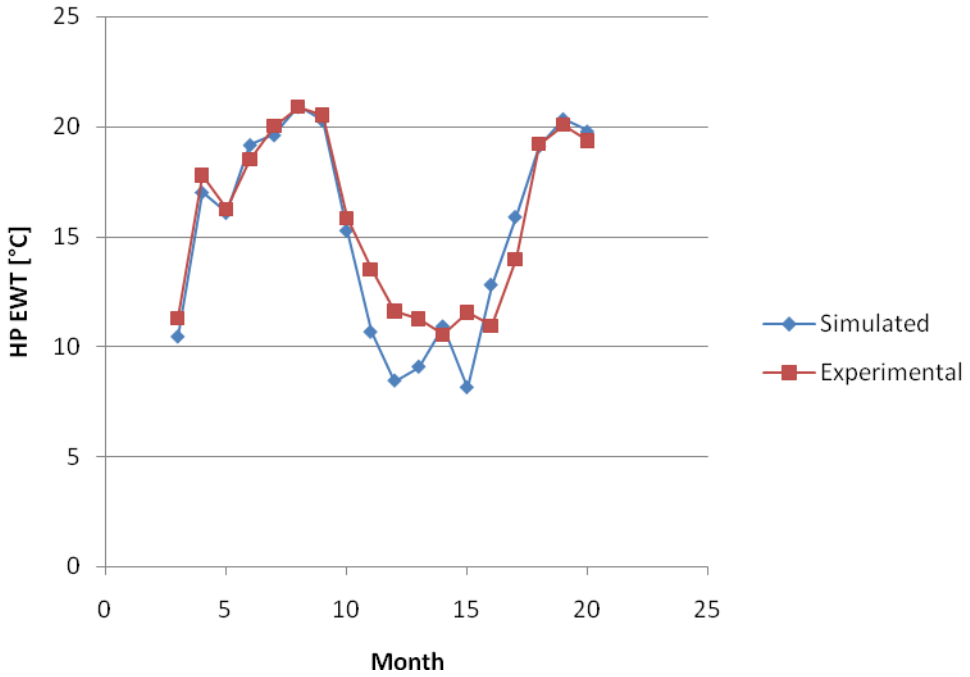

Figure 5-4: 18 month simulation results - minimum heat pump EWT

The average heat pump entering water temperatures match reasonably well, as shown in Figure 5-2. Here, "average" for the simulation means the end-of-month value. For the experiment, it refers to the average heat pump EWT over the last 48 hours of the month; this is done to smooth out any cycling effects that could obscure the results. The main differences occur in the months either containing or immediately adjacent to the transition between heating and cooling dominated profiles for the month (i.e. months 3-4, 10-11). This can be explained by noting how the simulation handles the loads for each month. The heating and cooling loads are added together, and the average value applied over the entire month. However, in actuality there is a rapid transition between the heating and cooling loads at the transition point. This effect can be seen in Figure 5-5, which shows both the hourly heat pump EWT as well as the simulated value over the course of the month; this simulated value is the heat pump EWT when an hourly simulation is performed using the constant monthly average load utilized in GLHEPRO. Even with this multiple degree discrepancy during the transition months, the average heat pump entering water temperature still matches fairly closely.

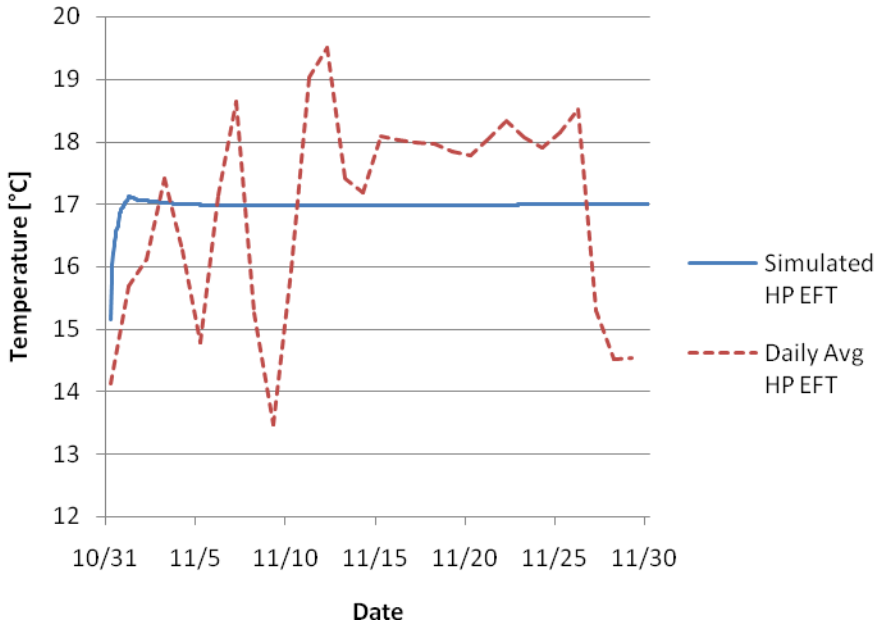

Figure 5-5: Month 11 heat pump EWT transitioning

The maximum and minimum heat pump entering water temperatures (Figures 5-3 and 5-4, respectively) show some mixed results. For the simulation, they are determined by computing the temperature response due to the monthly peak load at the end of the month, and finding the extreme values. For the experiment, the maximum and minimum temperatures are the one-hour intervals with the highest/lowest temperature value (averaged over the hour). While some months match quite closely, many have a large difference between the simulated value and the experimental data. These differences may be somewhat misleading, however, due to issues with both the simulation and the experimental data. There are three main causes for differences in the maximum and minimum temperatures: the experimental facility operation does not match the continuous operation assumed by the simulation, the peak load does not occur at the end of the month, and issues with the calculation of the peak load itself. These sources of error will now be discussed individually and in detail.

5.3.1 Mismatch Between Experimental Operation and Simulation

The heating months, with the exception of month 14, show a sizable difference in the minimum EWT, which is somewhat disconcerting. The problem here, in months 11-13, lies in the lack of equivalence between the experimental and simulated heating loads. While it is true that, by design, the same amount of heat is extracted from the ground, the time period over which that heat is extracted is not the same. The experimental facility was shut down for nearly three weeks consecutively between late November 2005 and mid-December 2005—months 11 and 12 in the simulation—and for a couple of shorter periods (several days each) in January 2006. The hourly heating loads are shown in Figure 5-6; the zero value for the first two weeks, as well as the short gap around 12/18, indicate that the experimental facility was not operational.

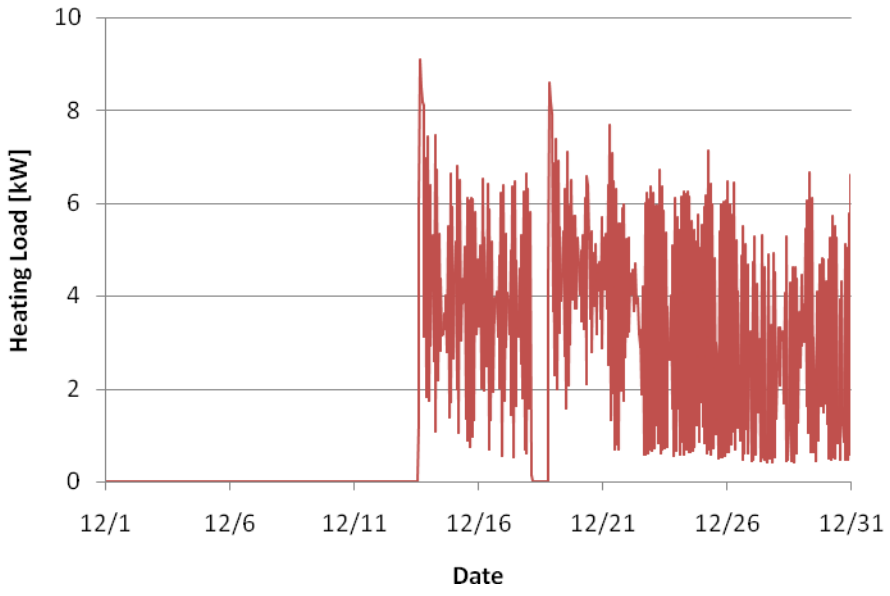

Figure 5-6 Month 12 hourly heating loads

Since the same amount of heat is extracted in a shorter time in the case of the experiment, it is not entirely unexpected that the temperatures would be lower. This can be verified by checking what would happen to the simulated heat pump EWT if the load were simulated only over the time during which the system was running (about 16 days); indeed, the results of this simulation in Figure 5-7 show this behavior. During the system downtime, the loop temperature has a chance to creep back toward the undisturbed ground temperature of 16.3 °C. This creeping behavior also helps to explain the somewhat counterintuitive temperature rise upon further application of the heating load for the month, as the further application of the load is insufficient to further decrease the temperature from the value at the beginning of the load application. The heat pump EFT from a simulation using the hourly load profile, plotted using a 12-hour rolling average to smooth out the curve, shows the same temperature rise over the month. Ignoring the initial upward spike on restart, the temperature plot in Figure 5-8 also shows this. The temperature during the month, when the peak load occurs (at the restart), is not at the same level in the simulation. The experimental downtime caused the peak load to occur at a time when the loop temperature is higher than the monthly simulation can possibly predict; as a result, the temperature response to that peak load is higher in the simulation than the actual experimental value. Using the value of about 15.7 °C that occurs in the offset or hourly simulations at the restart, instead of the 14.1 °C value at the end of the month with the simulation using the average load, would cause the simulated minimum EFT for the month to be 1.6 °C higher, reducing the prediction error for month 12 from 25% to about 10%.

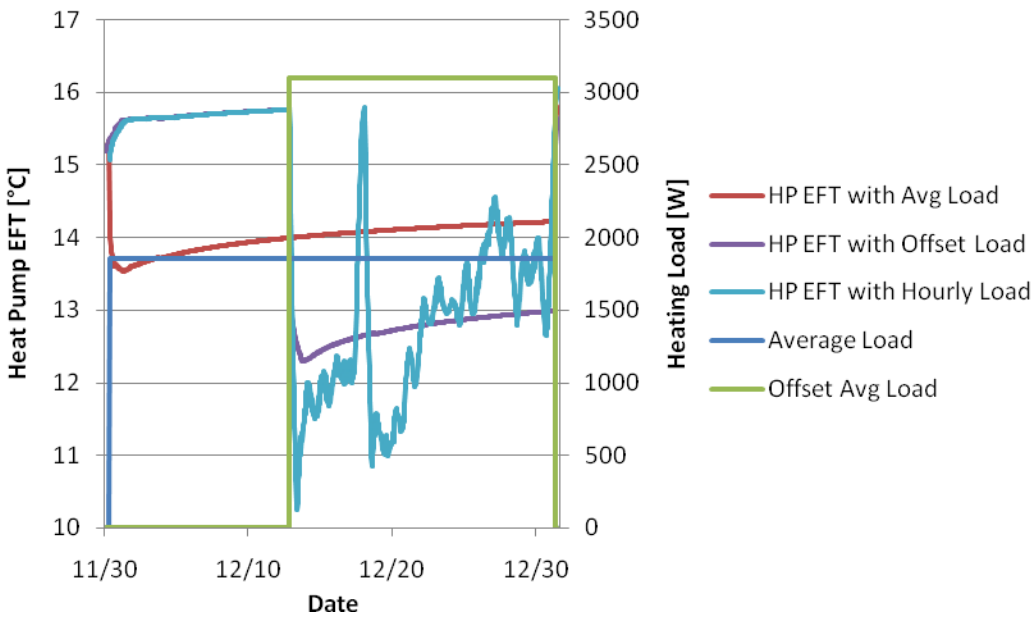

Figure 5-7: Month 12 simulation with offset load

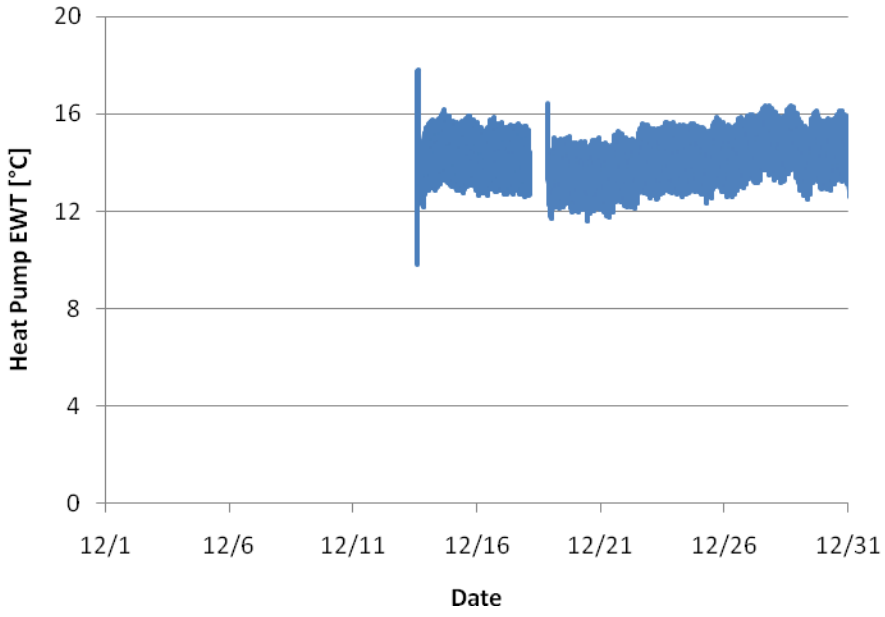

Figure 5-8: Month 12 hourly heat pump EWT

Month 14 is accurate because there were no such outages, and the peak heating load duration was specifically attuned to this month. Month 15 shows such a large differential because that same peak heating load duration is not very appropriate for this month. The peak load duration issue will be discussed in further detail momentarily.

5.3.2 Peak Load Not at End of Month

In months 10 through 14, the simulated maximum EWT is significantly lower than the measured experimental value. Although the maximum heat pump EWT is of little practical importance for the winter months, it is still important to understand why these differences occur. There are two separate reasons for these differences. First, for months 10 and 11, the maximum temperature occurs within the first several days of the month, as shown in Figure 5-9; the plot for month 11 shows the same behavior, and therefore is not shown. The peak occurring at the beginning of the month is an issue with the simulation because it computes the maximum temperature at the end of the month, with the peak load applied to the average temperature at that time. The difference occurs because, while both months are cooling dominated, the cooling load is in both cases lower than the previous month and decreases throughout the month. The average daily cooling load for month 10 demonstrates this behavior, as seen in Figure 5-10; this is a decrease from month 9, where the average cooling load is about 5.8 kW. This causes the temperature in the borehole to drop over the course of the month, so the simulation uses a base temperature (the cooler, end-of-month value) that is too low when computing the peak effects. Adding the effect of the peak load to the temperature at the end of month 9 (as an approximation to the peak load occurring on the first day of month 10) instead of the

temperature at the end of month 10, reduces the error in the prediction of month 10's maximum EFT from about 16% down to just above 6%.

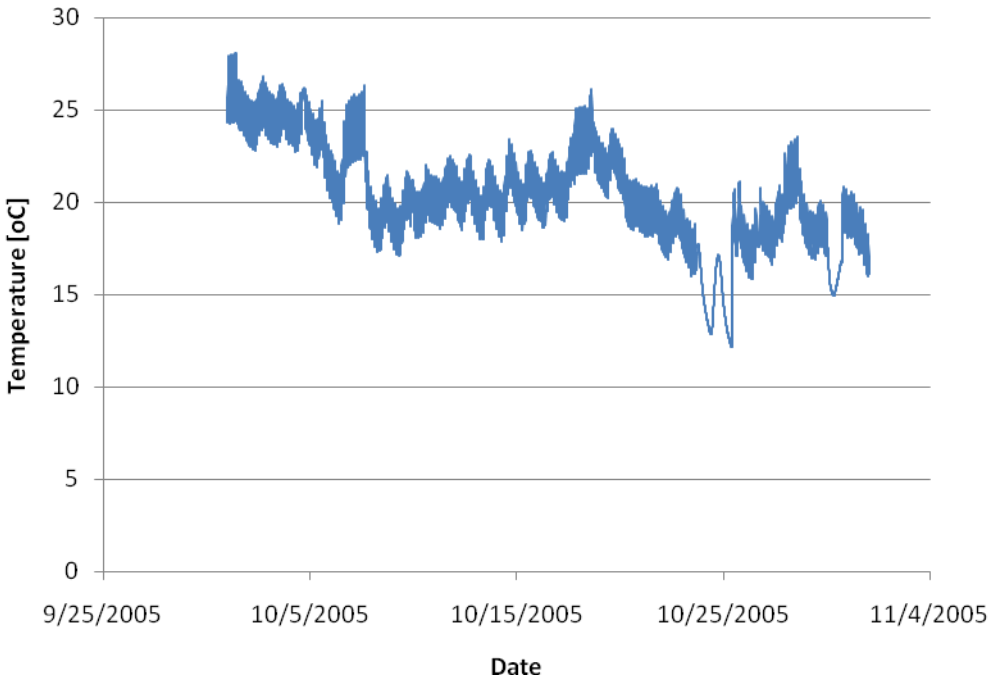

Figure 5-9: Month 10 hourly heat pump EWT

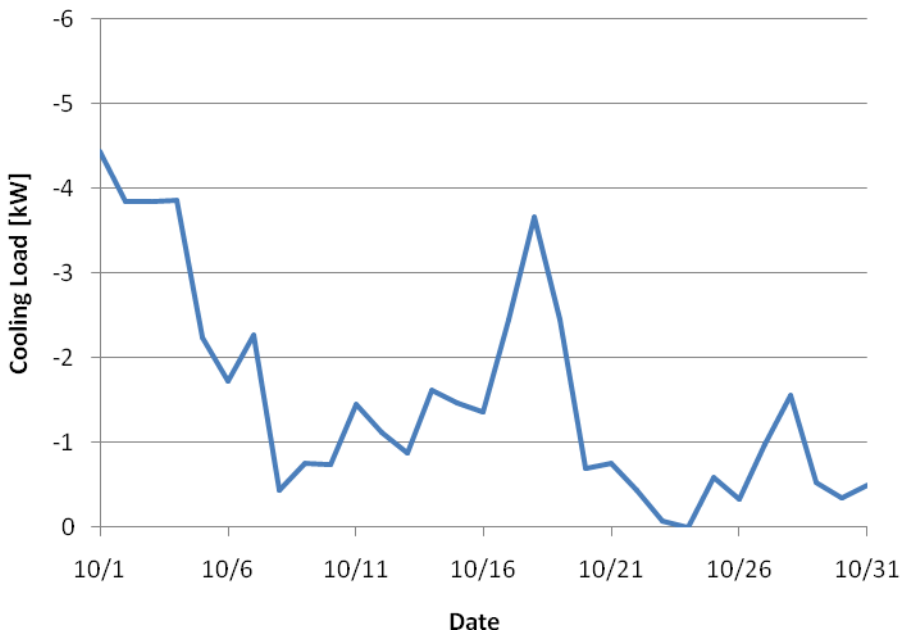

Figure 5-10: Month 10 daily average cooling loads

For the other three months (12-14), there is zero cooling load on the system, and consequently no peak cooling load either. As a result, the maximum temperature from the simulation is identical to the end-of-month value, which, though not realistic, is acceptable for a design simulation where maximum temperatures in winter months are of little practical importance.

The inaccuracies in the simulated minimum heat pump EWT in month 3, and in the simulated maximum heat pump EWT in months 4 and 15, are also due to the actual peak load not occurring at the end of the month. In all of these cases, the months in question are either during or adjacent to a month in which the system switches from heating to cooling or from cooling to heating; the switches occurred in months 3, 11, and 15.

5.3.3 Peak Load Calculation Issues

The remainder of the discrepancies between the experimental data and the simulation results can be attributed to a peak load duration that is not appropriate for the month in question. As the simulation is currently designed, it only uses one peak duration for heating and one for cooling; this same duration is used for every month of the simulation. Thus, because it is most desirable to match the data during the months with the most extreme temperatures, the durations—and, subsequently, the values of the peak loads themselves—are determined by using the peak loads for those months. In the case of the experimental facility, the months used in determining the peak durations were month 14 for heating and month 18 for cooling; the resulting peak load durations were five hours for heating and three hours for cooling, with the values of the peak loads being the average load value of the highest cumulative five- or three-hour total. Both of these months match quite well in their respective modes of operation, but, curiously, neither is actually the most extreme temperature. The aforementioned issues with experimental downtime depressed the water temperature such that the minimum does not actually occur at the time it would be expected if the heating load for each month were evenly distributed over the entire month. As for the maximum temperature, the selection of the peak cooling duration was based on the month with the highest individual hourly load, and not the highest temperature. It is often the case that the day with the highest hourly load will also have the highest temperature, but that is simply not so here. This represents a flaw in the methodology of the peak load determination, but this is much less of a factor than being limited to a single peak duration for every month of the simulation.

It is quite clear that not every month is best served by the same heating and cooling peak load duration. Consider the minimum and maximum heat pump entering water temperatures for different peak load durations, shown, respectively, in Figures 5-11 and 5-12. In each plot, the first three simulation peak load durations use the average load over the time span with the highest cumulative load, while the last uses the absolute maximum load for the month and applies it for two hours consecutively. The load durations used in the validation were five hours for heating, and three hours for cooling, as these were the durations that led to the best match in the month with the absolute maximum heating or cooling load over the span of the experiment. Consequently, the months used in developing these durations (14 in heating and 18 in cooling) show very close agreement. By utilizing a different peak load duration and, occasionally, changing the method in which the magnitude of the peak load is computed, non-design months could be improved in prediction accuracy. It is worth noting, though, that matching a peak load duration for an arbitrary month requires the hourly heating or cooling loads for that month, or, at the very least, the peak day during that month. If these loads are known for every month, it would be entirely possible to use a different peak load duration for each month, and as a result potentially lessen the required borehole depth determined by the simulation when sizing a GSHP system.

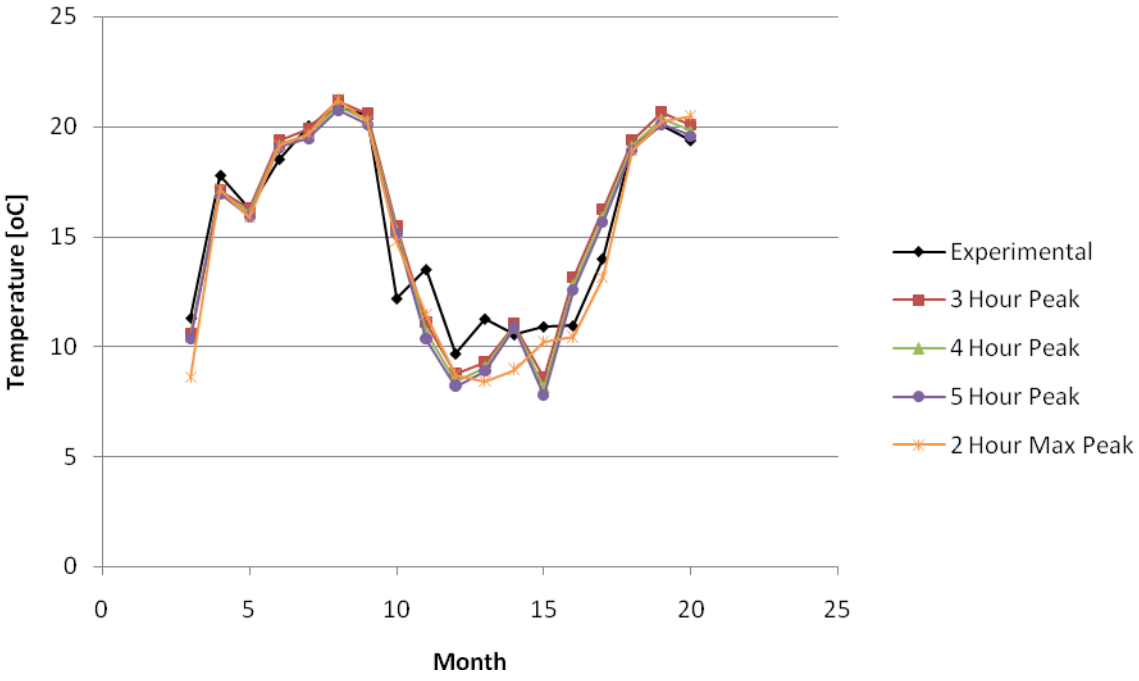

Figure 5-11: Monthly minimum heat pump EWT for different peak load durations

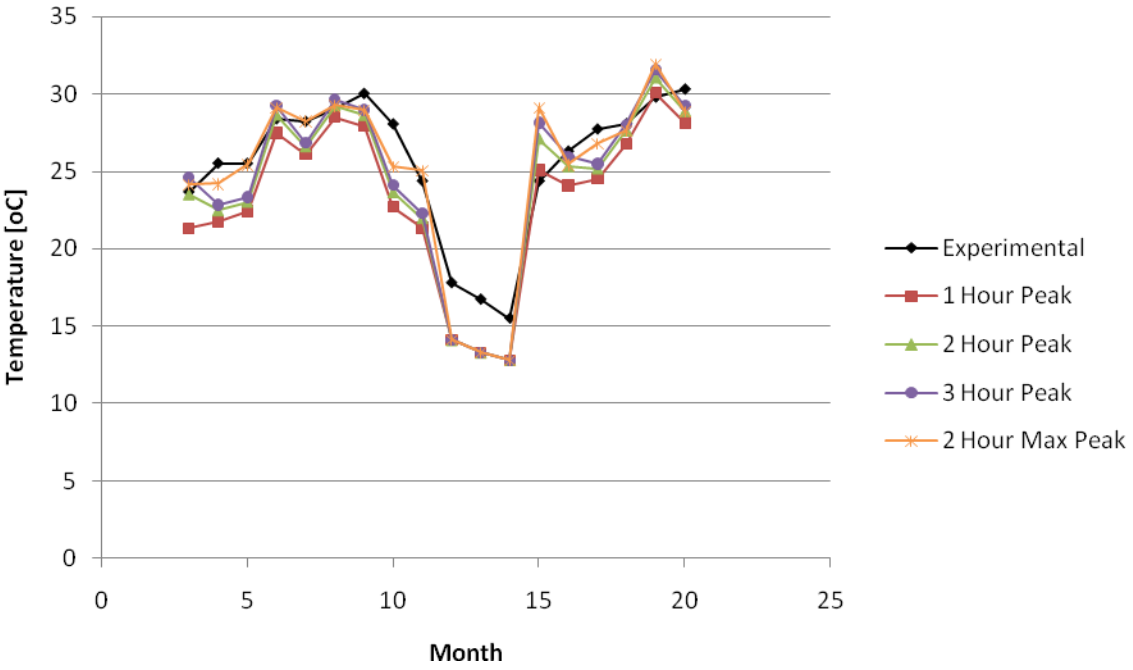

Figure 5-12: Monthly maximum heat pump EWT for different peak load durations

The choice of peak load duration also causes some of the inaccuracies in the simulated minimum heat pump EWT in months 15-17, and in the simulated maximum heat pump EWT in months 5, 16, 17, and 19.

5.4 Conclusions and Recommendations

Experimental data has from a hybrid ground source heat pump test facility has been used to check the validity of GLHEPRO, a software tool for simulating ground source heat pump systems. The simulation routine that forms the backbone of the software was modified slightly in order to handle the 18 months of noncyclical loads computed from the experimental data. Using heat extraction and rejection rates determined from the experimental data, temperature prediction values were checked. Results were typically within about a degree of the experimentally measured values, but could definitely be improved with a more refined treatment of the peak loads. The differences between the experimental and simulated monthly maximum and minimum heat pump entering water temperature were typically fairly small, with the larger errors being mostly explained by looking at the switch between heating and cooling seasons and the appropriateness of the peak load durations. Experimental downtime also played a role in the accuracy of the results; it might be possible to get more accurate results by artificially adjusting the number of days in the simulated month to match the number of days of actual facility operation. Overall, the simulation is adequate for design purposes, although there are a few places for improvement.

The simulation methodology could serve to be refined somewhat, especially in the handling of peak loads. It is obvious that assuming that the peak load occurs at the end of the month, an assumption currently used in the ground loop simulation, may not always be correct; while the errors occasionally produced by this assumption are generally not very large, this is definitely a place where improvements could be made. This could potentially be achieved by weighting the peak load depending on the time of month in which it occurs, which would dampen the effect of the peak load in the simulation if it occurred toward the beginning of the month. Also, it is painfully obvious that not every month is best served by the same peak load duration; this should definitely be addressed as well. However, the trade-off between improved accuracy and simulation time must be carefully weighed, as the purpose for this simulation is to be a useful tool for design, and not a perfectly accurate depiction of the system (though that would be nice as well!).

CHAPTER VI

CONCLUSIONS AND RECOMMENDATIONS

This work presents several new developments in design procedures for ground source and hybrid ground source heat pump systems. First, a much improved GSHP simulation and design tool was presented, with refinements including a more advanced borehole thermal resistance calculation and consideration of the thermal mass of the system. Next, a new methodology was introduced to determine the magnitude and duration of peak heating and cooling loads for use in GSHP system design; this method attempts to equate the temperature response due to the peak period for a monthly simulation to the response for the peak day if the simulation were performed hourly. Then, an optimization-based algorithm for designing hybrid ground source heat pump systems was introduced; the algorithm tries to minimize system cost by maximizing the usage of the available range of entering fluid temperatures to the heat pump. Finally, the monthly GSHP system simulation used in the design tool presented at the beginning of the work was validated against eighteen months of experimental data from the Oklahoma State University hybrid ground source heat pump research facility. Specific conclusions are as follows:

- The refined computation of the borehole thermal resistance and borehole convection coefficient, as well as consideration of thermal mass effects, lead to a

more complete representation of the behavior of a vertical borehole without sacrificing computational efficiency.

- Expansion of the g-function approach via a curve fit of existing g-function data and extrapolation to rectangular borefields of up to 900 boreholes allows for reasonable simulation and design of larger GSHP systems.
- When undisturbed ground temperature data is not available, a reasonable estimate may be obtained by adjusting the annual mean air temperature. This value is, in some cases, much more readily obtainable, although more verification of the approximation is needed.
- The peak load analysis procedure is simple to implement for design engineers, requiring nothing other than a full year's hourly heating and cooling loads. It is also quick and efficient from a computational perspective, requiring very little time to run.
- Validation of the peak load procedure showed generally good results on a variety of building types and locations. The procedure tends to slightly oversize GSHP systems; differences in sizing results can be accounted for by noting that the simplifying assumptions are not always perfectly true. Nevertheless, this approach is better than the nearly complete lack of guidance as to the selection of peak loads that was previously available.
- The current terminology of "heating-dominated" and "cooling-dominated" systems is insufficient to fully identify the type and behavior of a GSHP system; the new terms "heating-constrained" and "cooling-constrained" more fully capture the behavior.

- The simulation-based, temperature limit-optimized design procedure for HGSHP systems is relatively easy to implement and computationally efficient. On a computer with typical hardware, a GLHE length and supplemental heat rejection/addition device size may be obtained within a couple of minutes.
- The new HGSHP design methodology compared favorably to a cost-optimized design method, and outperformed the existing method, for the test cases examined. The new methodology is superior to the cost-optimized method in that it requires far less computation time, even though the cost-optimized method produces the most desirable system from a design engineer's perspective.
- The temperature prediction capability of the GSHP design tool is adequate for design purposes, with most errors being small (within a degree or so).
- Mismatches between the experimental and simulated data were due to the nature of the switch between heating and cooling seasons in the experiment, the appropriateness of the peak load approximation, and the handling of experimental downtime.

There are still quite a few areas in which the methodology for designing ground source and hybrid ground source heat pump systems, as well as the simulation of such systems, may be improved. Some particular recommendations for future work include:

- Optional hourly simulation of all or part of a GSHP system in a design tool. This must be carefully considered to balance the improved accuracy from an hourly simulation with the heavy increase in computation time.

- The capability to simulate a wide variety of supplemental heat rejection and heat addition devices in a design tool, thus creating the ability to design, via simulation, a complete HGSHP system.
- A more thorough investigation into the optimal shape of a peak heating or cooling load in a monthly simulation. It is obvious that, in some cases, assuming a square heat pulse is not the best approximation.
- Adaptation of the peak load procedure to consider different peak load durations for each month. This might allow for a better overall prediction of system behavior.
- Complete automation of the peak load analysis procedure into a design tool. While the procedure currently requires user decision of the best approximating method and duration, this could be implemented into a design tool; this would also easily allow selection of different durations for different months.
- Further comparison of the HGSHP design methodology to both existing and future methods, using a wide variety of test cases. Parts of this are currently underway.
- Investigation into the optimal control of HGSHP systems, as pertaining to the design of those systems.
- Further validation of the general GSHP simulation procedure, especially using data from different locations and of varying building types.

REFERENCES

Austin, W. A. 1998. Development of an In-Situ System for Measuring Ground Thermal Properties. M.S. Thesis, Oklahoma State University, School of Mechanical and Aerospace Engineering. Available online at http://www.hvac.okstate.edu.

Austin, W., C. Yavuzturk, and J.D. Spitler. 2000. Development of an In-Situ System For Measuring Ground Thermal Properties. *ASHRAE Transactions*. 106(1): 365-379.

Bennet, J., J. Claesson, and G. Hellström. 1987. Multipole Method to Compute the Conductive Heat Flows to and Between Pipes in a Composite Cylinder. Notes on Heat Transfer 3-1987, Department of Building Technology and Mathematical Physics, University of Lund, Sweden.

Bose, J. E. 1988. Closed-Loop/Ground-Source Heat Pump Systems—Installation Guide. National Rural Electric Cooperative Association, NRECA Research Project 86-1.

Bose, J. E., Editor. 1989. Soil and Rock Classification for the Design of Ground-Coupled Heat Pump Systems—Field Manual. Electric Power Research Institute Special Report, EPRI CU-6600.

Chiasson, A. D., J. D. Spitler, S. J. Rees and M. D. Smith. 2000a. A Model for Simulating the Performance of a Shallow Pond as a Supplemental Heat Rejecter with Closed-Loop Ground-Source Heat Pump Systems. ASHRAE Transactions. 106(2): 107-121.

Chiasson, A. D., J. D. Spitler, S. J. Rees and M. D. Smith. 2000b. A Model for Simulating the Performance of a Pavement Heating System as a Supplemental Heat Rejecter with Closed-Loop Ground-Source Heat Pump Systems. ASME Journal of Solar Energy Engineering. 122: 183-191.

Chiasson, A. D. and C. Yavuzturk. 2003. Assessment of the Viability of Hybrid Geothermal Heat Pump Systems with Solar Thermal Collectors. ASHRAE Transactions. 109(2): 487-500.

Chiasson, A. D., C. Yavuzturk and W. J. Talbert. 2004. Design of school building HVAC retrofit with hybrid geothermal heat-pump system. Journal of architectural engineering. 10(3): 103-111.

Claesson, J., and G. Hellström. 1987. Thermal Resistances to and Between Pipes in a Composite Cylinder. Department of Mathematical Physics and Building Technology, University of Lund, Sweden.

Collins, W.D. 1925. Temperature of Water Available for Industrial Use in the United States. United States Geological Survey Water Supply Paper 520-F. Washington: USGS.

DOE. 2007. EnergyPlus Energy Simulation Software. http://www.eere.energy.gov/buildings/energyplus/.

Dowell, M., and P. Jarratt. 1971. A Modified Regula Falsi Method for Computing the Root of an Equation. *BIT Numerical Mathematics* 11(2): 168-174.

Eskilson, P. 1987. Thermal Analysis of Heat Extraction Boreholes. Ph.D. Dissertation, University of Lund, Sweden, Department of Mathematical Physics.

Falvey, D. M. 1968. Increase Accuracy of Soil Resistivity Measurements. *Electrical World* 107(11): 79-80.

Feng, X. 1999. Energy Analysis of BOK Building. M.S. Thesis, Oklahoma State University, School of Mechanical and Aerospace Engineering. Available online at http://www.hvac.okstate.edu.

Gehlin, S., and G. Hellström. 2003. Comparison of Four Models for Thermal Response Test Evaluation. ASHRAE Transactions Vol. 109, Pt. 1.

Gentry, J. E. 2007. Simulation and Validation of Hybrid Ground Source and Water-Loop Heat Pump Systems. M.S. Thesis, Oklahoma State University, School of Mechanical and Aerospace Engineering. Available online at http://www.hvac.okstate.edu.

Gnielinski, V. 1976. New Equations for Heat and Mass Transfer in Turbulent Pipe and Channel Flow. *International Chemical Engineering* Vol.16, pp.359-368.

Hellström, G., and B. Sanner. 1994. Software for Dimensioning of Deep Boreholes for Heat Extraction. Proceedings of Calorstock Conference 1994, Espoo/Helsinki, Finland.

Hellström, G., and B. Sanner. 2000. EED/Earth Energy Designer User Manual, Version 2.0.

Hellström, G., B. Sanner, M. Klugescheid, T. Gonka, and S. Mårtensson. 1997. Experiences with the Borehole Heat Exchanger software EED. Proceedings of Megastock Conference 1997, Sapporo, Japan.

Hern, S.A. 2004. Design of an Experimental Facility for Hybrid Ground Source Heat Pump Systems. M.S. Thesis, Oklahoma State University, School of Mechanical and Aerospace Engineering. Available online at http://www.hvac.okstate.edu.

Hooper, F. C., and S. C. Chang. 1953. Development of the Thermal Conductivity Probe. *ASHVE Transactions*. Vol. 59, pp. 463-472.

Katsura, T., K. Nagano, S. Takeda, T. Ibamoto, and S. Narita. 2006. Development of a Design and Performance Prediction Tool for the Ground Source Heat Pump System. Proceedings of Ecostock Conference 2006, Pomona, NJ.

Kavanaugh, S.P. 1992. Simulation of Ground-Coupled Heat Pumps with an Analytical Solution. Proceedings of the ASME International Solar Energy Conference, Maui, HI, 5-9 April 1992.

Kavanaugh, S.P., and S. Rafferty. 1997. Ground-Source Heat Pumps: Design of Geothermal Systems for Commercial and Industrial Buildings. Atlanta: ASHRAE.

Khan, M. 2004. Modeling, Simulation and Optimization of Ground Source Heat Pump Systems. M.S. Thesis, Oklahoma State University, School of Mechanical and Aerospace Engineering. Available online at http://www.hvac.okstate.edu.

Khan, M. H., A. Varanasi, J. D. Spitler, D. E. Fisher and R. D. Delahoussaye. 2003. Hybrid Ground Source Heat Pump System Simulation Using Visual Modeling Tool for HVACSIM+. Proceedings of Building Simulation 2003. pp: 641-648. Eindhoven, Netherlands. August 11-14, 2003.

Knoblich, K. 1997. EED/Earth Energy Designer User's Manual, Version 1.0.

Marshall, C.L., and J.D. Spitler. 1994. GLHEPRO: The Professional Ground Loop Heat Exchanger Design Software—User's Guide.

Melinder, Å. 1997. Thermodynamic Properties of Liquid Secondary Refrigerants. International Institute of Refrigeration.

Mitchell, J. K., and T. C. Kao. 1978. Measurement of Soil Thermal Resistivity. Journal of the Geotechnical Engineering Division, Proceedings of the ASCE. Vol. 104, No. GT7. pp. 1307-1320.

Morrison, A. 2000. GS2000™ Software. Proceedings of the Fourth International Heat Pumps in Cold Climates Conference, Aylmer, Québec, 17-18 August.

Nagano, K., T. Katsura, and S. Takeda. 2006. Development of a Design and Performance Prediction Tool for the Ground Source Heat Pump System. *Applied Thermal Engineering*. Vol. 26, pp. 1578-1592.

Nelder, J.A., and R. Mead. 1965. A Simplex Method for Function Minimization. Computer Journal 7(4): 308-313.

Paul, N. D. 1996. The Effect of Grout Thermal Conductivity on Vertical Geothermal Heat Exchanger Design and Performance. M.S. Thesis. South Dakota State University.

Pikul, Jr., J.L. 1991. Estimating soil surface temperature from meteorological data. *Soil Science* 151(3):187-195.

Rees, S.J. 2000. An Introduction to the Finite Volume Method: Tutorial Series. Stillwater, OK: Oklahoma State University.

Šafanda, J., D. Rajver, A. Correia, and P. Dědeček. 2006. Monitoring of the Air-Ground Temperature Coupling in Three European Climatic Provinces. *Geophysical Research Abstracts*, Vol. 8, 07663.

Sanner, B., G. Hellström, J. Spitler, and S. Gehlin. 2005. Thermal Response Test – Current Status and World-Wide Application. Proceedings of the World Geothermal Congress 2005, Antalya, Turkey, April 24-29.

Signorelli, S. and T. Kohl. 2004. Regional Ground Surface Temperature Mapping from Meteorological Data. *Global and Planetary Change*. Vol. 40, pp. 267-284.

Spitler, J.D. 2000. GLHEPRO -- A Design Tool for Commercial Building Ground Loop Heat Exchangers. Proceedings of the Fourth International Heat Pumps in Cold Climates Conference, Aylmer, Québec, 17-18 August.

Stolpe, J. 1970. Soil Thermal Resistivity Measured Simply and Accurately. IEEE Transactions on Power Apparatus and Systems. Vol. PAS-89, No. 2. pp. 297-304.

Thornton, J.W., T.P. McDowell, J.A. Shonder, P.J. Hughes, D. Pahud, and G. Hellstrom. 1997. Residential Vertical Geothermal Heat Pump System Models: Calibration to Data. *ASHRAE Transactions* 103(2): 660–674.

Webb, R. L. 1984. A Unified Theoretical Treatment for Thermal Analysis of Cooling Towers, Evaporative Condensers and Fluid Coolers. ASHRAE Transactions. 90(2): 398-415.

Webb, R. L. and A. Villacres. 1984. Algorithms for Performance Simulation of Cooling Towers, Evaporative Condensers and Fluid Coolers. ASHRAE Transactions. 90(2): 416-458.

Witte, H.J.L., G.J. van Gelder, J.D. Spitler. 2002. In Situ Measurement of Ground Thermal Conductivity: The Dutch Perspective. *ASHRAE Transactions* 108(1): 263-272.

Xu, X., and J.D. Spitler. 2006. Modeling of Vertical Ground Loop Heat Exchangers with Variable Convective Resistance and Thermal Mass of the Fluid. Proceedings of the EcoStock 2006 Conference, Pomona, NJ

Yavuzturk, C. 1999. Modeling of Vertical Heat Exchangers for Ground Source Heat Pump Systems. Ph.D. Dissertation, Oklahoma State University, School of Mechanical and Aerospace Engineering. Available online at http://www.hvac.okstate.edu.

Yavuzturk, C., and J.D. Spitler. 1999. A Short Time Step Response Factor Model for Vertical Ground Loop Heat Exchangers. *ASHRAE Transactions*. 105(2):475-485.

Yavuzturk, C. and J.D. Spitler. 2000. Comparative Study to Investigate Operating and Control Strategies for Hybrid Ground Source Heat Pump Systems Using a Short Time-Step Simulation Model. ASHRAE Transactions. 106(2): 192-209.

Young, T.R. 2004. Development, Verification, and Design Analysis of the Borehole Fluid Thermal Mass Model for Approximating Short Term Borehole Thermal Response. M.S. Thesis, Oklahoma State University, School of Mechanical and Aerospace Engineering. Available online at http://www.hvac.okstate.edu.

VITA

James R. Cullin

Candidate for the Degree of

Master of Science

Thesis: IMPROVEMENTS IN DESIGN PROCEDURES FOR GROUND SOURCE AND HYBRID GROUND SOURCE HEAT PUMP SYSTEMS

Major Field: Mechanical Engineering

Biographical:

Personal Data: Born in Ponca City, Oklahoma, on 3 July 1984 to John F. and Celia R. Cullin

Education: Graduated from Ponca City High School in May 2002. Received Bachelor of Science degrees in Mechanical Engineering and Aerospace Engineering from Oklahoma State University, Stillwater, Oklahoma, in May 2006. Completed the requirements for the Master of Science in Mechanical Engineering at Oklahoma State University in December 2008.

Experience: Employed as a graduate research assistant for the Oklahoma State University Building and Environmental Thermal Systems Research Group from June 2006 to present.

Professional Memberships: American Society of Heating, Refrigerating, and Air-Conditioning Engineers (ASHRAE).

ABSTRACT

Name: James R. Cullin Date of Degree: December 2008

Institution: Oklahoma State University Location: Stillwater, Oklahoma

Title of Study: IMPROVEMENTS IN DESIGN PROCEDURES FOR GROUND SOURCE AND HYBRID GROUND SOURCE HEAT PUMP SYSTEMS

Pages in Study: 137 Candidate for the Degree of Master of Science

Major Field: Mechanical Engineering

Scope and Method of Study: This study focuses on improvements made in design procedures for ground source and hybrid ground source heat pump systems. Revisions were made to a ground source heat pump system design tool that allow for more accurate simulations without sacrificing computation time. Additionally, a new methodology to best approximate the magnitude and duration of peak heating and cooling loads for monthly design simulations is introduced, as is an algorithm for determining the optimum hybrid ground source heat pump system design (both ground loop and supplemental device sizes). Finally, the ground source heat pump simulation and design tool is validated against eighteen months of experimental data.

Findings and Conclusions: The new additions to the ground source heat pump design tool allow for accurate simulation of a much wider variety of systems than has previously been available. When validated against an hourly simulation, the peak load approximation technique performs well, showing better guidance for selection of the peak load. The hybrid ground source heat pump design algorithm outperforms the method available in the literature, and compares favorably to a cost-optimized design procedure, especially when computation time is taken into account. Finally, the validation of the ground source heat pump design tool shows that it is accurate enough for design purposes, although more refinement is undoubtedly needed.

ADVISER'S APPROVAL: Dr. Jeffrey D. Spitler